Nanoplasmonics: From Surface-Enhanced Raman Spectroscopy to Nanophotonic Circuits

Hongxing Xu

Institute of Physics, CAS
Wuhan University

2014, 4, 17 Beijing

表面等离激元及其研究意义

表面等离激元：

金属自由电子气的集体振荡

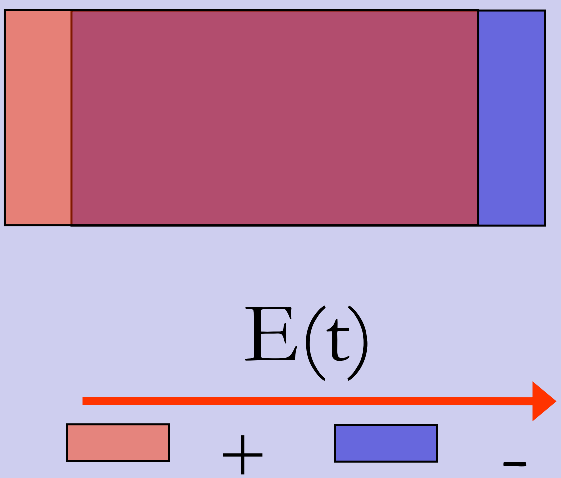

特殊的共振特性

局域电场增强效应

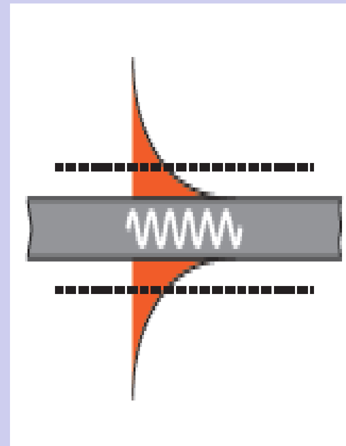

等离激元结构
尺寸小于波长

突破衍射极限

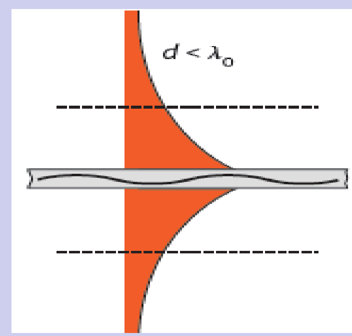

介质光传输结构
尺寸大于波长

衍射极限

- 亚波长的光束缚和远程传播
- 纳米尺度上光的调控

例1—共振频率可调

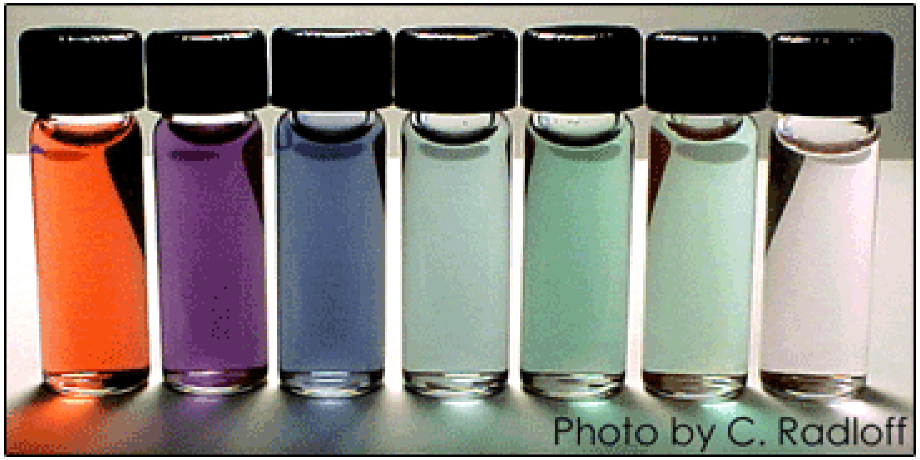

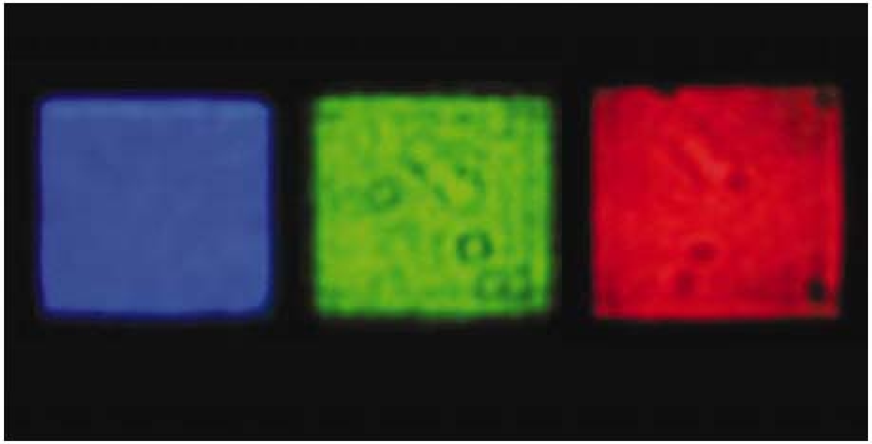

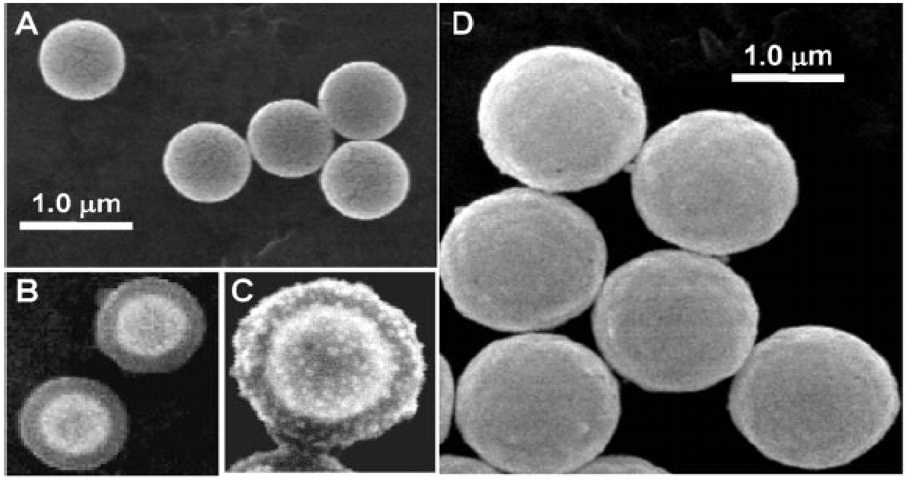

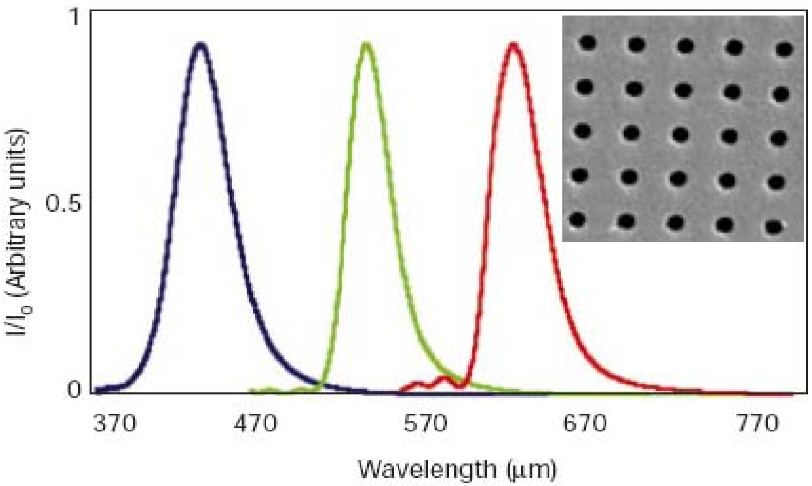

Halas et al. Science, **302**, 419 (2003)

Ebbesen et al. Nature **424**, 824 (2003)

金属纳米颗粒的奇特的散射和透射

The Lycurgus Cup

Gold Bull **2007,** *40*, 270-277

例2—巨大电磁增强效应

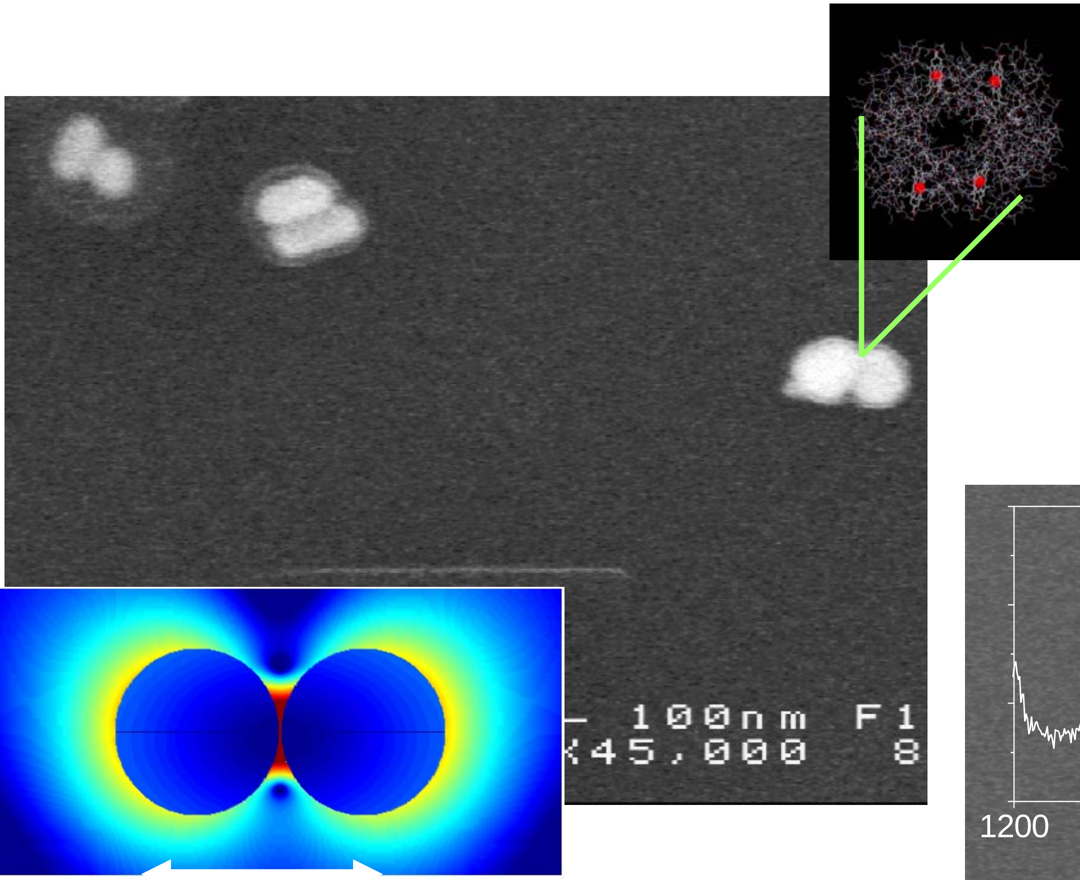

- 当银胶溶液与血红蛋白溶液混合后，两个银颗粒被单个血红蛋白分子粘在一起
- 血红蛋白分子/银颗粒 ~ **1:4**

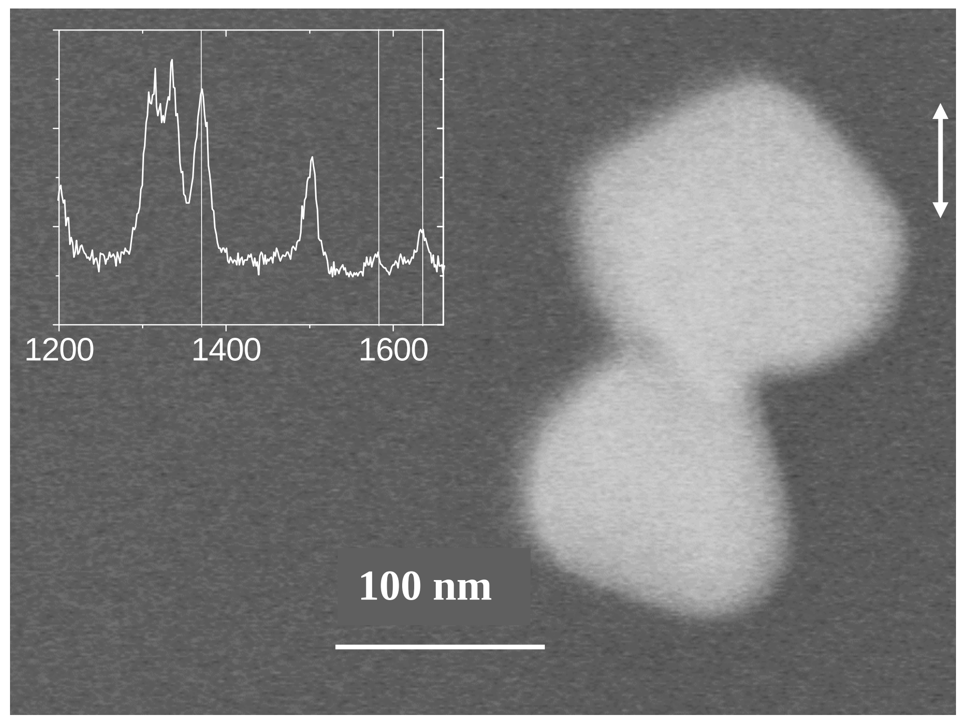

徐红星 等 **PRL 83** 4357 (1999)

巨大的电磁增强效应，解释了单分子表面增强拉曼散射的机理。

例3—纳米尺度光的传导

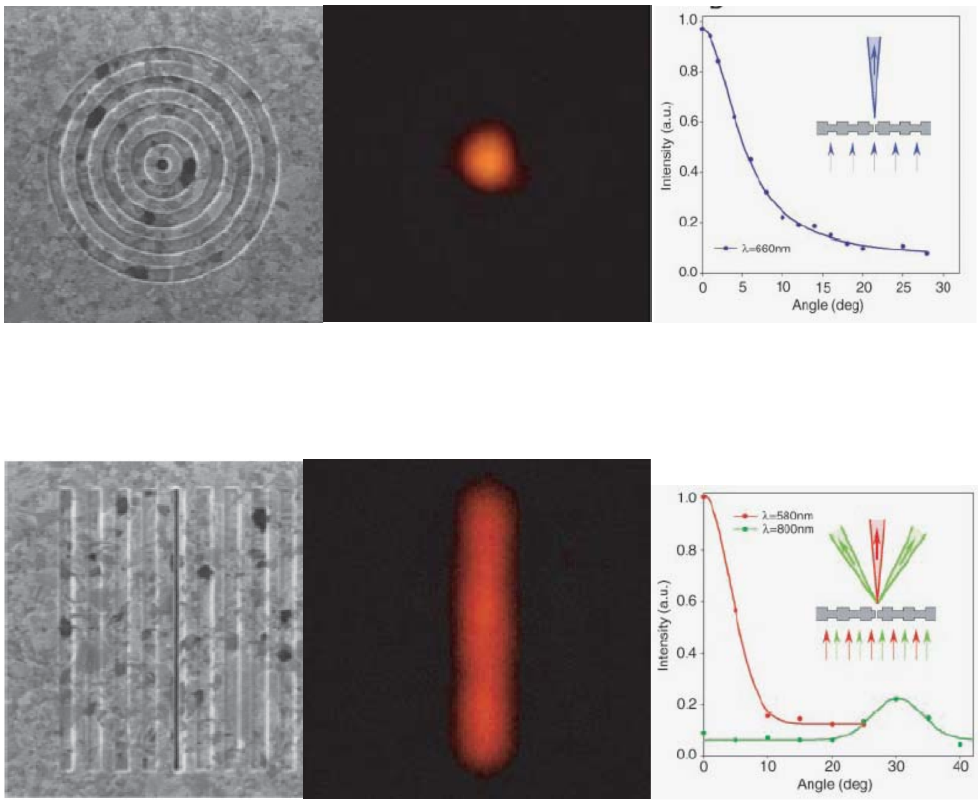

Lezec *et al*. *Science* **297**, 820 (2002)

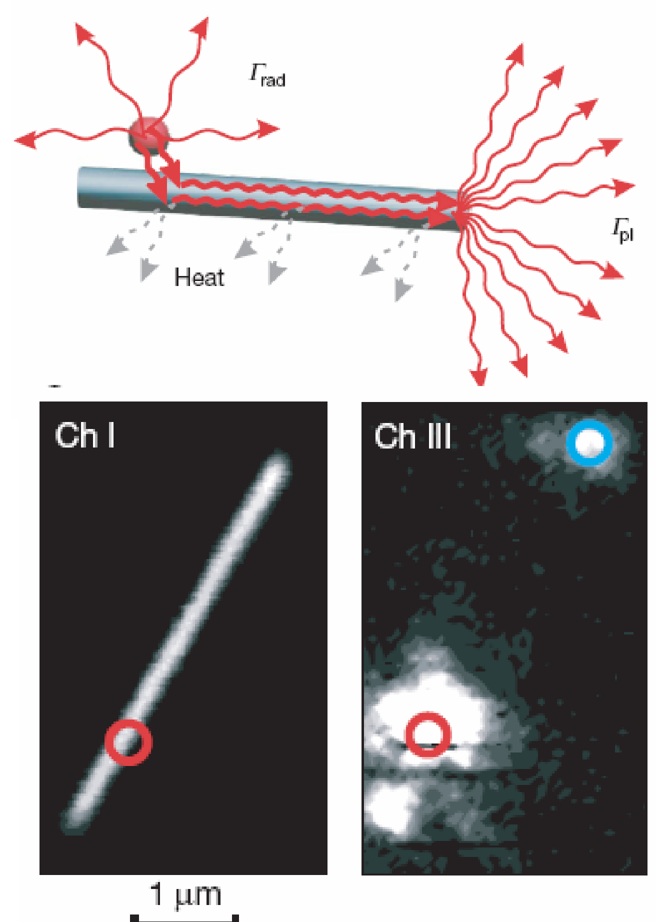

Akimov *et al.* nature **450**，402 (2007)

克服光的衍射极限的传播！

例4—任意的透射和反射规律

Metasurfaces

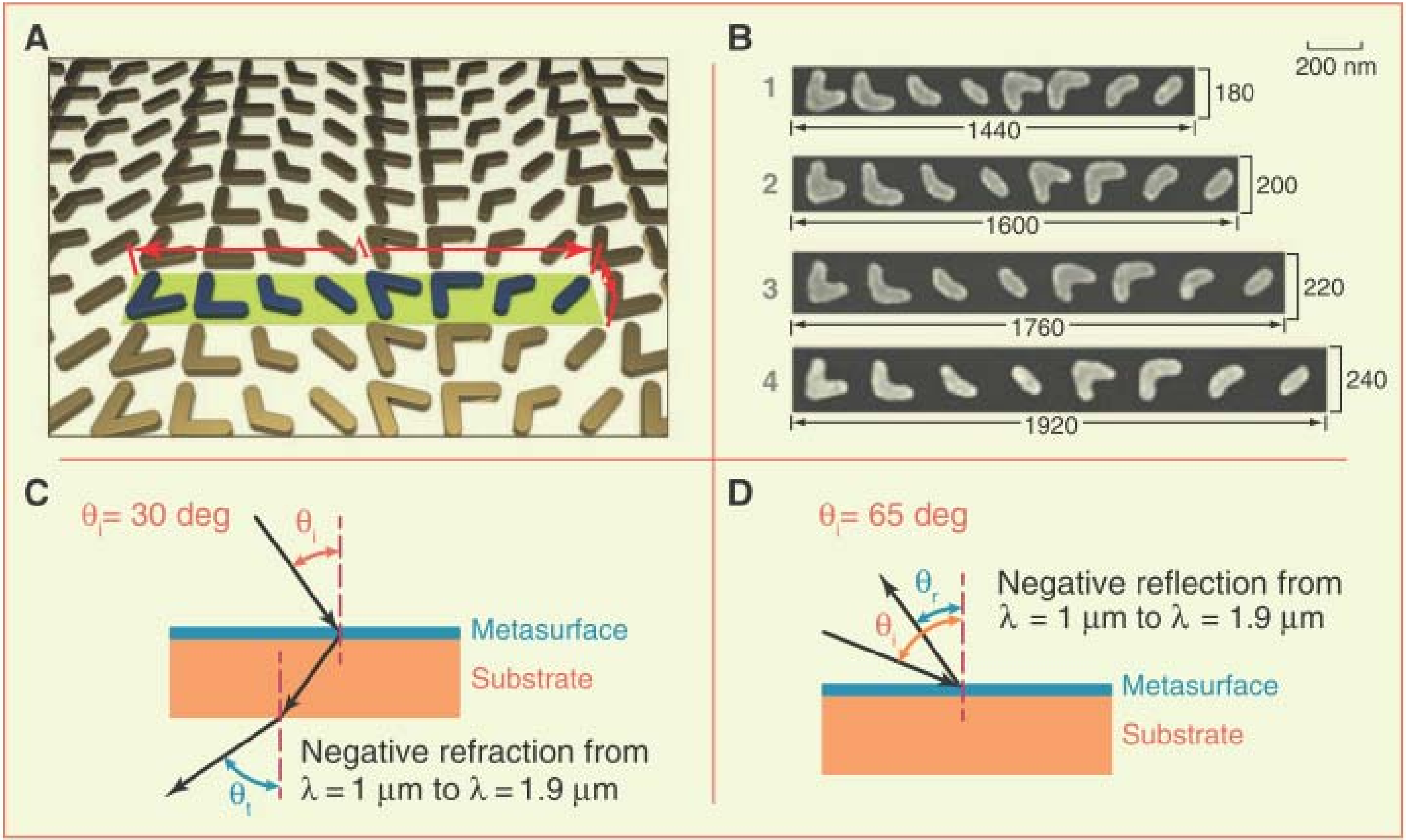

Science **2013,** 339, 123009

例5—增强光学非线性效应

二阶和频产生

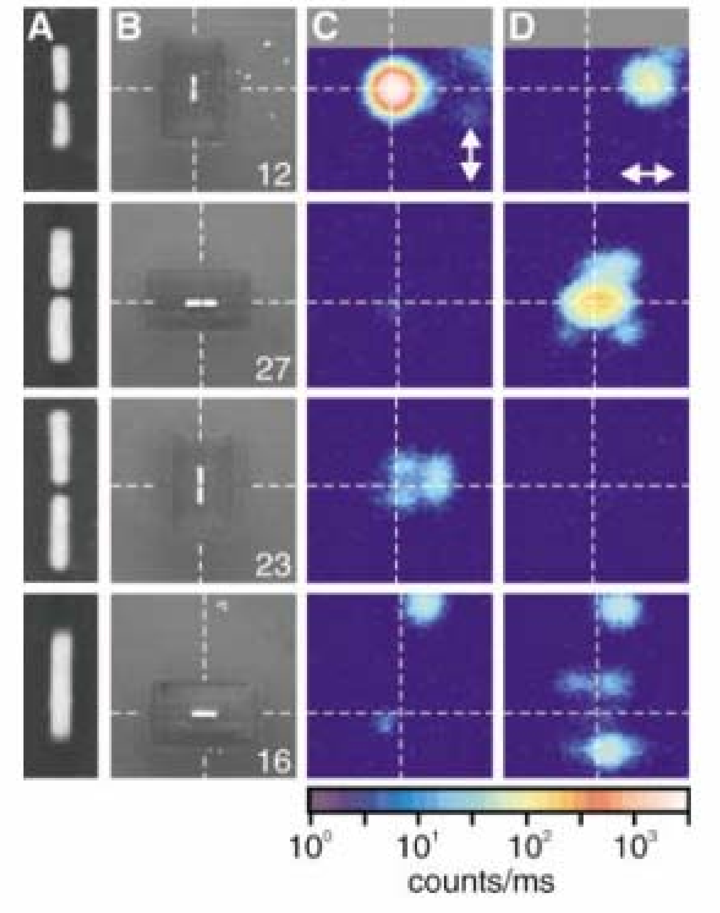

Science **2005,** *308*, 1607-1609

高阶和频产生

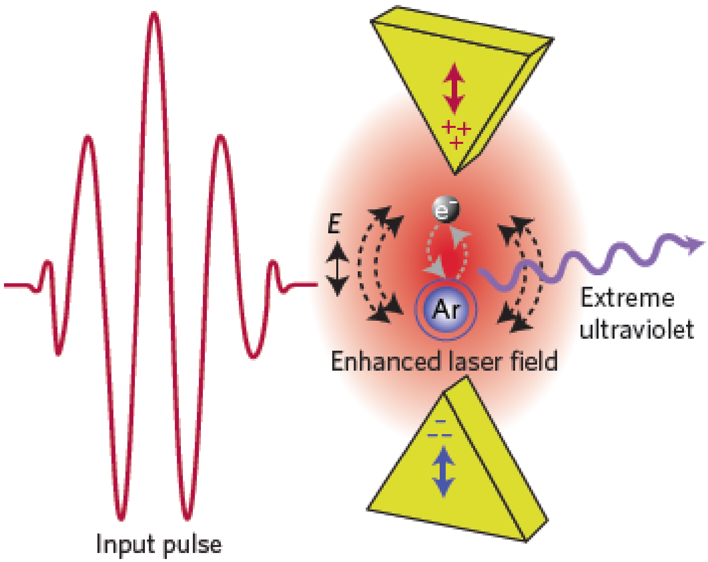

Nature 453, 757-760 (2008)

例6—癌症热疗与太阳能电池

癌症热疗

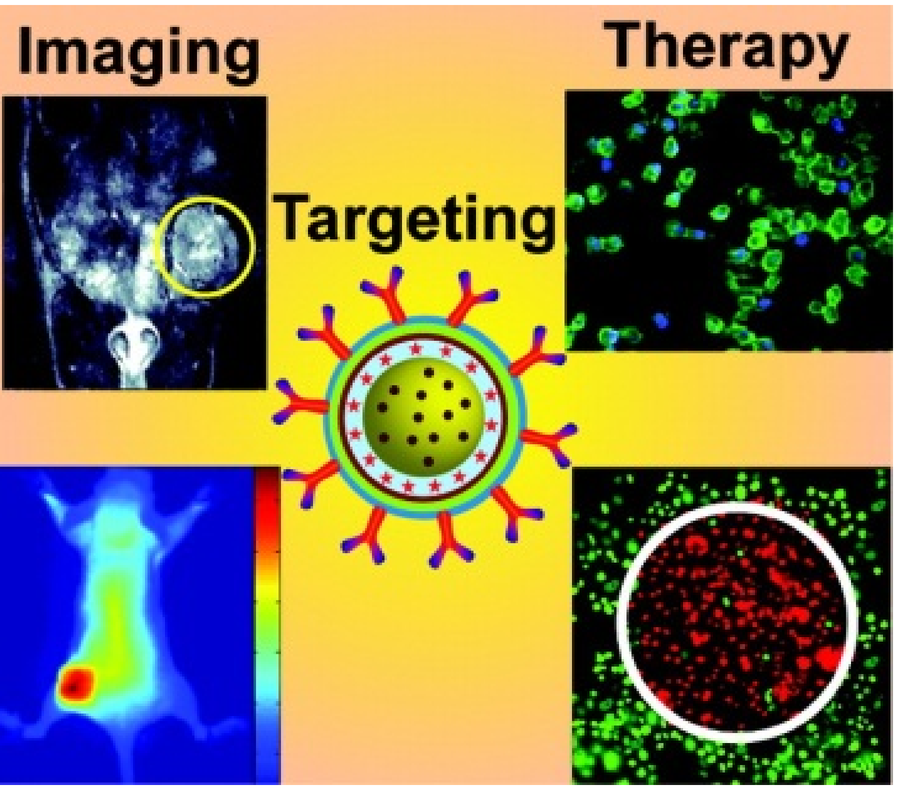

Acc. Chem. Rev. DOI: 10.1021/ar200023x

太阳能电池

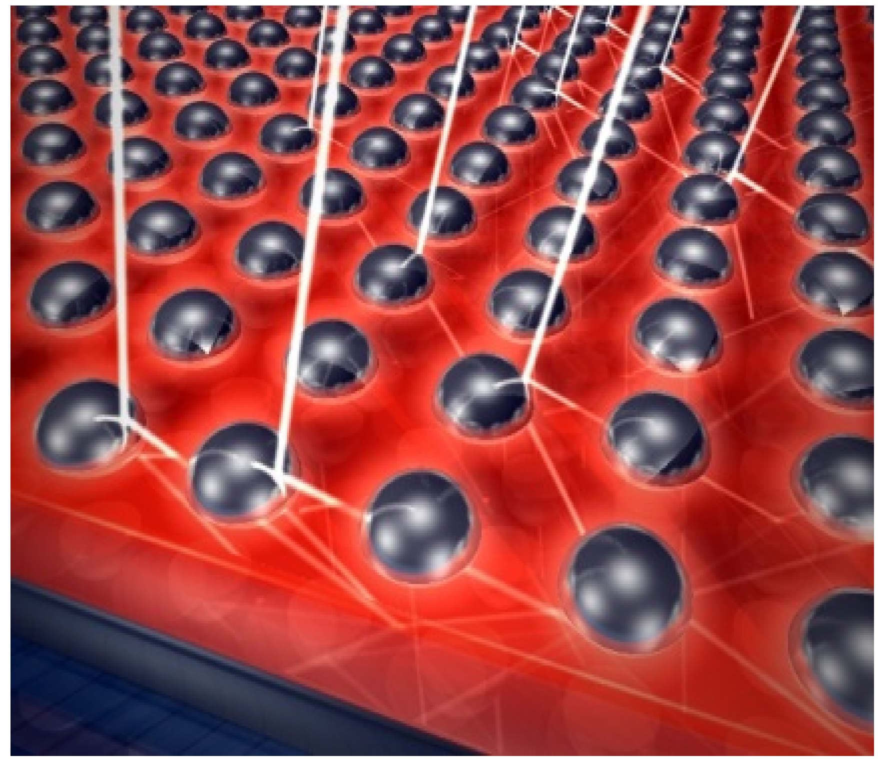

Nat. Mater., 9, 205-213 (2010)

例6—微纳光器件

亚波长波导

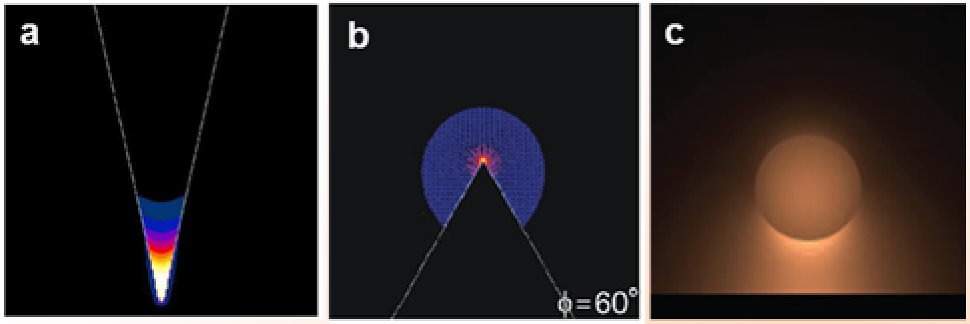

Opt. Lett. **2006,** *31*, 3447-3449; *Phys. Rev. Lett.* **2008,** *100*, 023901; *Nat. Photon.* **2008,** *2*, 496-500

耦合器

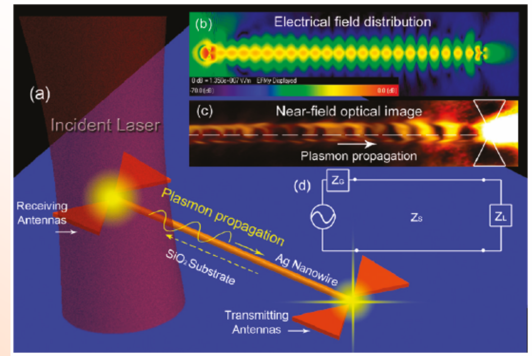

Nano Lett., **2011**, *11* (4), 1676–1680

干涉器

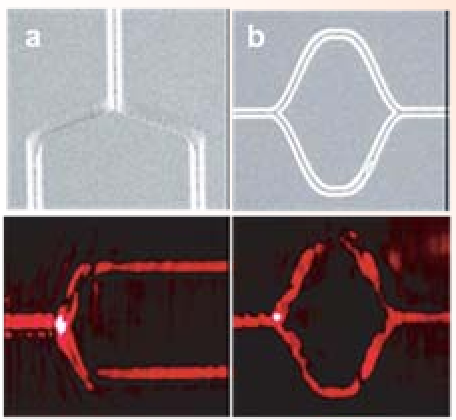

Nature, 440(23), 508-511(2006)

分光器

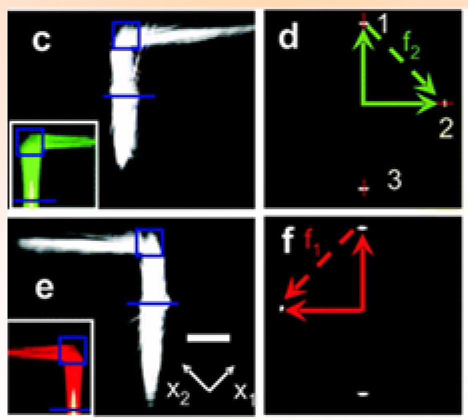

Nano Lett. **2007,** *7*, 1697-1700

纳米激光器

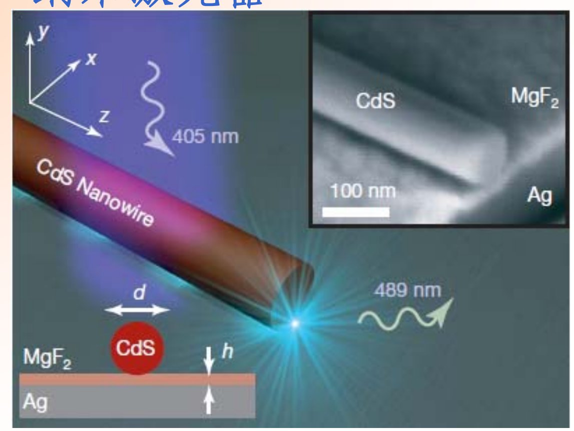

Nature **2009,** *461* (7264), 629-632

还有聚焦元件、反射器、滤波器……

广阔的应用前景

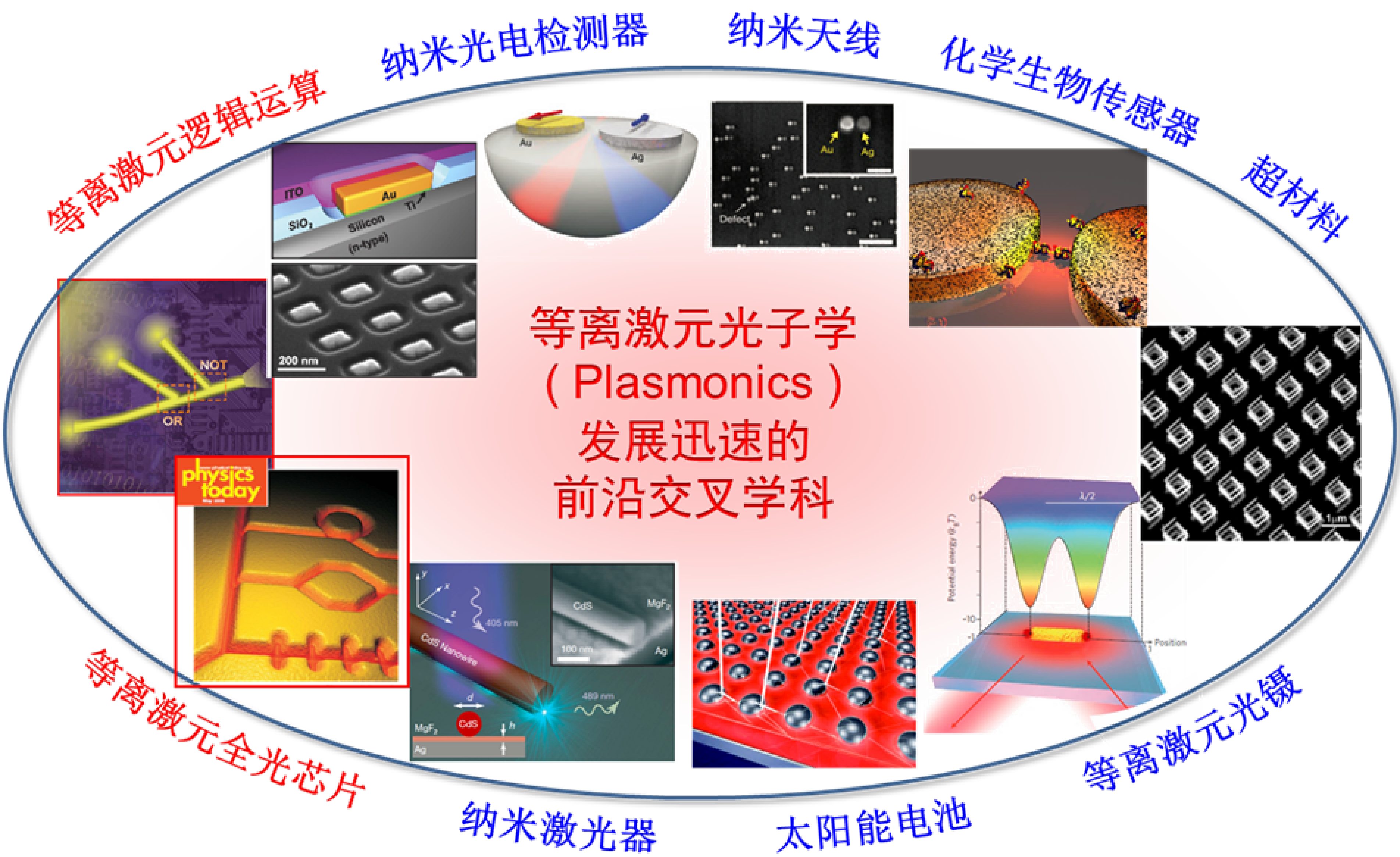

等离激元逻辑运算
纳米光电检测器
纳米天线
化学生物传感器
超材料
等离激元光子学
（Plasmonics）
发展迅速的
前沿交叉学科
等离激元全光芯片
纳米激光器
太阳能电池
等离激元光镊
ITO
Au
Ti
SiO2
Silicon
(n-type)
200 nm
Au
Ag
Defect
NOT
OR
physics today
CdS Nanowire
405 nm
489 nm
CdS
MgF2
100 nm
Ag
λ/2
Position

1. Surface enhanced Raman spectroscopy

Hot spot/ Nanogap for huge SERS(EM) enhance

Coupling Plasmons for Single Molecule SERS

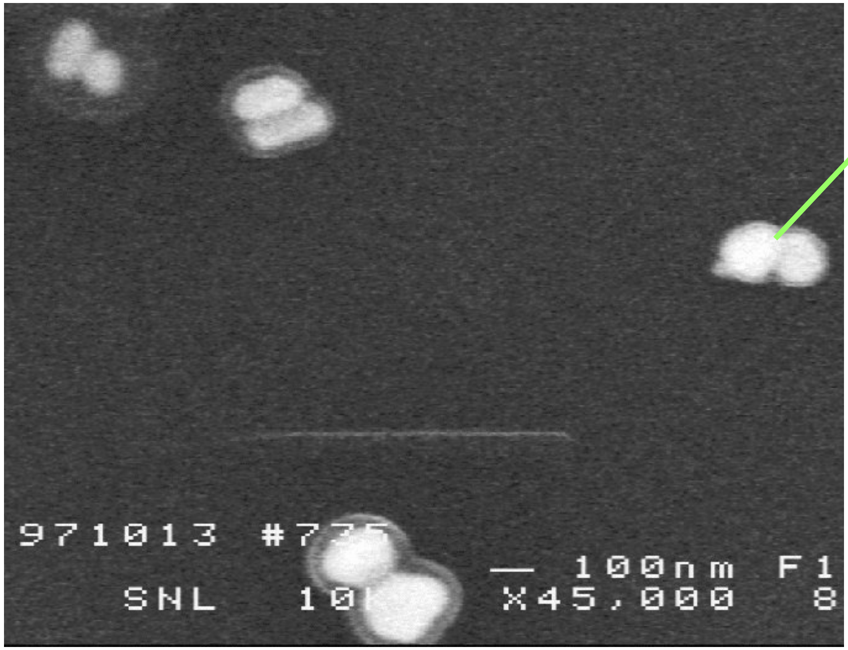

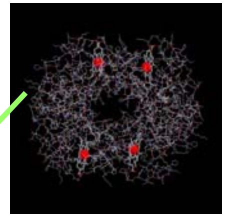

- Ag sol mixed with 10^{-11}M Hb
  Hb / Ag particles ~ 1:4
- Ag dimers can be observed, which is most likely connected by Hb

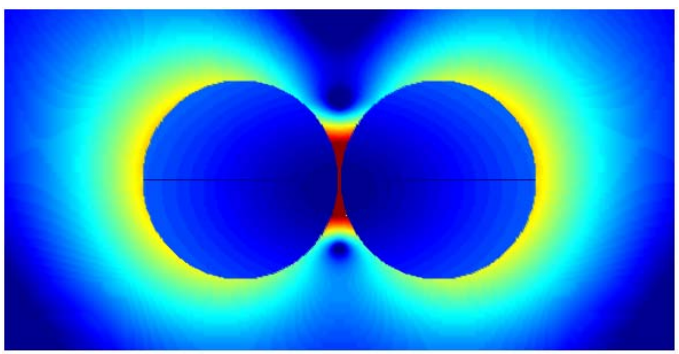

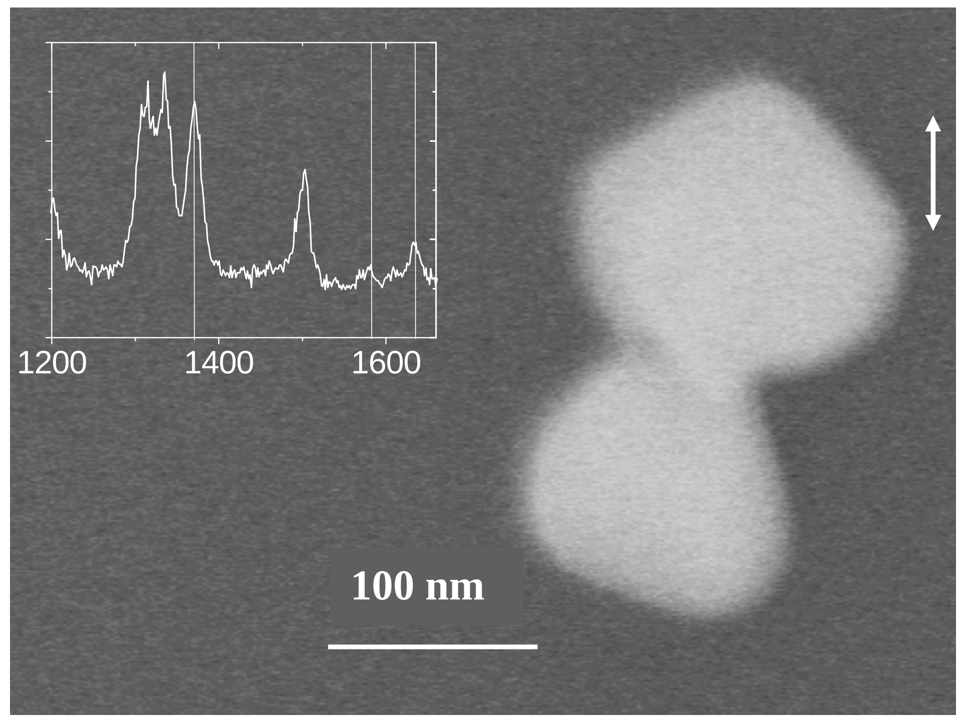

Xu *et al*. PRL **83** 4357 (1999)
&
Xu &Aizpurua et al. PRE **62** 4318 (2000)

Plasmon optical forces

Plasmochemistry

Dimer Antenna

Receival Antenna ($|E/E_0|^2$)

Emission Antenna ($|E/E_0|^2$)

Plasmon hybrization

Quantum plasmon (coupling)

Nanogap/Hot spot … for SERS

Nonlinear plasmonic effects

The base of many directions in plasmonics

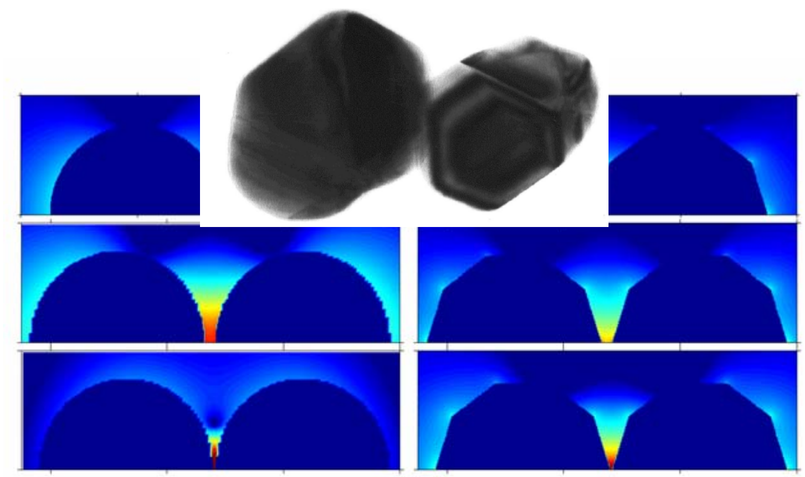

Xu *et al*. PRL **83** 4357 (1999); Xu &Aizpurua et al. PRE **62** 4318 (2000)

Remote-Excitation Raman Using Propagating Surface Plasmons

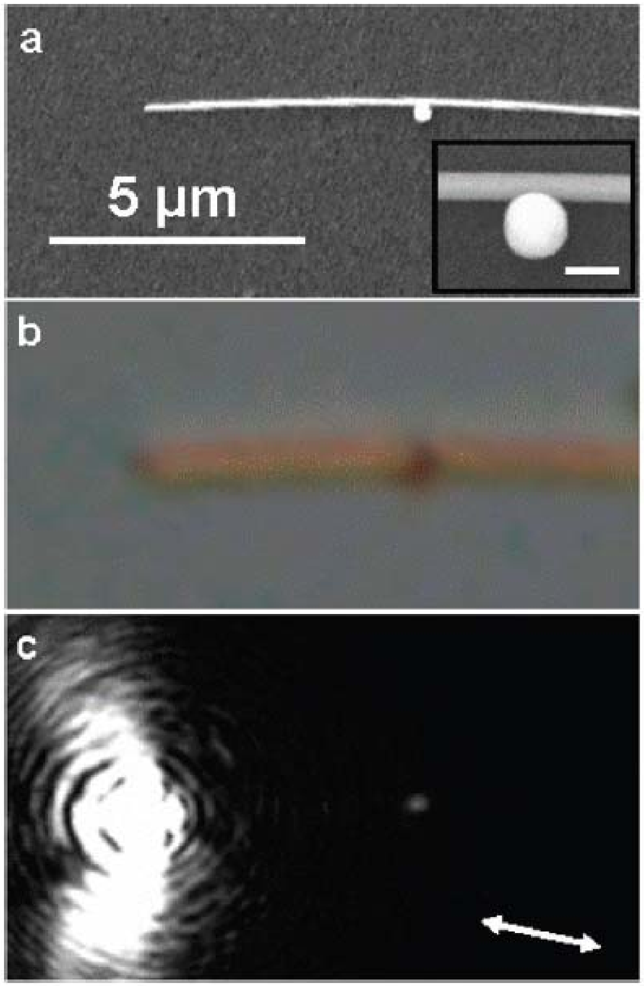

Fang&Wei et al, Nano Lett. 9, 2049 (2009)

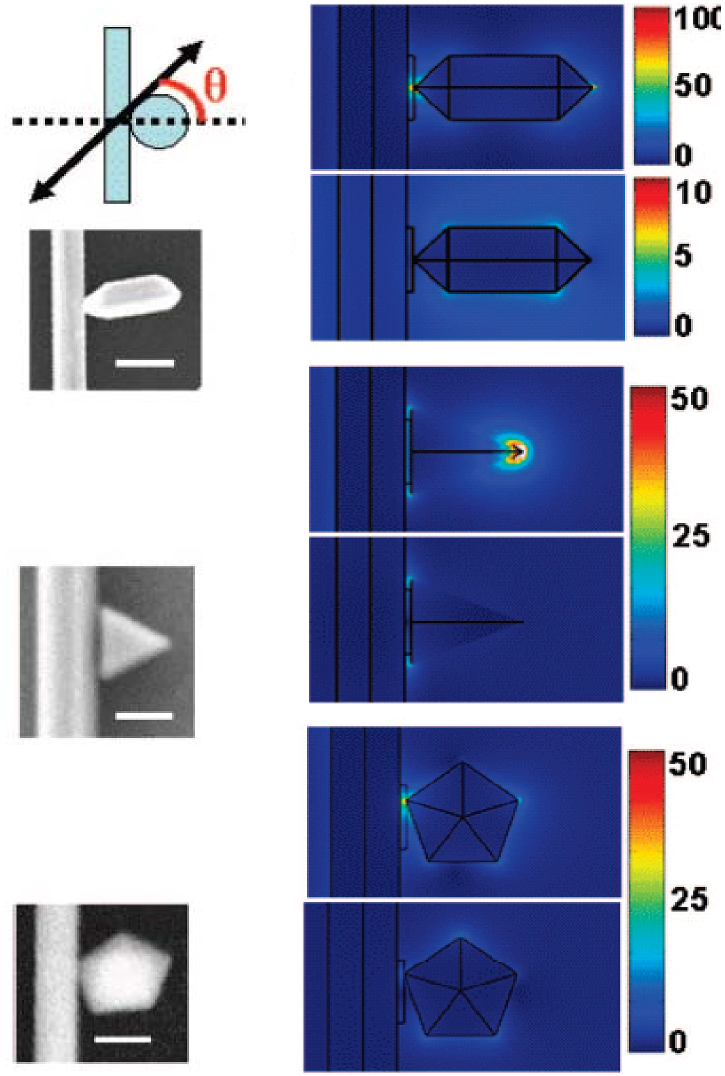

Wei et al., Nano Lett., 8, 2497, 2008

Remote-Excitation Raman Using Propagating Surface Plasmons

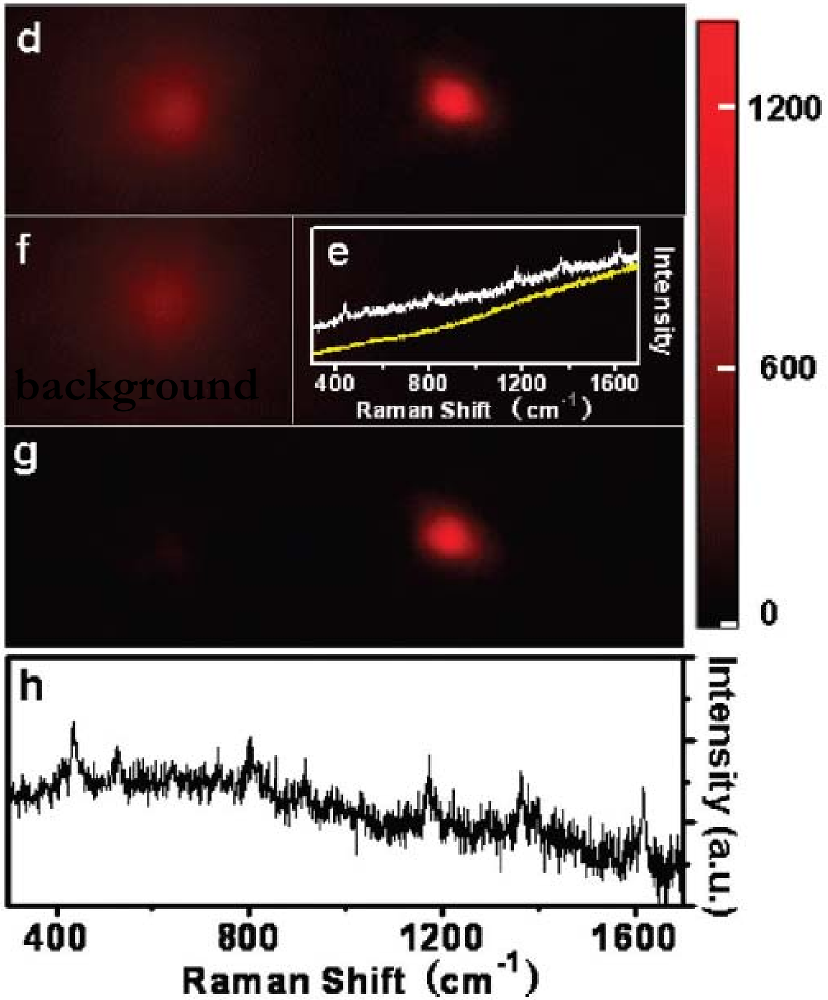

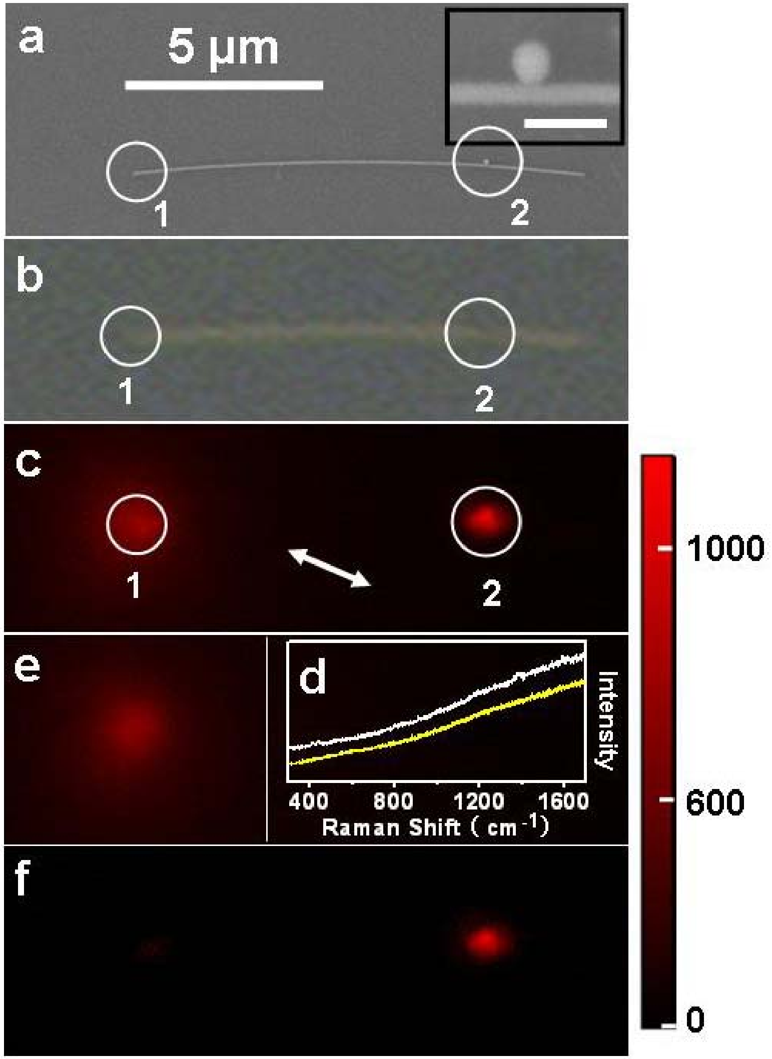

Raman spectra of
malachite green isothiocyanate
(MGITC)

Fang&Wei et al, Nano Lett. 9, 2049 (2009)

Remote-Excitation Raman Using Propagating Surface Plasmons

Finite Element Method COMSOL

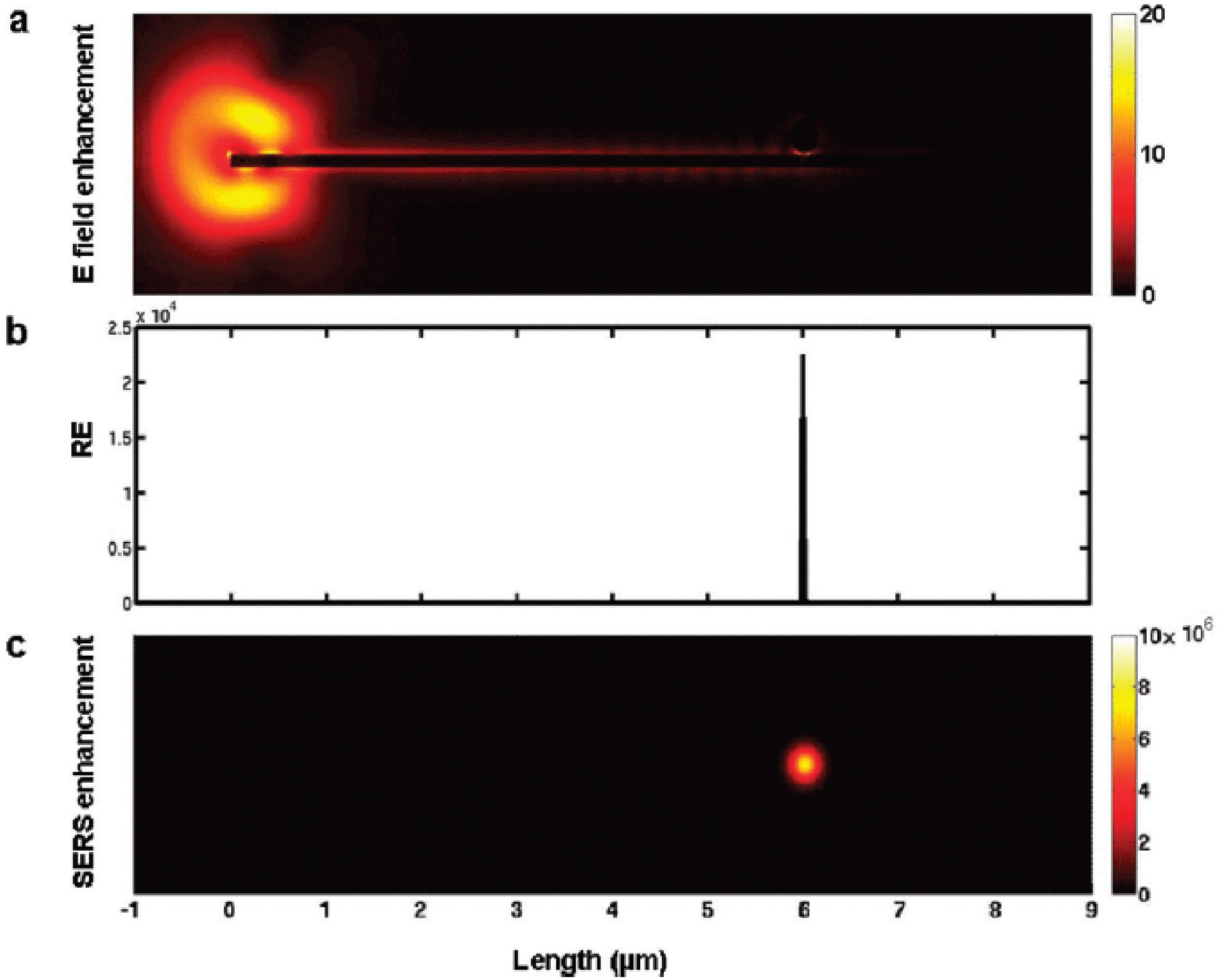

Fang&Wei et al, Nano Lett. 9, 2049 (2009)

Remote-Excitation Raman Using Propagating Surface Plasmons

Advantages of Remote sensing for SERS

- ***Nano light source***
- ***Background free***
- ***Low damage***

Nano Lett. 9, 2049 (2009)

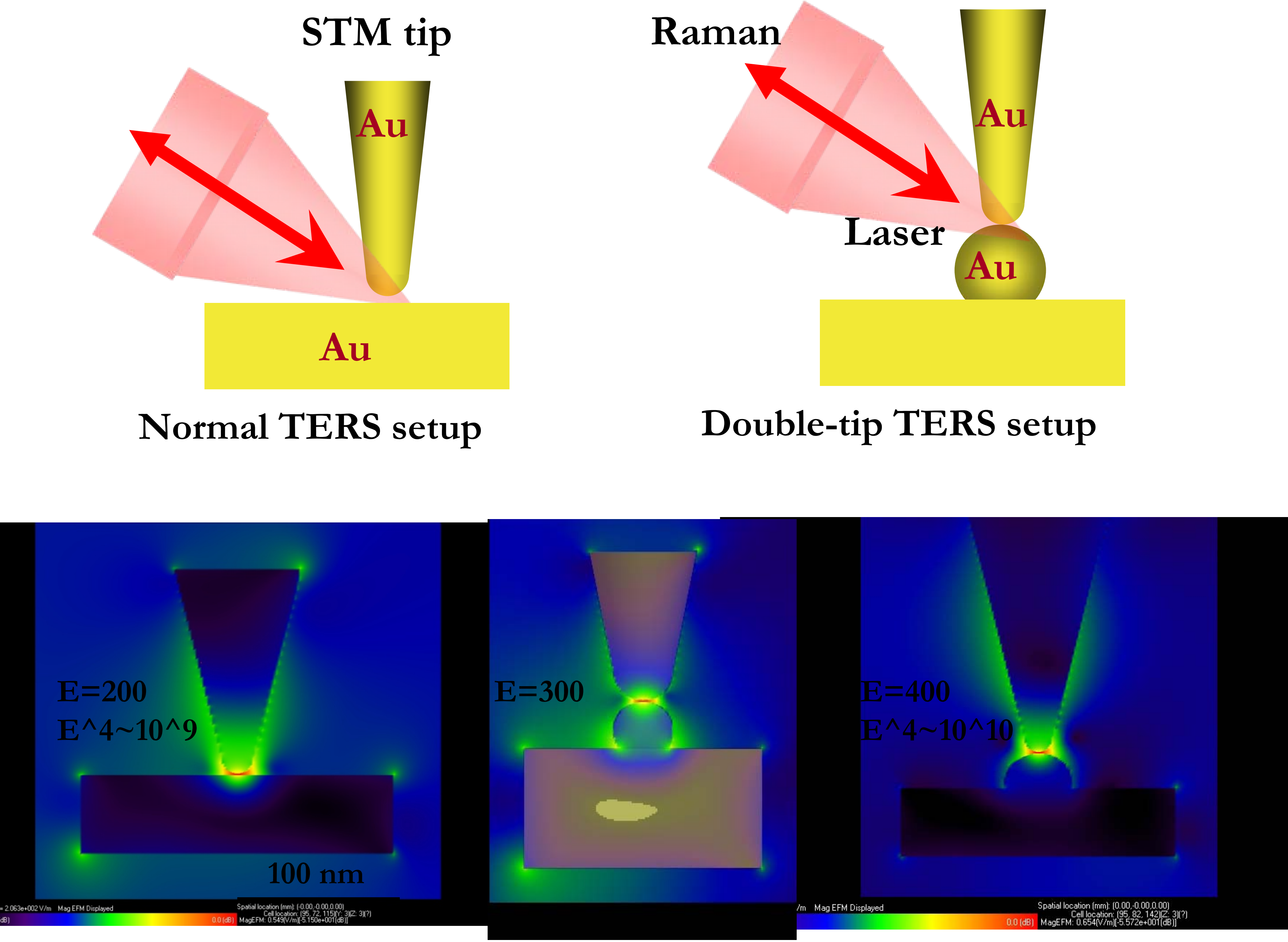
STM tip
Au
Au
Normal TERS setup
Raman
Au
Laser
Au
Double-tip TERS setup
E=200
E^4~10^9
100 nm
E=300
E=400
E^4~10^10
Mag EFM Displayed

Plasmon-Assisted Chemical Reactions

Surface catalyzed reaction of PATP dimerizing to DMAB

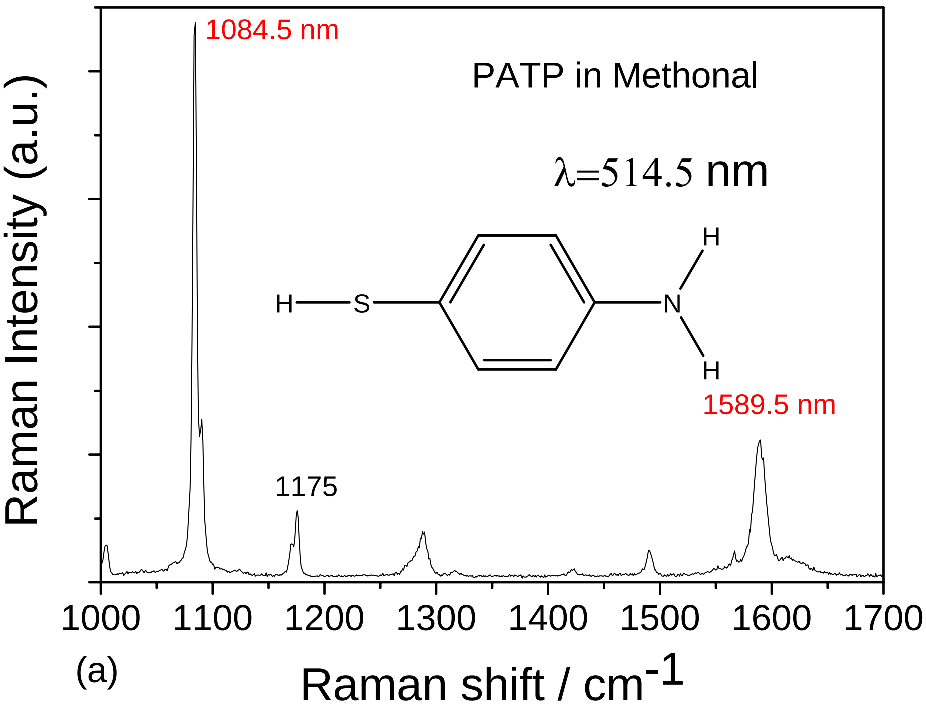

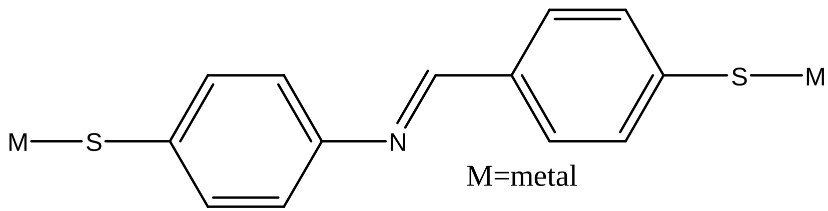

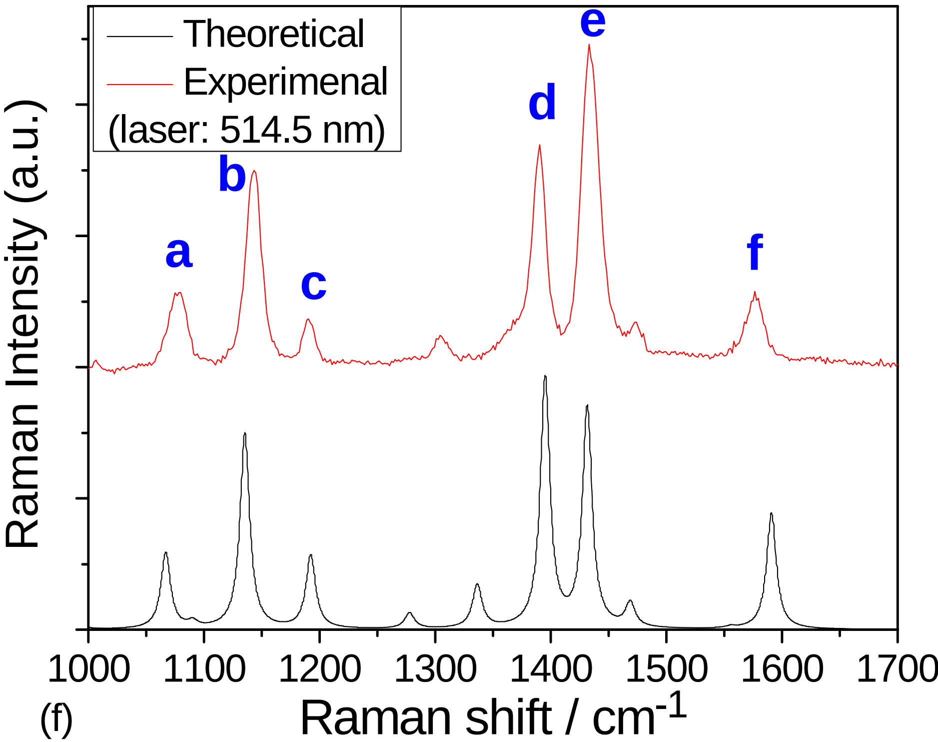

Fang et al., *Langmuir* **2010**, *26*, 7737.

Mechanism of surface catalyzed reaction

Hot electrons?

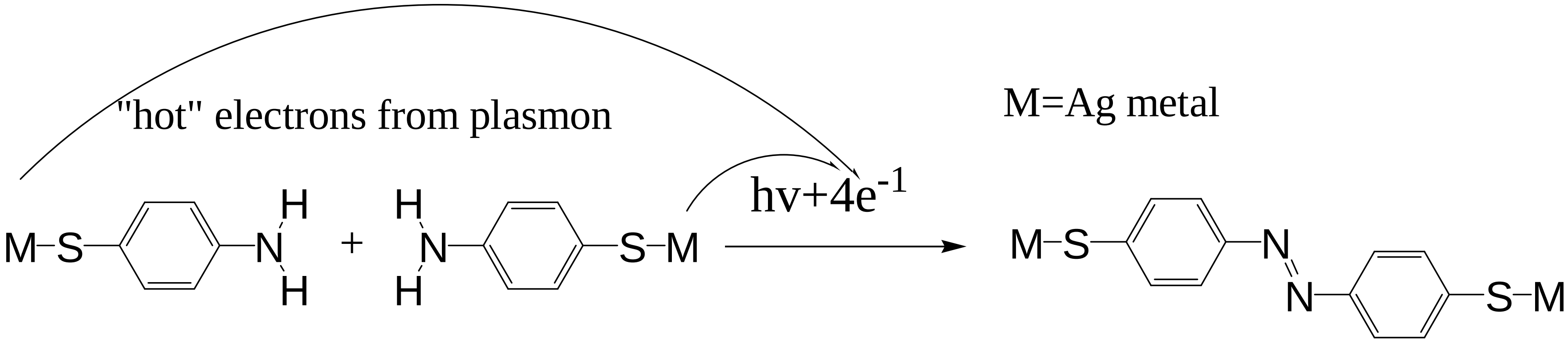

Scheme 1. The mechanism of plasmon-assisted surface catalyzed reaction.

The pH-controlled plasmon-assisted surface catalyzed reaction

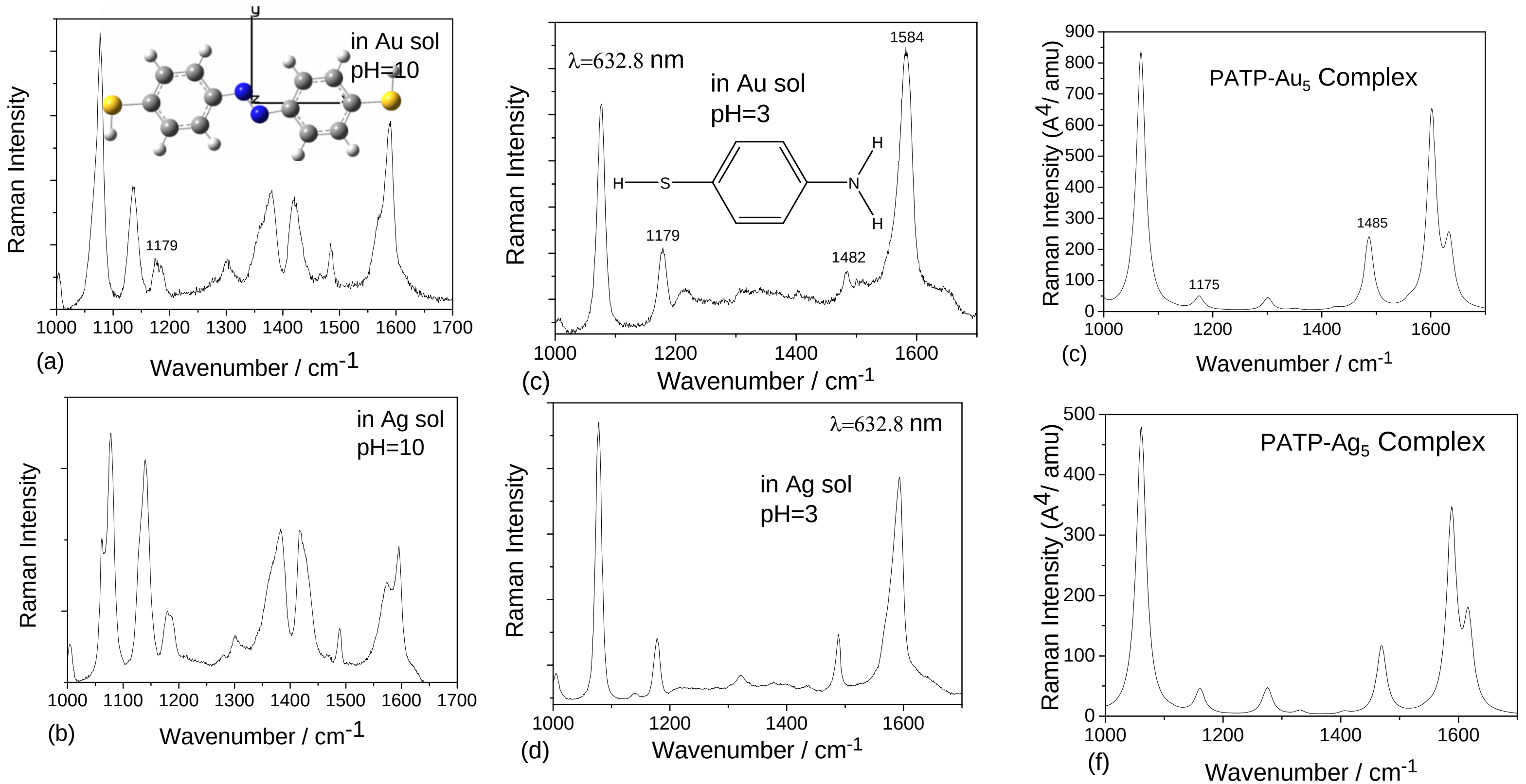

Sun, M. T. and H. X. Xu, *J. Phys. Chem. C*, ***2011***, *115*,*9629*.

Remote-excitation surface catalyzed reaction by plasmonic waveguide

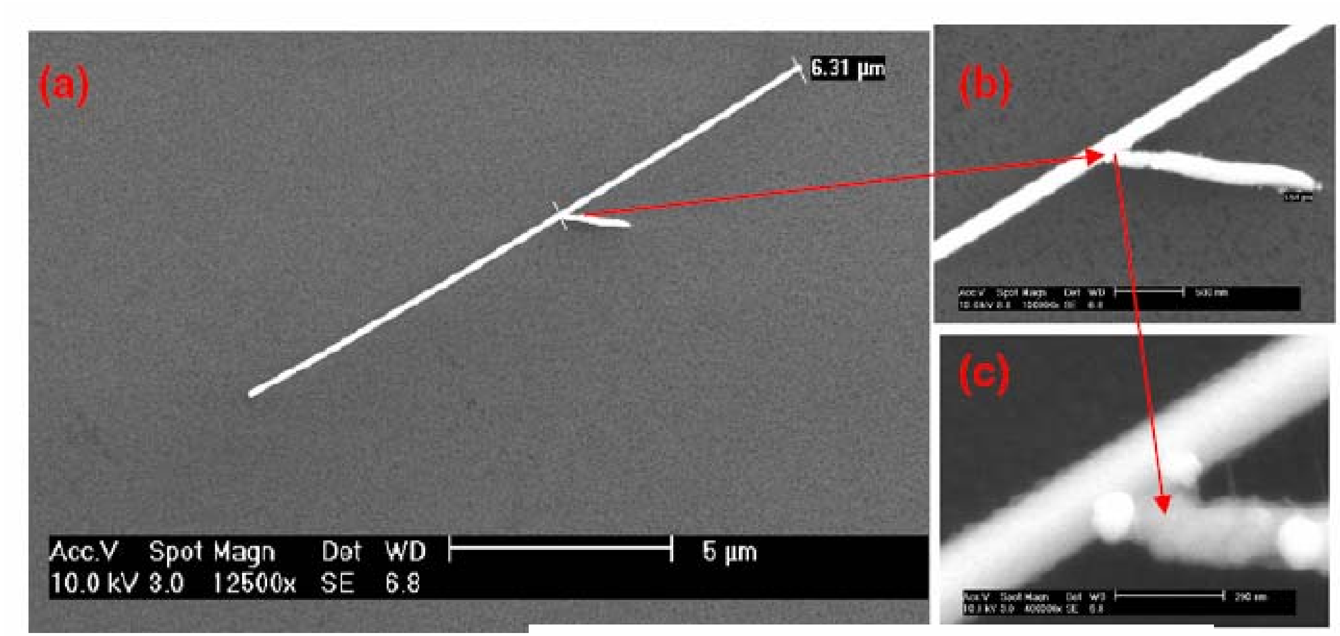

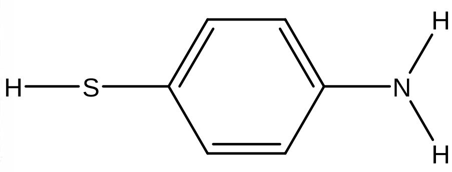

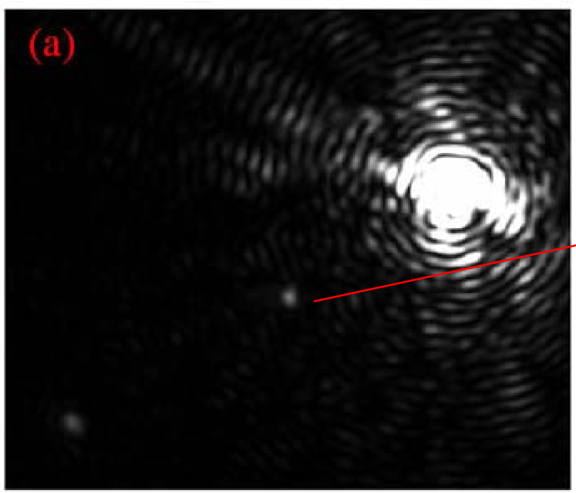

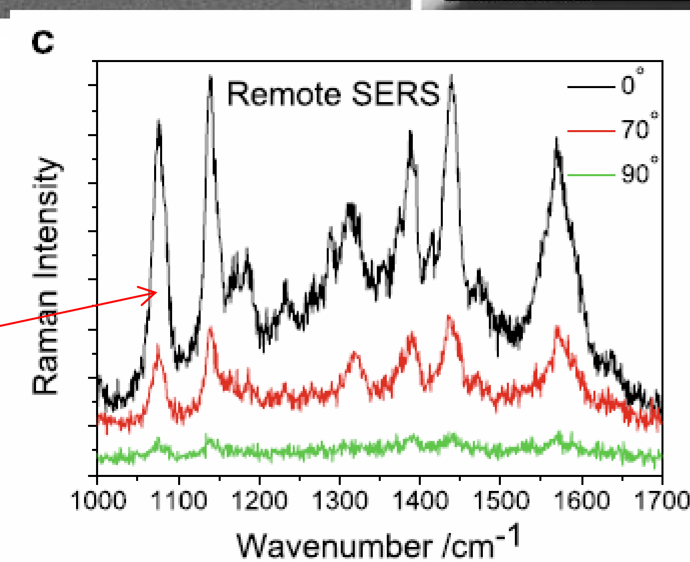

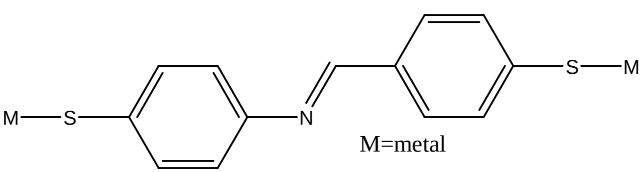

Plasmonics, 6, 681 (2011)

surface catalyzed reaction of 4NBT dimerizing to DMAB

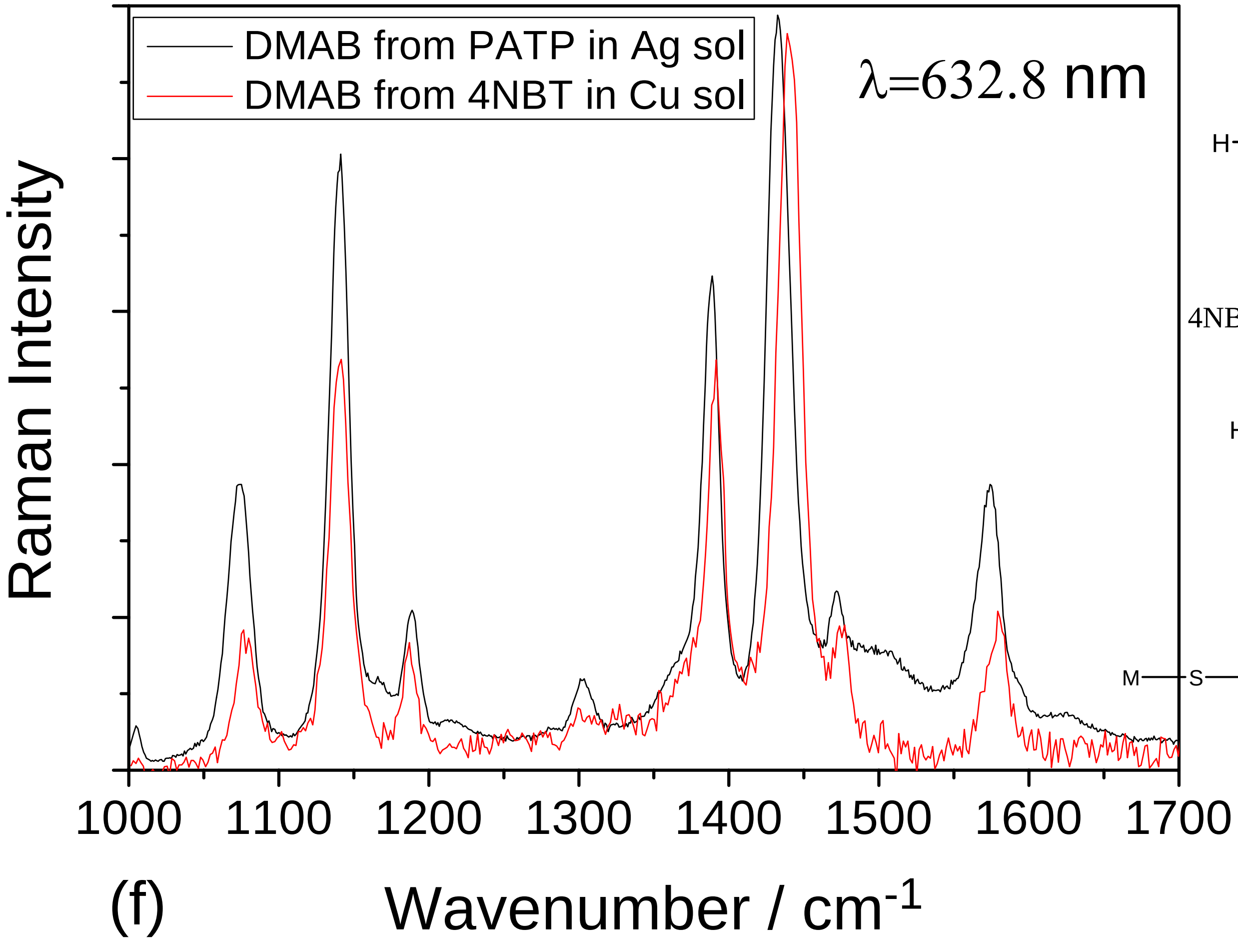

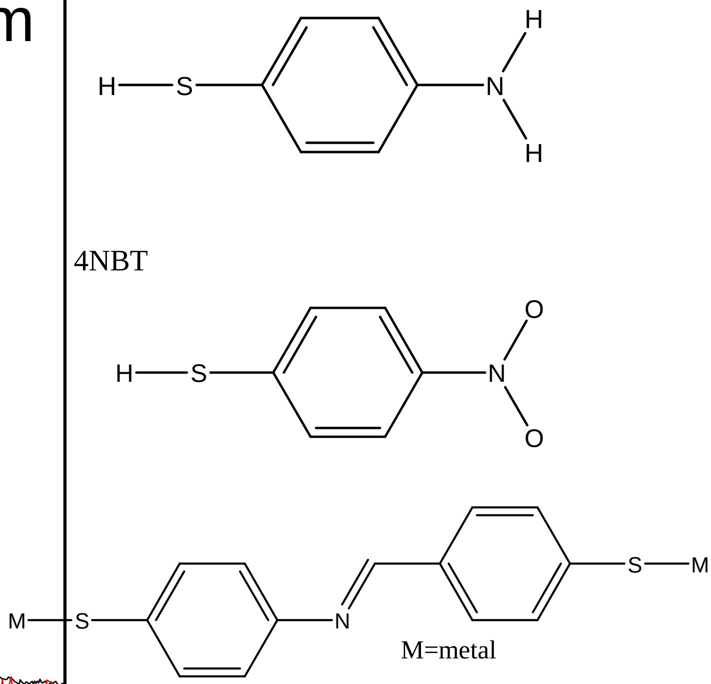

J. Raman Spectroscopy, 2011, 42, 1205.

Controlling such chemical reaction

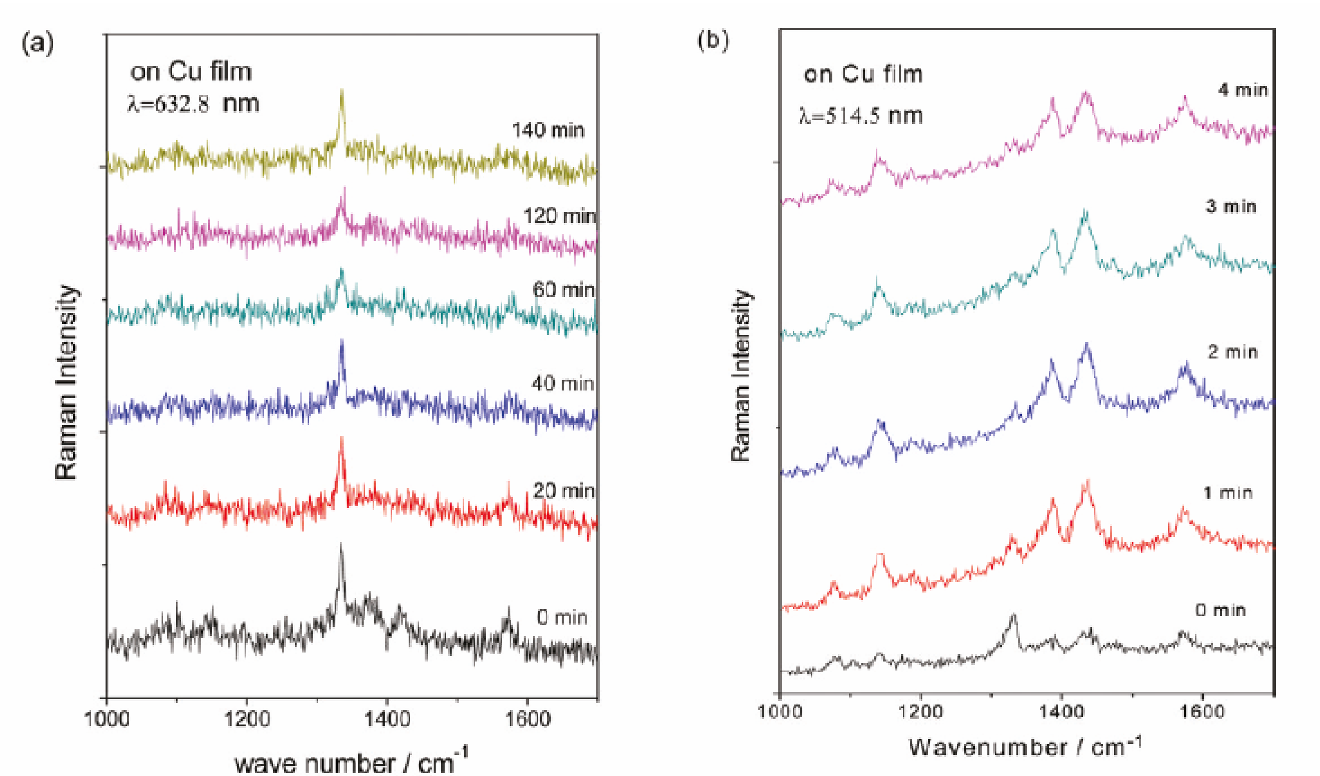

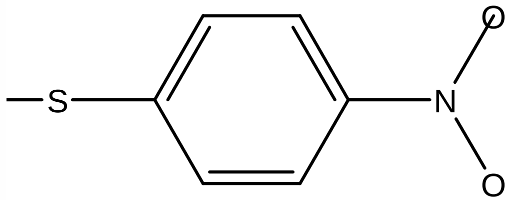

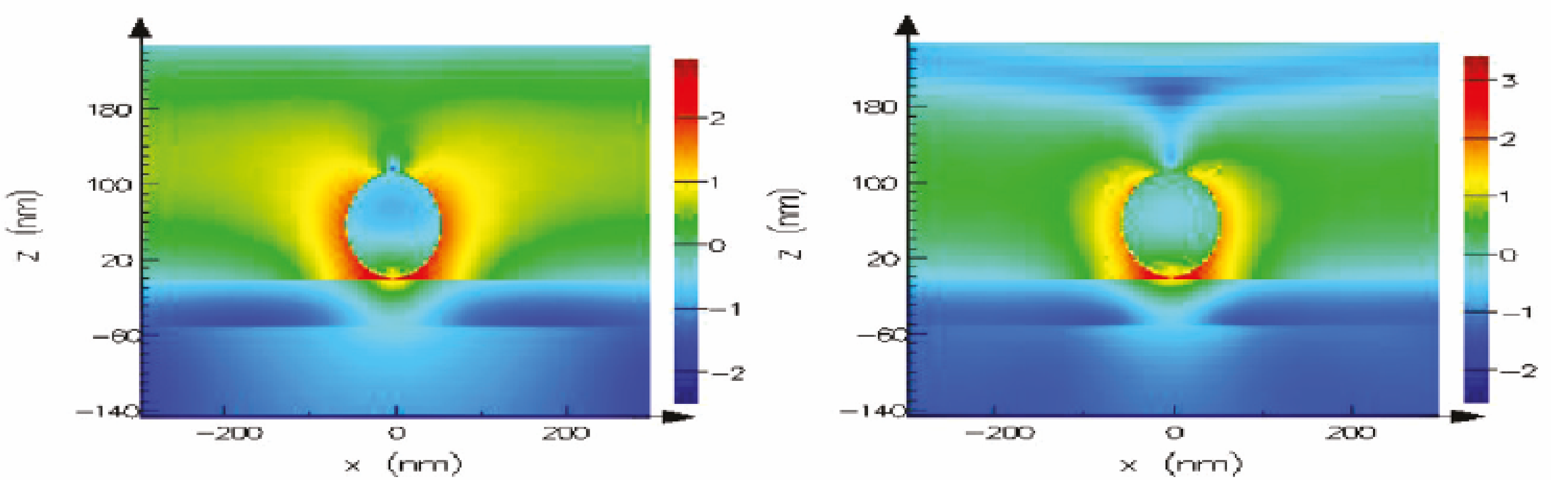

surface catalyzed reaction in Ag nanoparticle- molecule-Ag/Au films

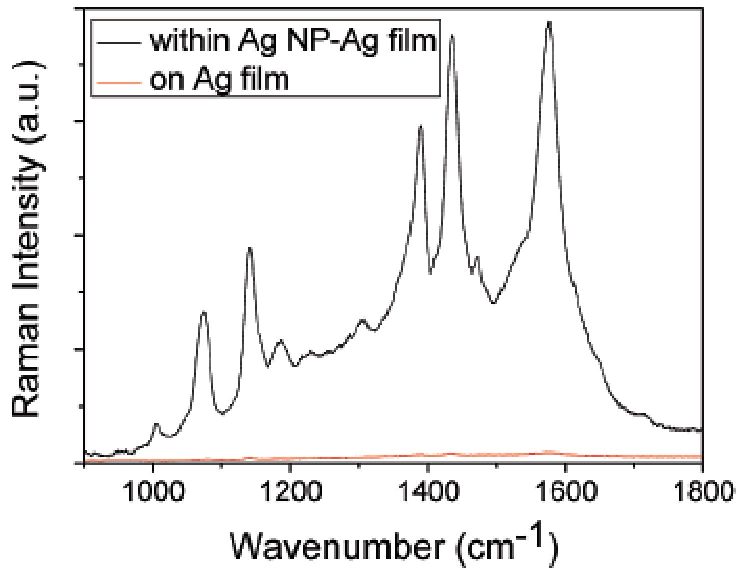

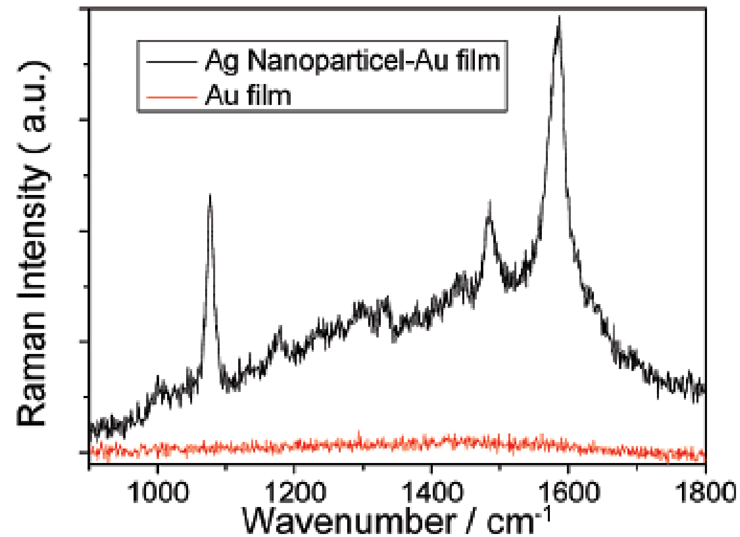

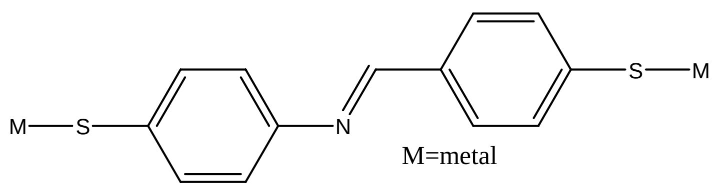

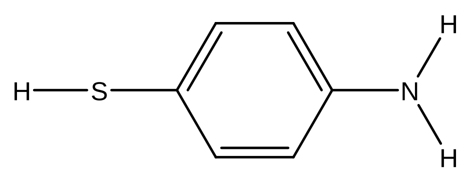

Huang et al., J. Phys. Chem. C **2010,** *114*, 18263

From Plasmon Chemical Reactions to

Surface catalyzed reaction on Au film in HV-TERS

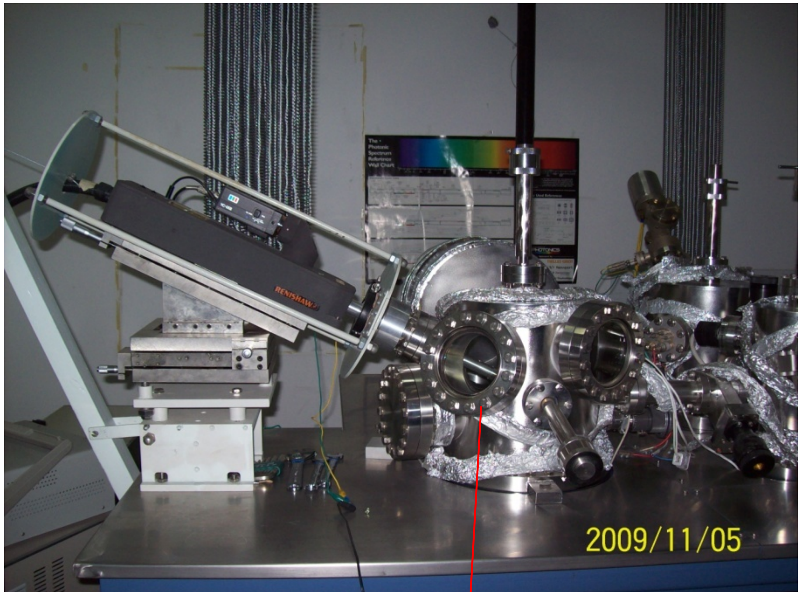

Institute of Physics, CAS

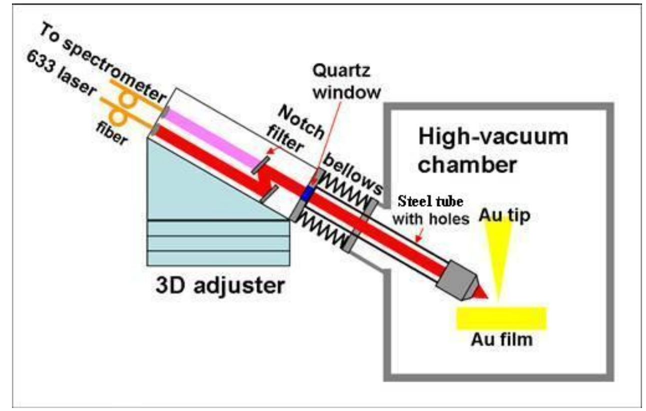

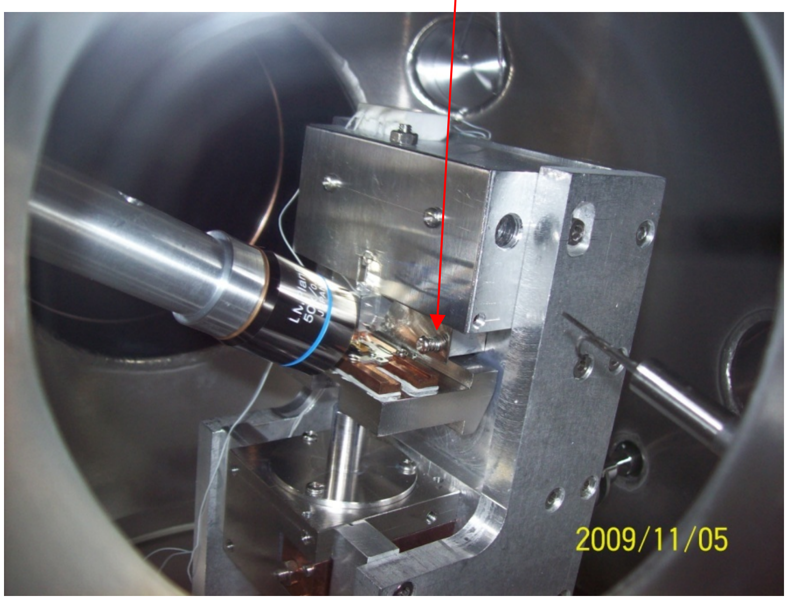

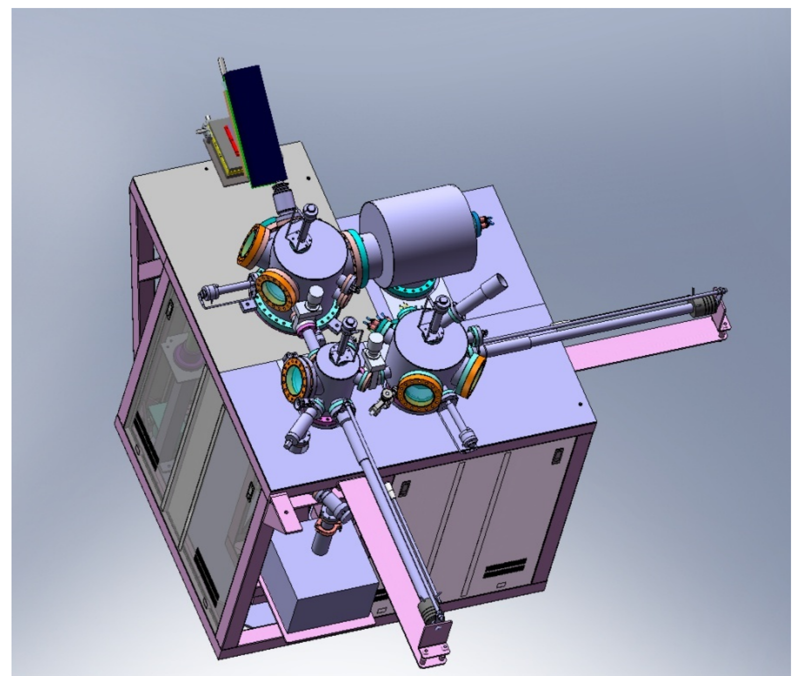

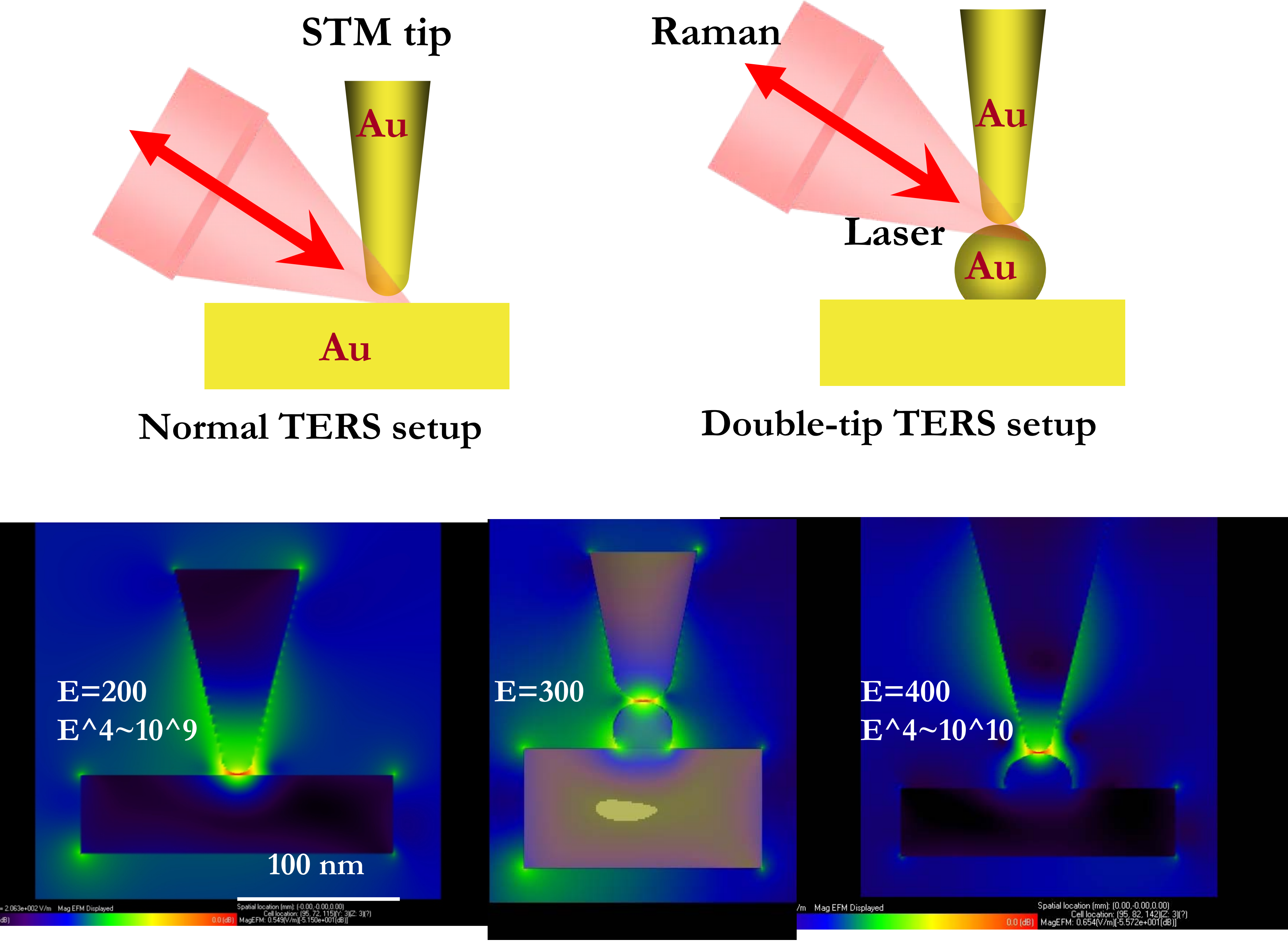
STM tip
Au
Au
Normal TERS setup
Raman
Laser
Au
Au
Double-tip TERS setup
E=200
E^4~10^9
100 nm
E=300
E=400
E^4~10^10
Mag EFM Displayed
Mag EFM Displayed

Plasmon-driven chemical reaction on Silver film

Motivations:
Capturing "hot" electrons in HV-TERS

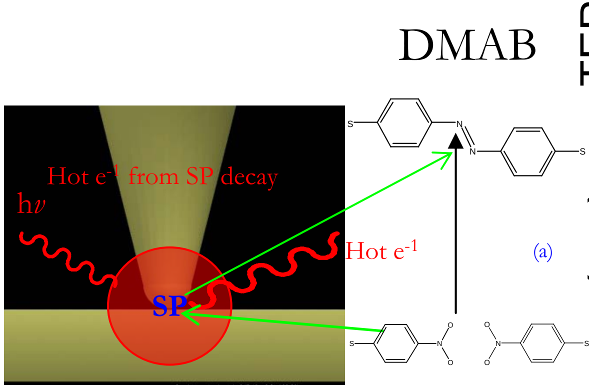

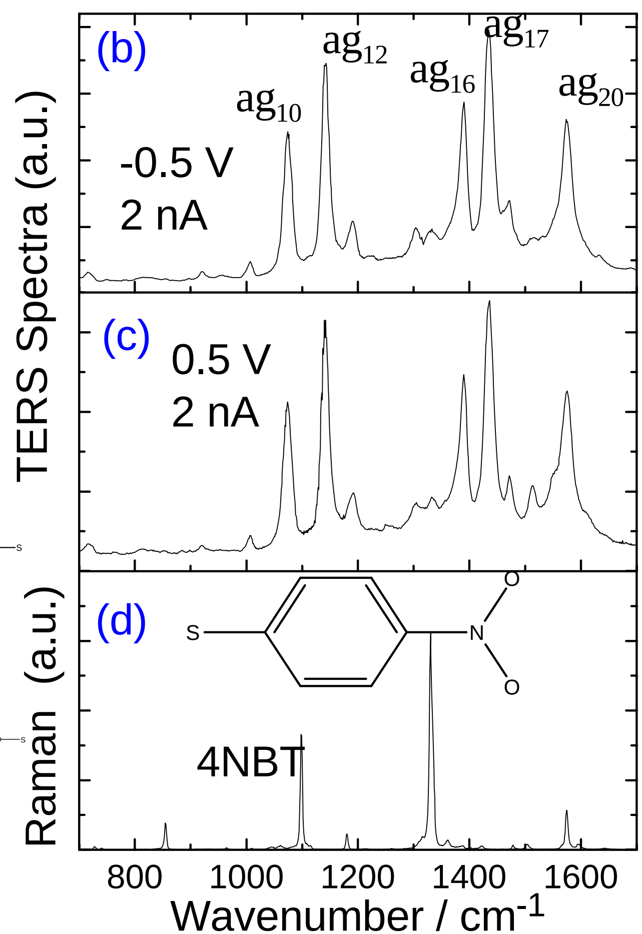

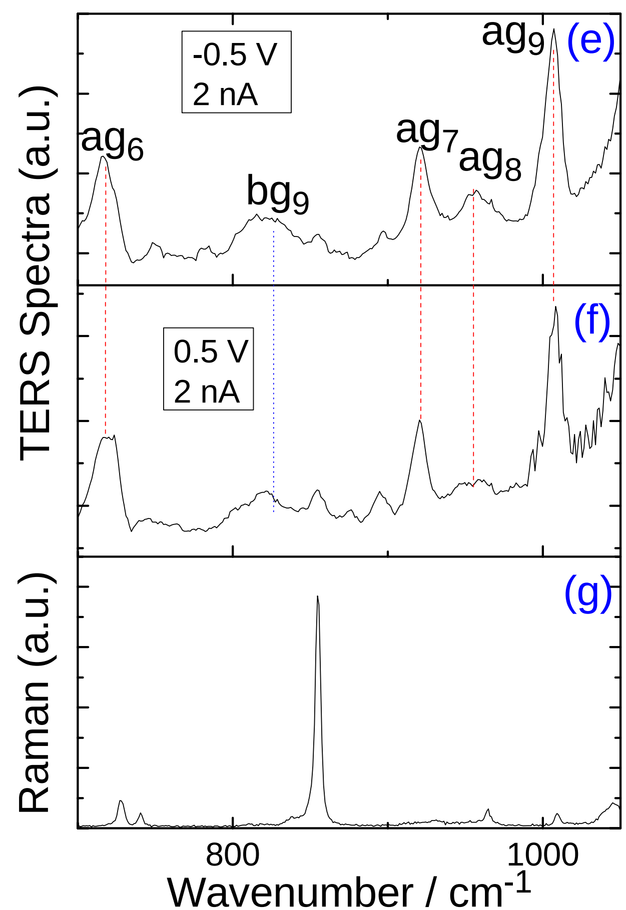

Controlled dynamics of chemical reaction

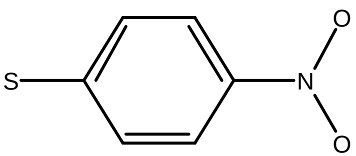

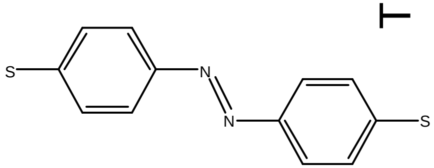

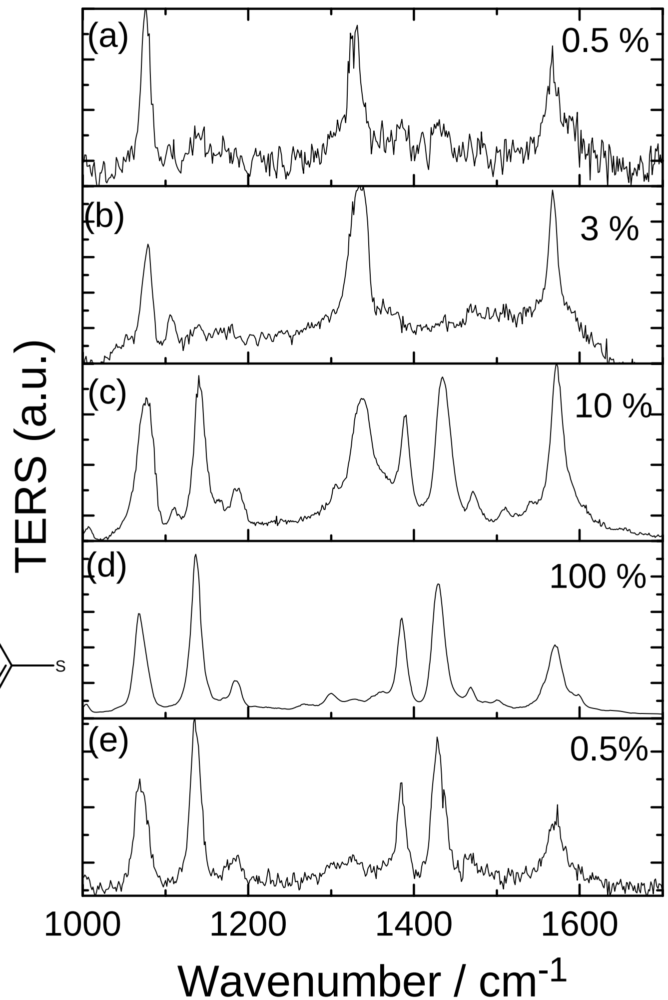

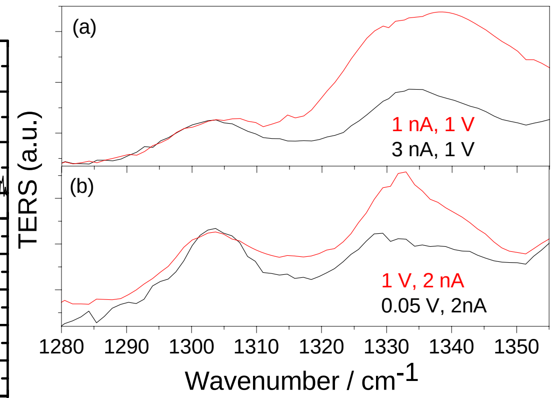

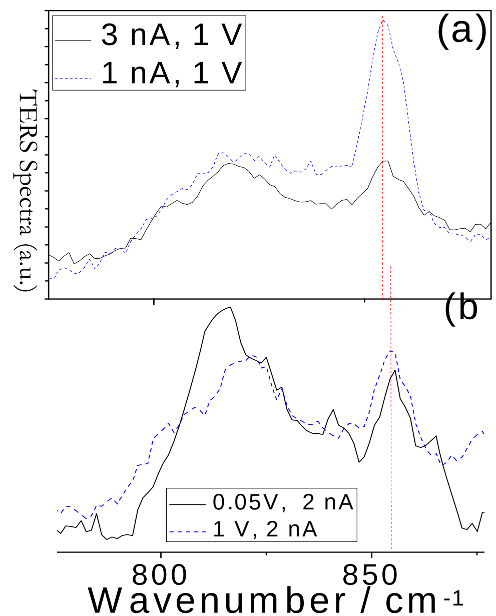

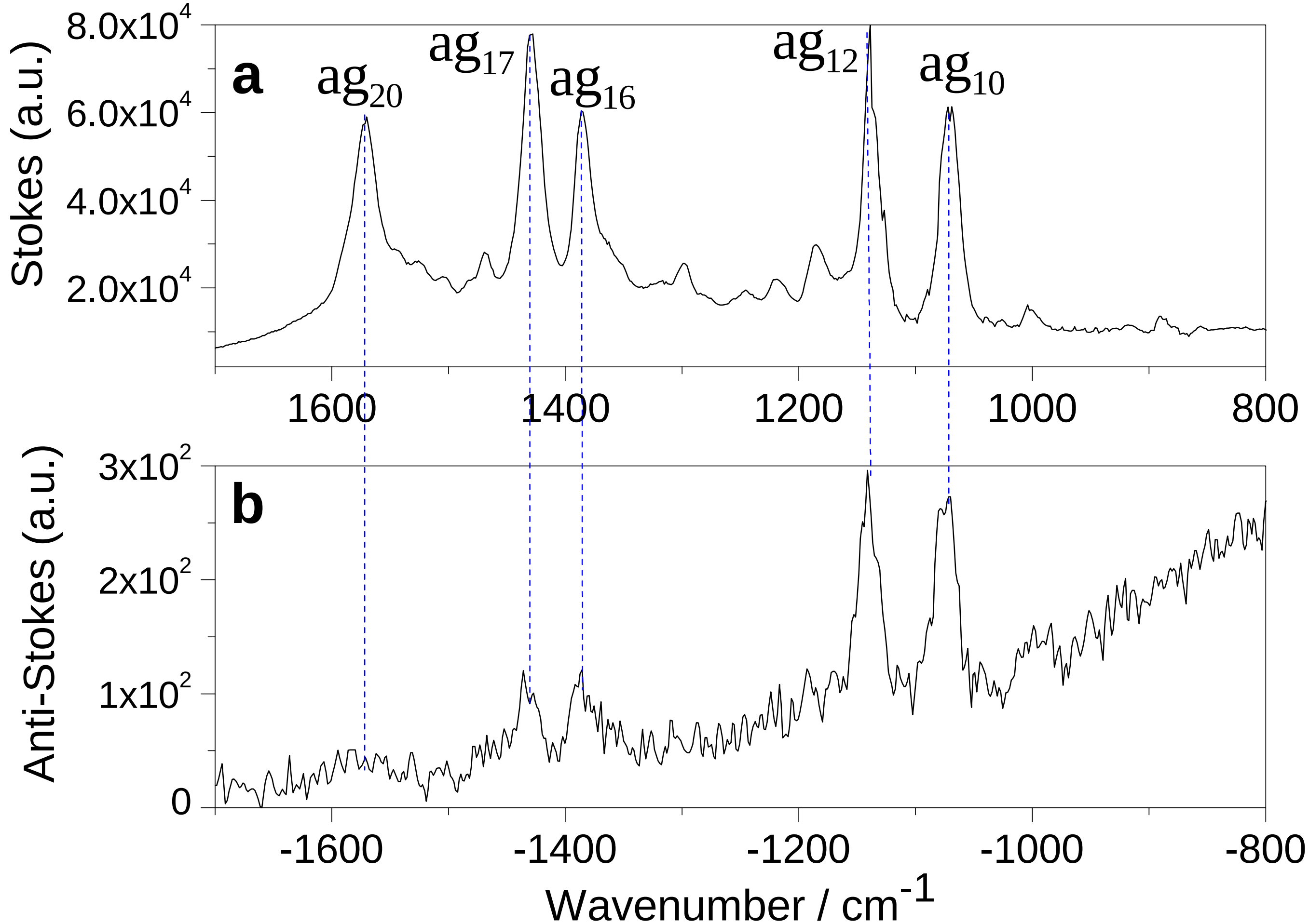

$$I_s / I_{as} = a \times e^{(\eta\omega / k_B T)}$$

T ~ 327 *K*

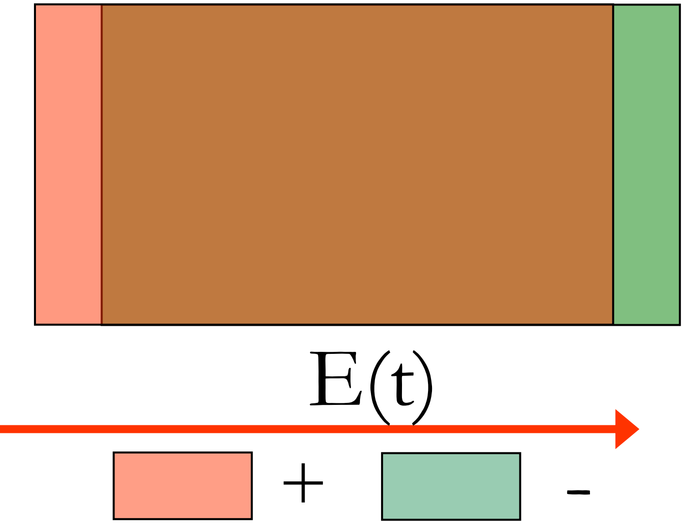

Hot-electrons

Laser/Plasmon

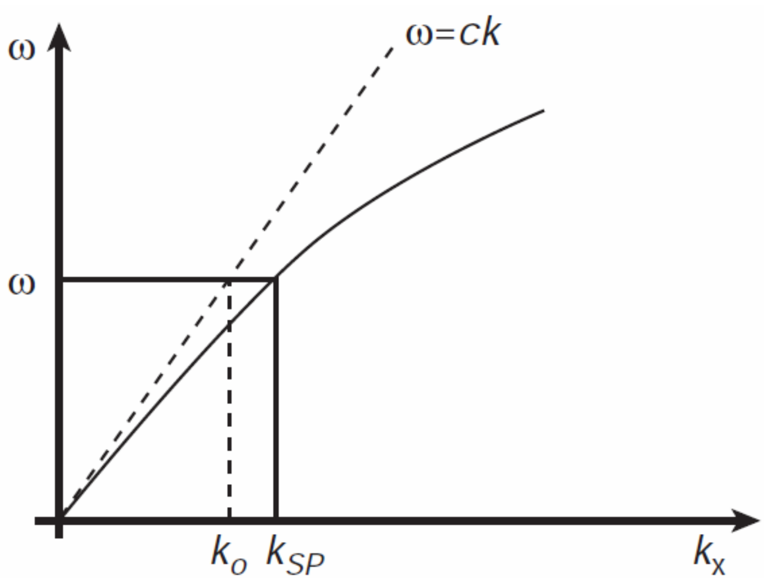

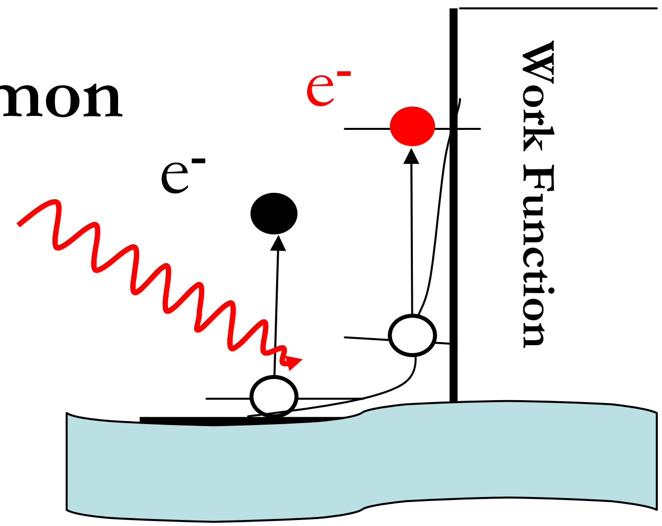

Plasmon Sea

$$N\_e \propto \exp(E^2)*\exp(E\_photon)/\exp(V\_work))$$

PATP

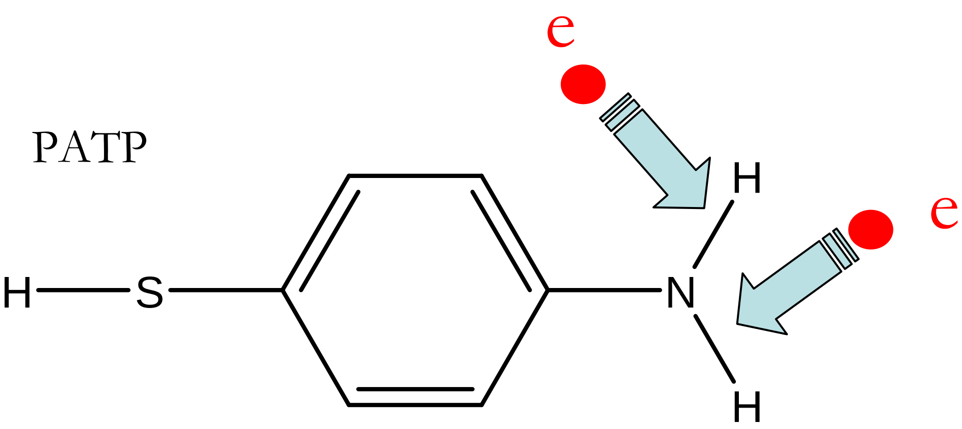

4NBT

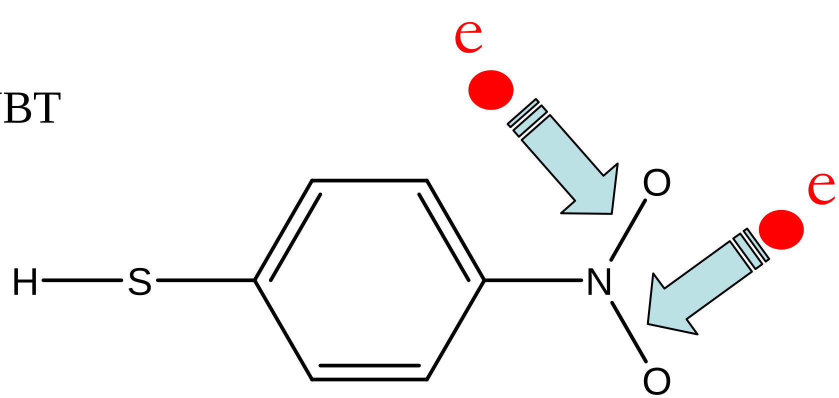

DMAB

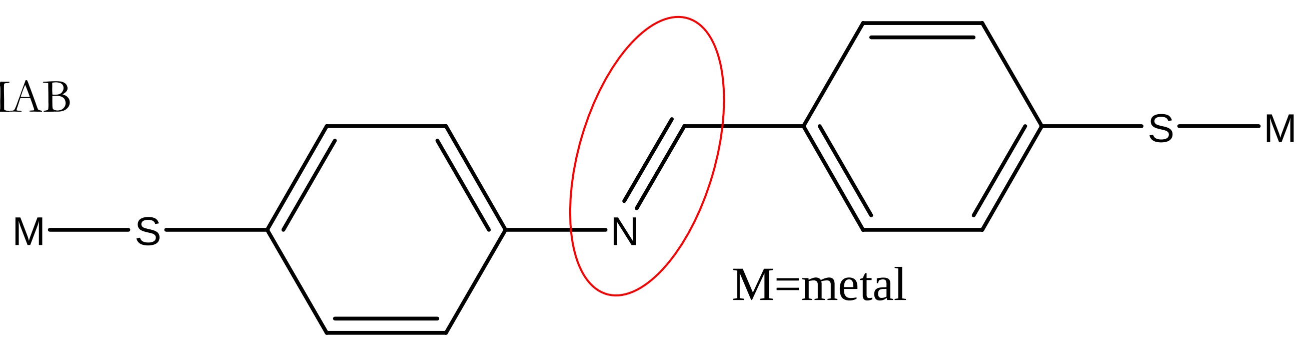

More complex chemical reactions on Au film?

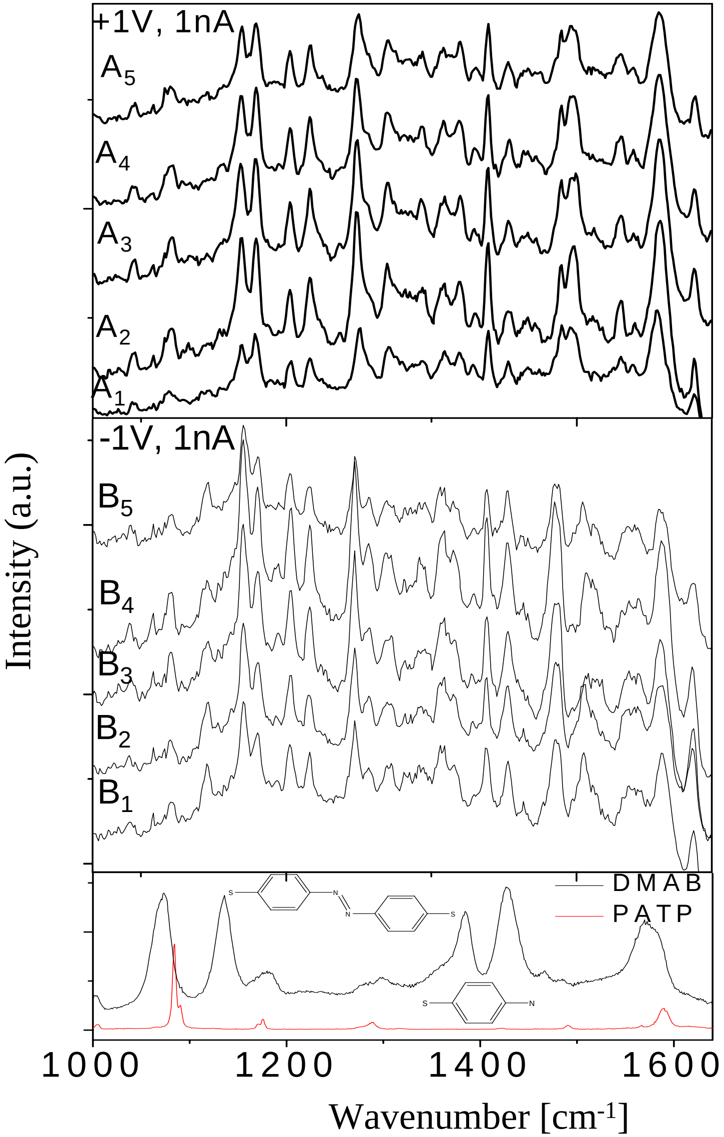

Fluctuation is weak

HV-TERS spectra is quilt different from SERS spectra of DMAB and NRS spectrum PATP powder

First conclusion:
Surface catalyzed reaction occurred on Au film, because above spectra

Why are they different ?
Produced new molecules (not DMAB)?

M. T. Sun, Y. Fang, Z. Y Zhang, H. X. Xu, **Activated Vibrational Modes and Fermi Resonance in Tip-Enhanced Raman Spectroscopy,** Submitted.

Assignment of HV-TERS spectra

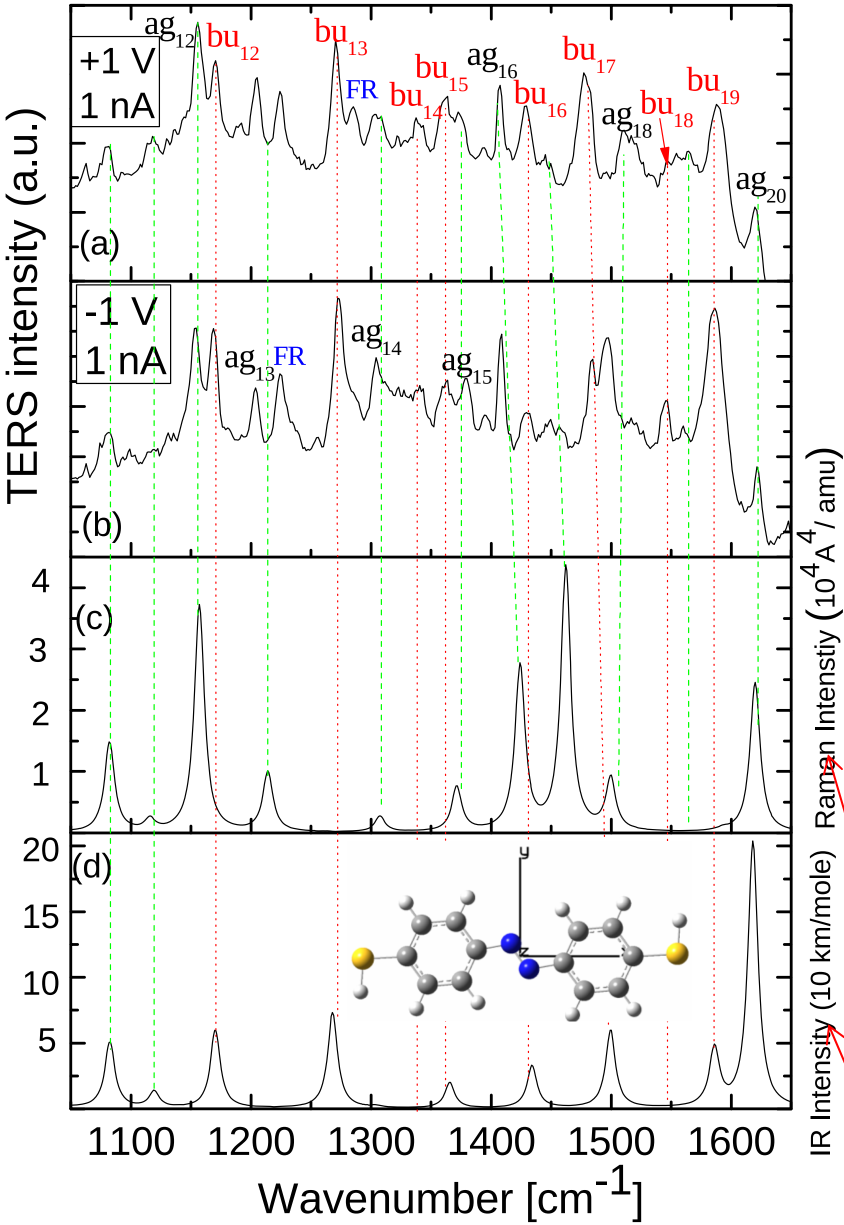

(a) and (b) HV-TERS spectra of DMAB
(c) Simulated Raman spectra
(d) Simulated IR spectra of DMAB.

VOLUME 85, NUMBER 19 PHYSICAL REVIEW LETTERS 6 NOVEMBER 2000

Electric Field Gradient Effects in Raman Spectroscopy

E. J. Ayars and H. D. Hallen
Physics Department, North Carolina State University, Raleigh, North Carolina 27695-8202

C. L. Jahncke
Physics Department, St. Lawrence University, Canton, New York 13617
(Received 15 February 2000)

Raman spectra of materials subject to strong electric field gradients, such as those present near a metal surface, can show significantly altered selection rules. We describe a new mechanism by which the field gradients can produce Raman-like lines. We develop a theoretical model for this "gradient-field Raman" effect, discuss selection rules, and compare to other mechanisms that produce Raman-like lines in the presence of strong field gradients. The mechanism can explain the origin and intensity of some Raman modes observed in SERS and through a near-field optical microscope (NSOM-Raman).

PACS numbers: 78.30.–j, 33.20.Fb, 78.66.Vs, 82.80.Ch

It was theoretically predicted that Raman-active and IR active modes could be observed simultaneously due to the enhanced electric field gradient effect in the nanocavity between tip and surface.

Our HV-TERS spectra realized their theoretical prediction 10 years ago

Electric field intensity and gradient

▪

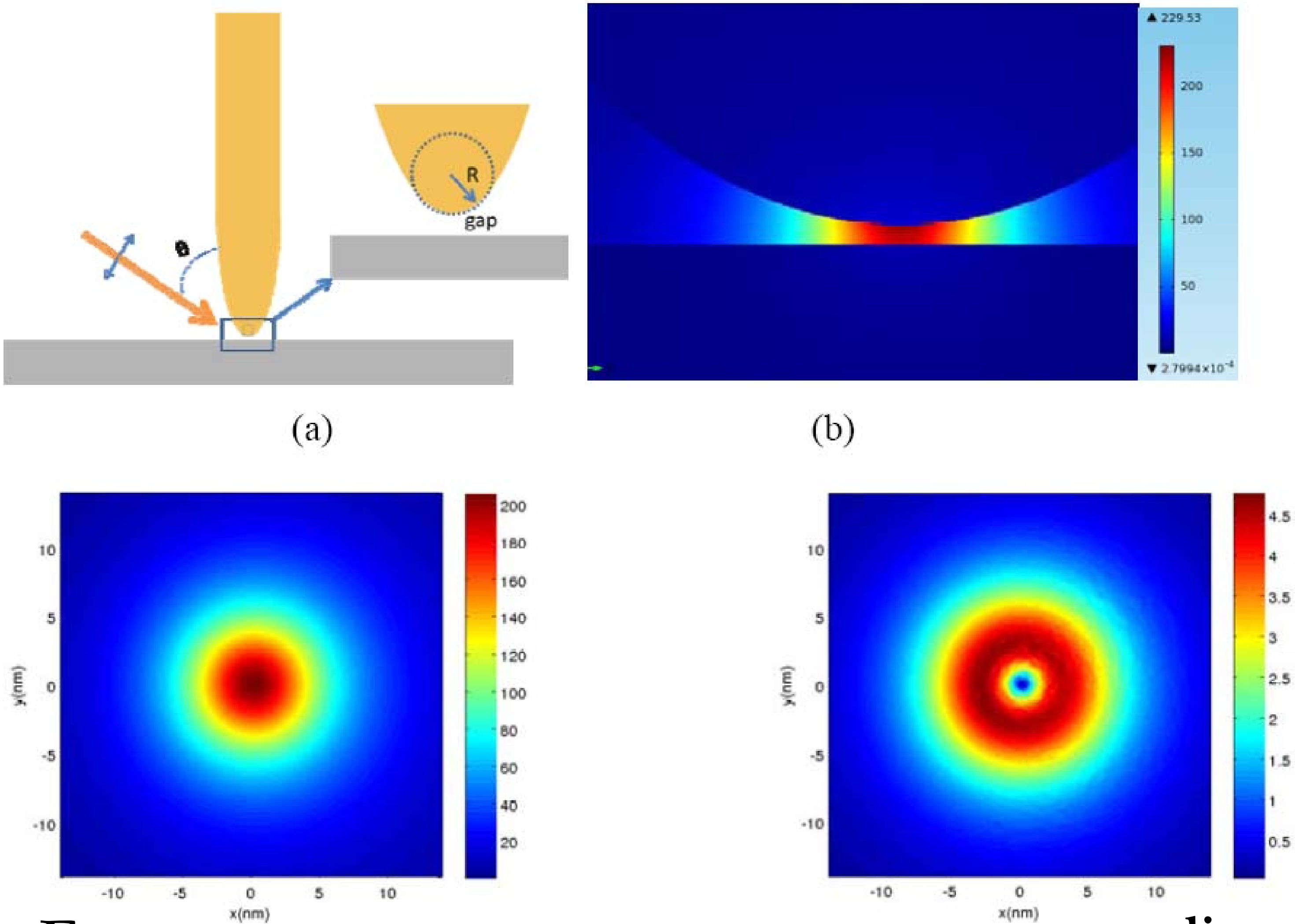

(a) (b)

Ez

gradient

(c) (d)

Electric field gradient effect

$$\mu_\alpha = \alpha_{\alpha\beta} E_\beta + \frac{1}{3} \mathrm{A}_{\alpha\beta\gamma} \frac{\partial E_\beta}{\partial r} + \Lambda$$

$$\alpha_{\alpha\beta} = \sum_j H(\omega) \left(\langle i | \mu_\alpha | j \rangle \langle j | \mu_\beta | f \rangle \right) / \eta.$$

$$A_{\alpha\beta\gamma} = \sum_j H(\omega) \left(\langle i | \mu_\alpha | j \rangle \langle j | \theta_{\beta\gamma} | f \rangle \right) / \eta$$

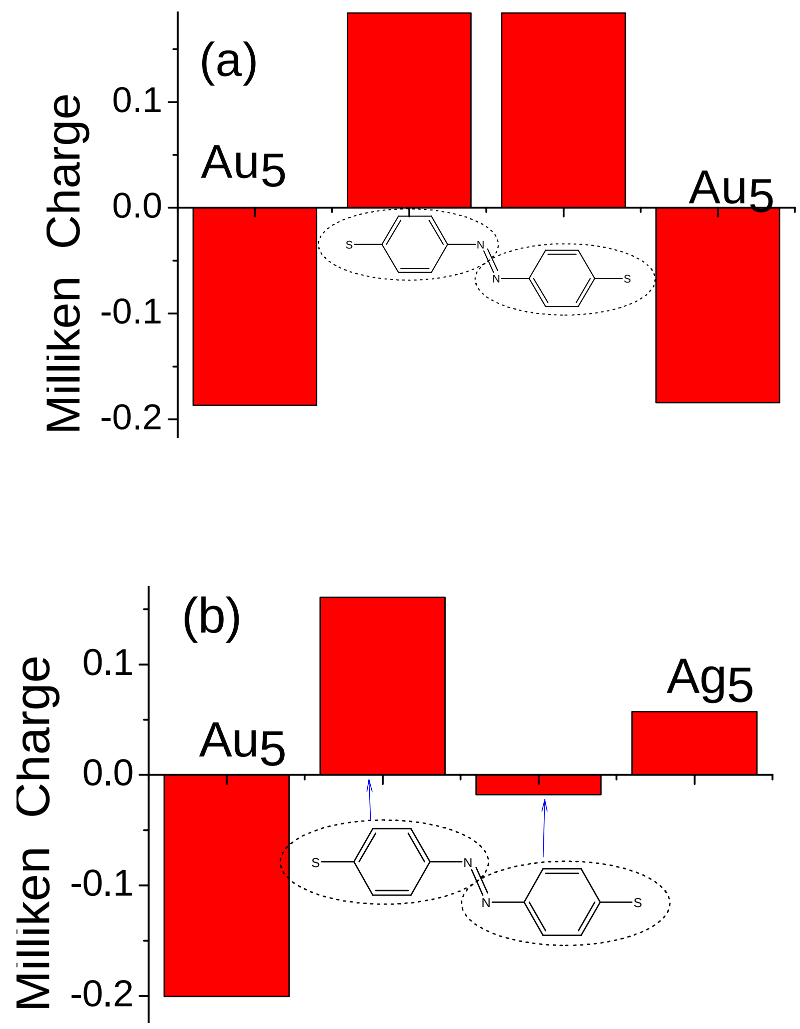

Additional peaks ? Why ?

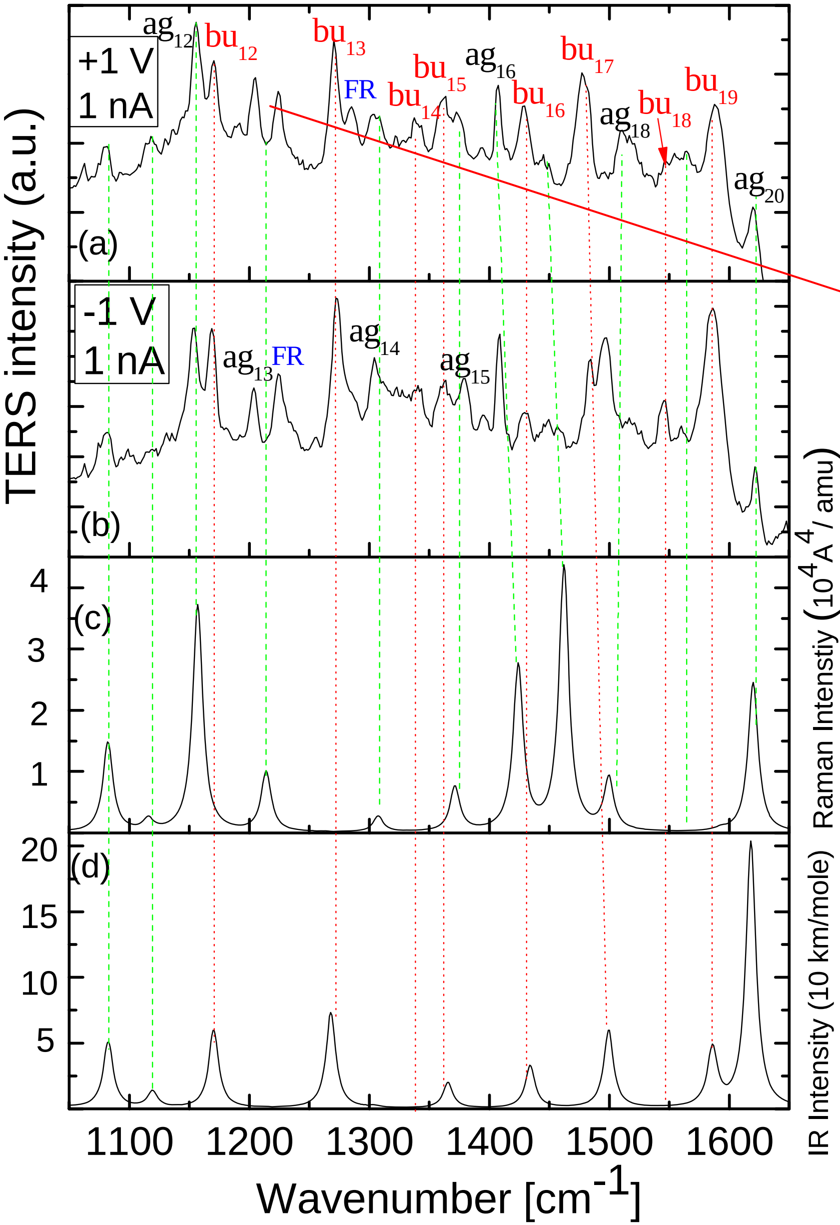

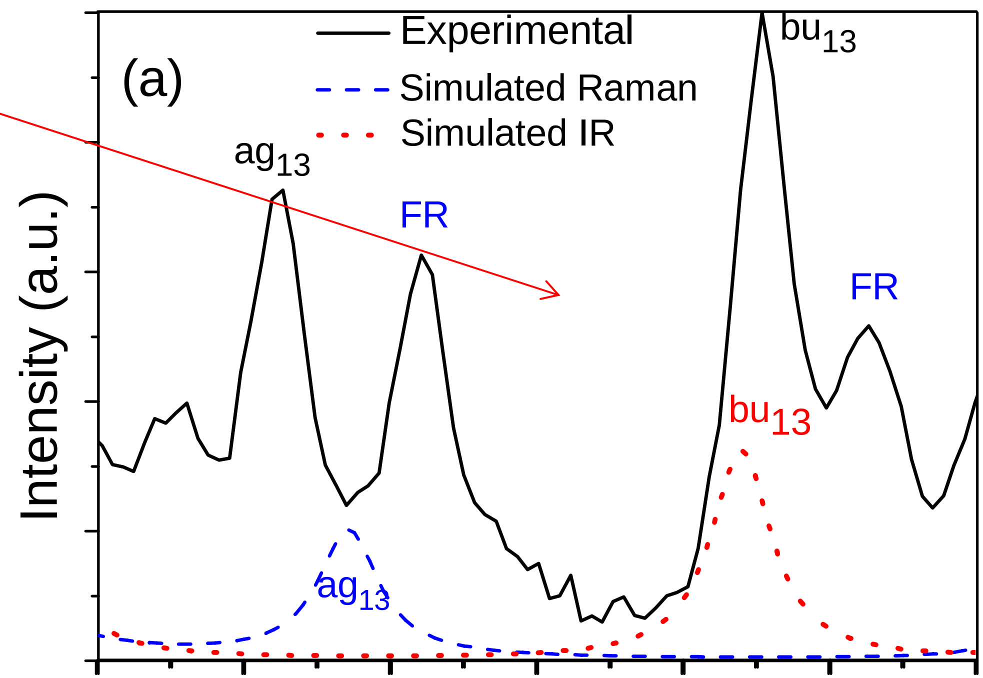

The experimentally observed Fermi resonance and simulated TERS spectra of DMAB for Raman-active symmetric ag_{13} and IR-active asymmetric bu_{13} modes.

Fermi Resonance

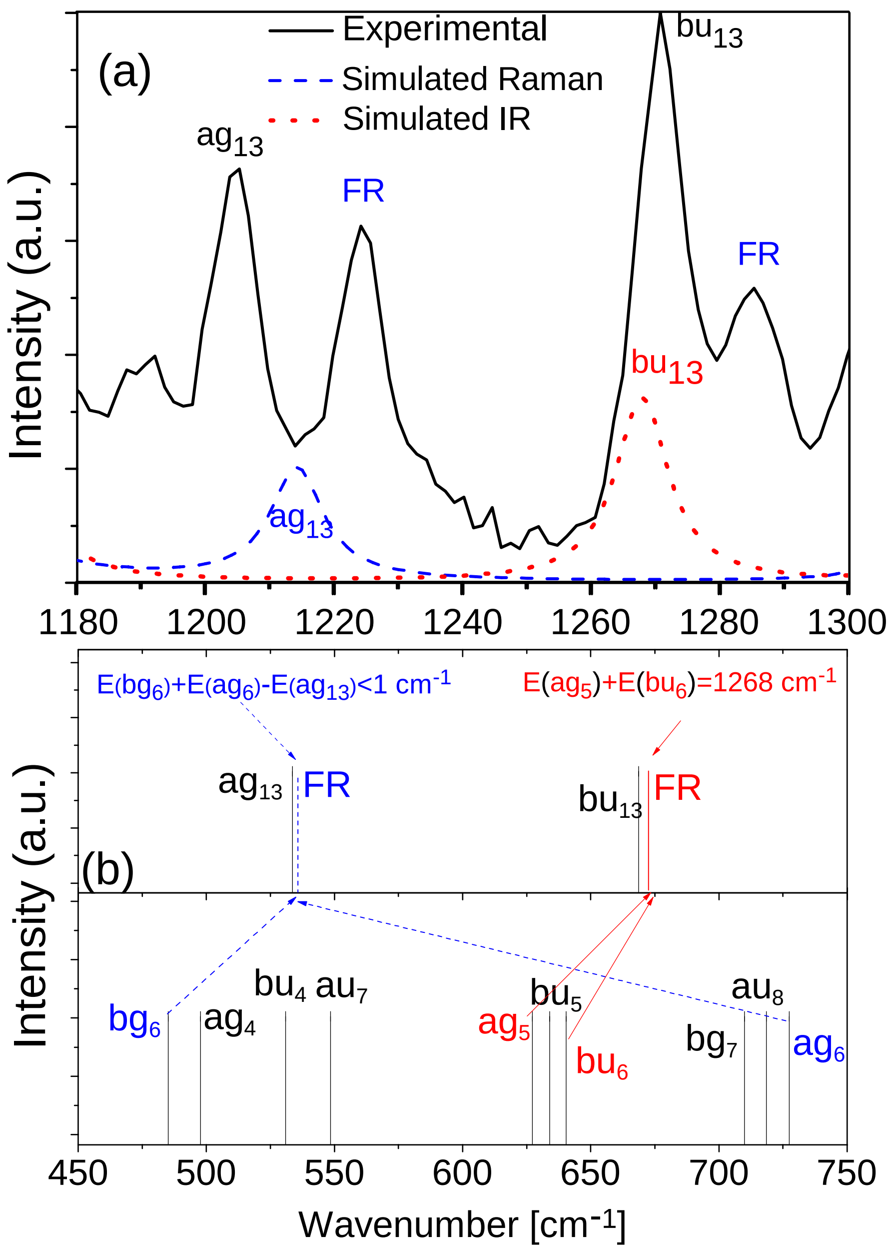

Fermi resonances:

overtone or a combination modes appearing in the vibrational spectra by gaining intensity from a fundamental mode.

E. Fermi, Z. Phys. **71**, 250 (1931).

Fermi Resonance

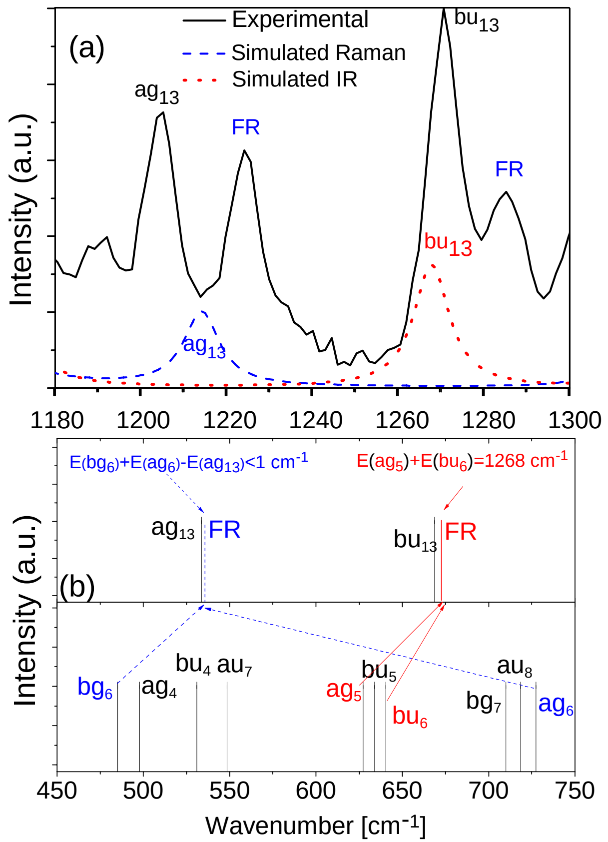

$$E_A = \frac{E_+ + E_-}{2} + \frac{E_+ - E_-}{2} \times \frac{I_+ - I_-}{I_+ + I_-}$$

$$E_B = \frac{E_+ + E_-}{2} - \frac{E_+ - E_-}{2} \times \frac{I_+ - I_-}{I_+ + I_-},$$

$$E_\pm = \frac{1}{2}(E_A + E_B) \pm \frac{1}{2}\sqrt{(E_A - E_B)^2 + 4\phi^2}$$

ϕ is the FR coupling coefficient

$$\phi(ag_{13}) = \frac{1}{2}\Delta E_\pm(ag_{13}) = 10.2\ \text{cm}^{-1}$$

$$\phi = \frac{\sqrt{2}}{3}\Delta E_\pm(bu_{13}) = 6.88\ \text{cm}^{-1}$$

(a) The experimentally observed Fermi resonance and simulated TERS spectra of DMAB for Raman-active symmetric ag_{13} and IR-active asymmetric bu_{13} modes. (b) The calculated vibrational modes and the combinational modes for Fermi resonance.

2.Nanophotonic Circuits
纳米光芯片

Propagating Surface Plasmons: to build plasmonic circuits

Nobel Prize in Physics 2009—K Kao: "for groundbreaking achievements concerning the transmission of light in fibers for optical communication"

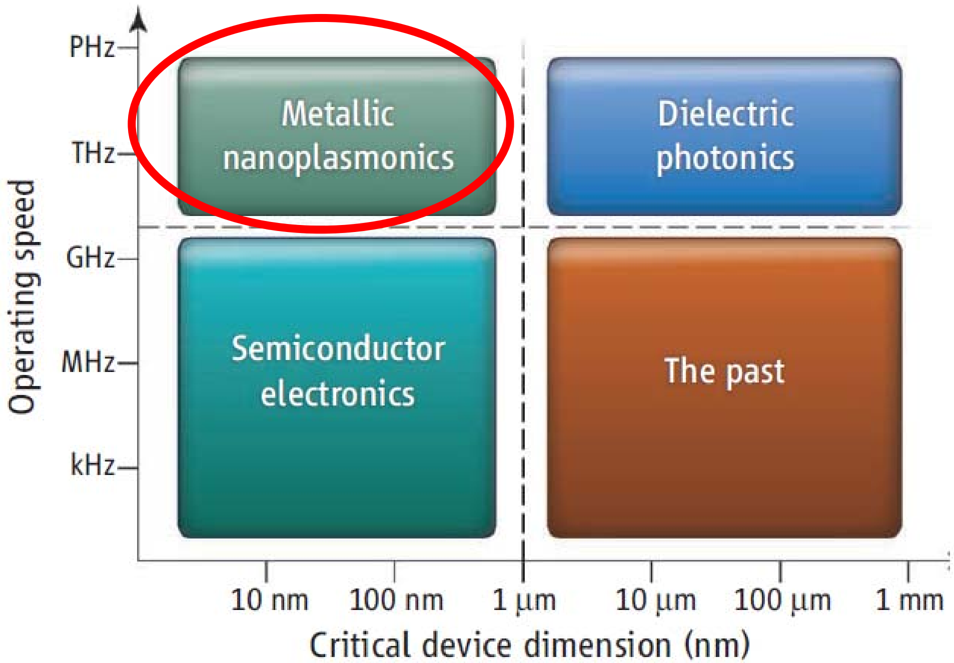

Science 328, 440 (2010)

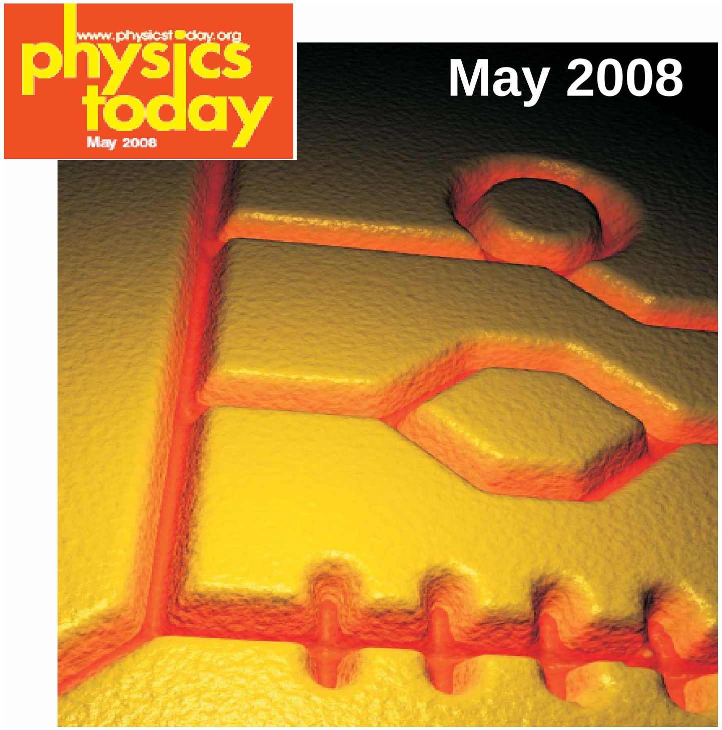

Surface-plasmon circuitry

Outline

- Near-field, Network and Logic
- Wire plasmon modes/Chiral wire plasmons
- Tunable wire plasmons
- Substrate-Mediated Plasmon
- Plasmon Amplification

Outline

- **Near-field, Network and Logic**
- Wire plasmon modes/Chiral wire plasmons
- Tunable wire plasmons
- Substrate-Mediated Plasmon
- Plasmon Amplification

Sample Structure

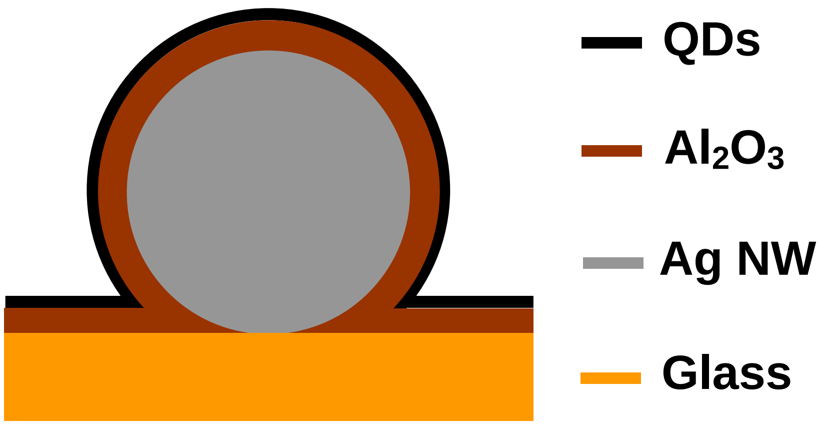

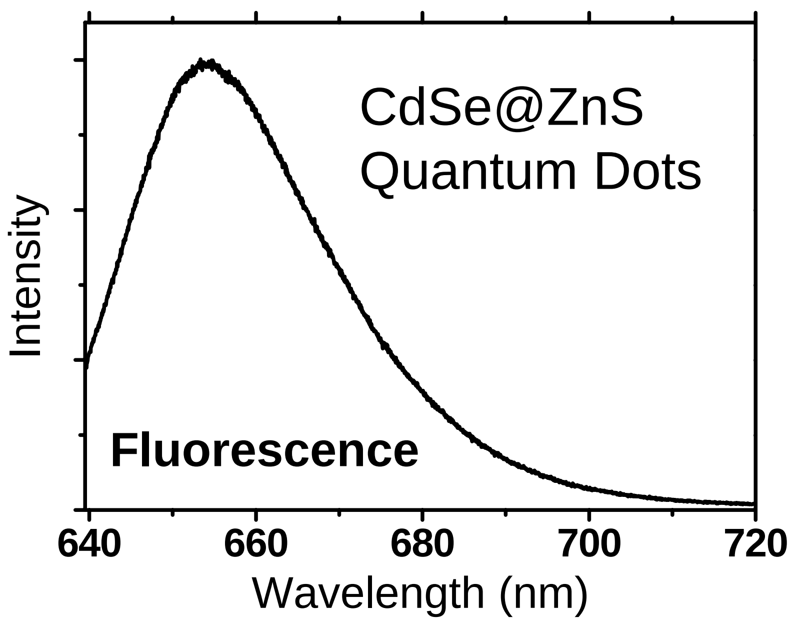

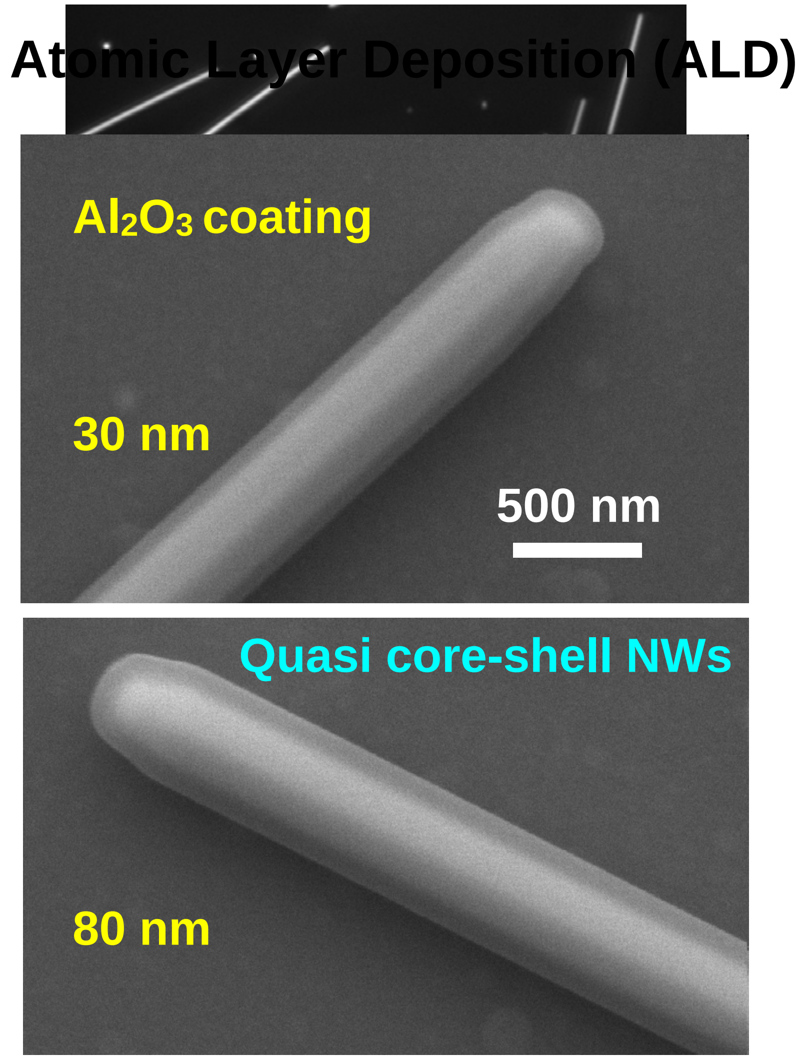

Quantum dot fluorescence imaging the near-field distribution

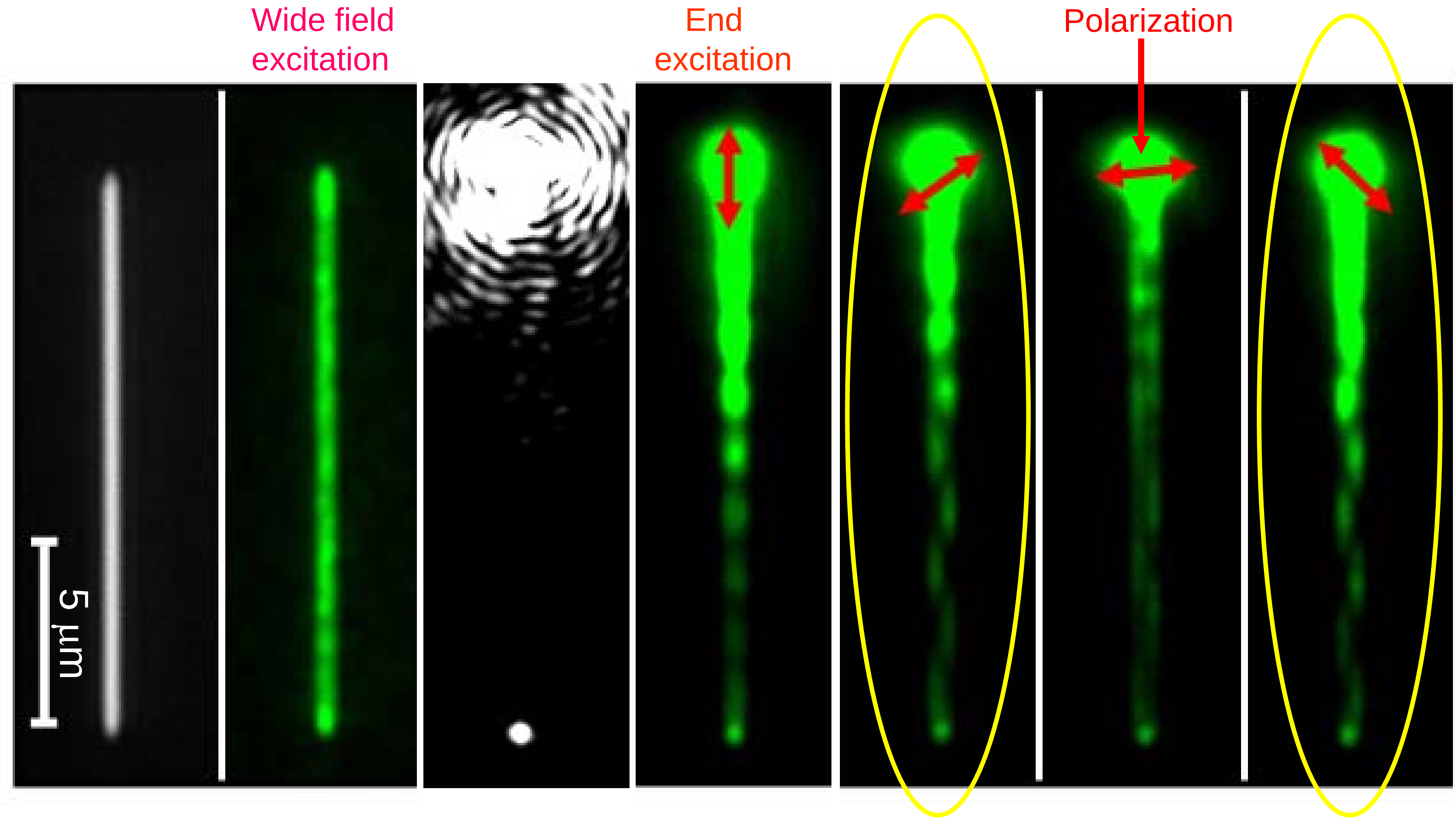

QD fluorescence images the near field of SPP.

Increasing the polarization angle shifts the local field from one side to the other.

H. Wei et al., Nano Lett. 11, 471 (2011)

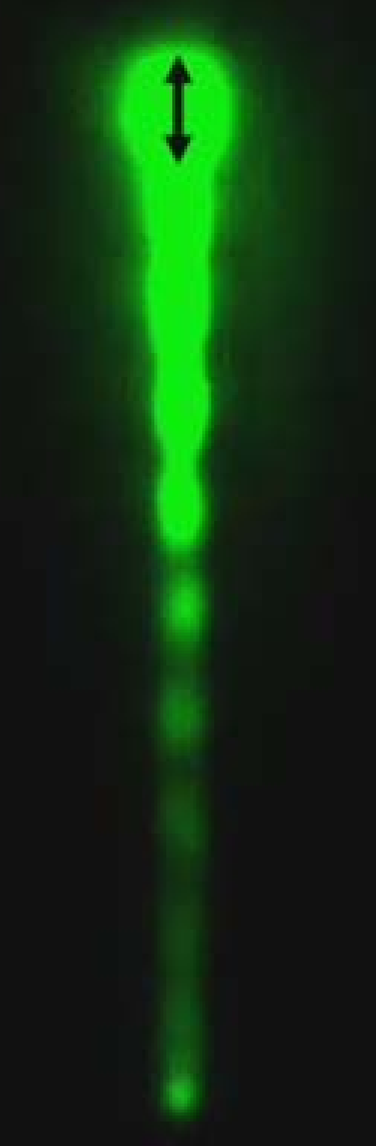

Hongxing Xu Lab, CAS

Origin of plasmon nodes in Ag NW waveguide

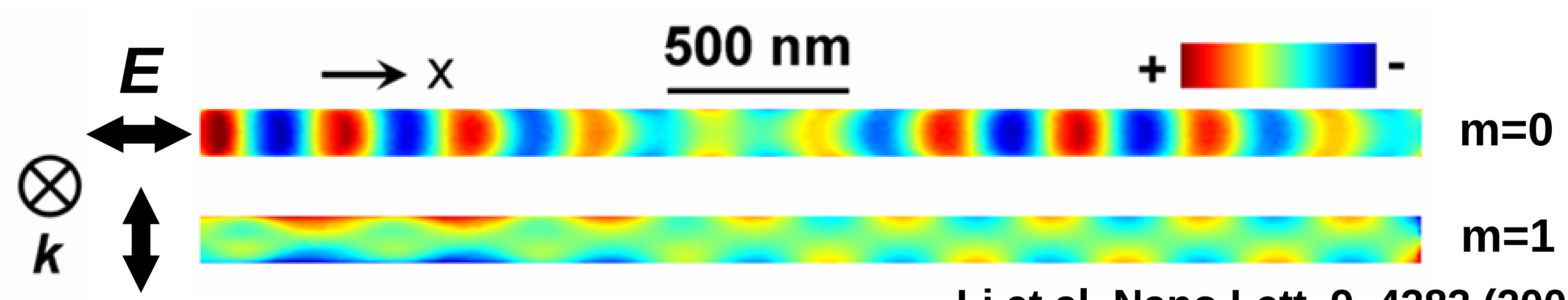

Li et al. Nano Lett. 9, 4383 (2009)

Interference of m=0 and m=1 plasmon modes result in large period near field modulation

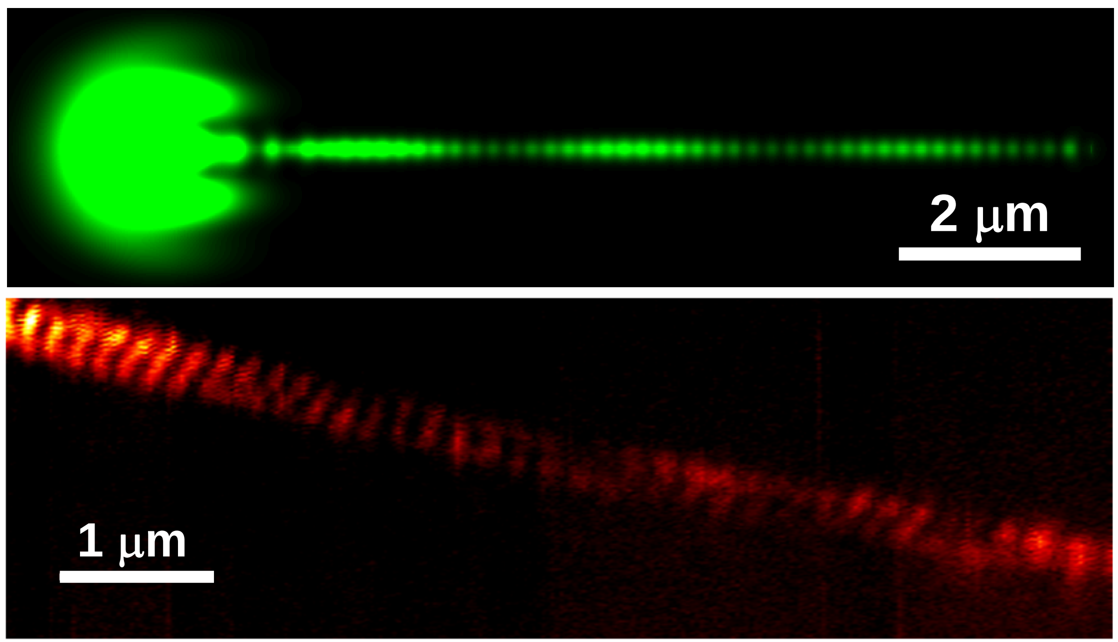

FDTD simulated E field intensity

SNOM image

Controlling scattering intensity by tuning near-field distribution

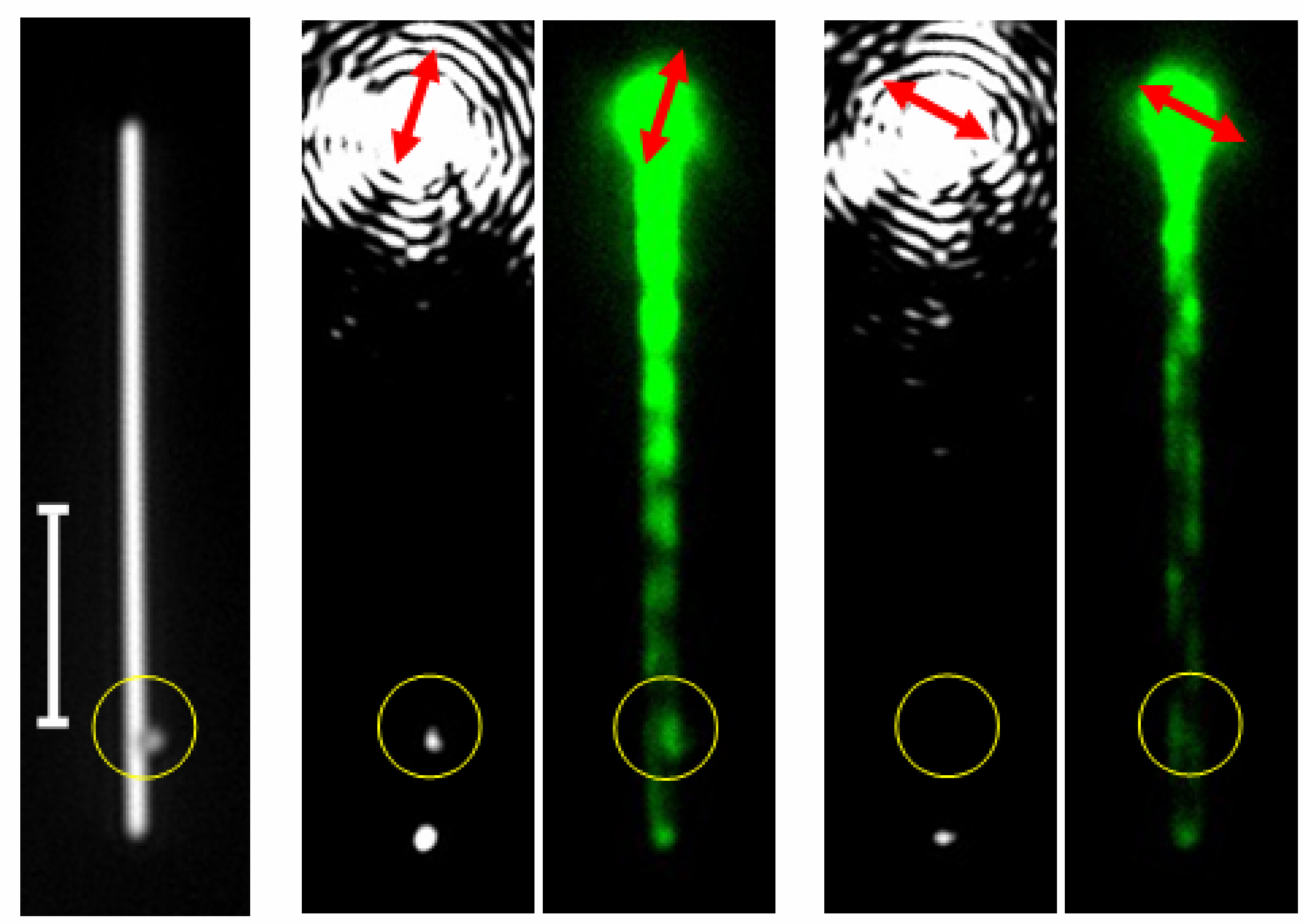

When the near-field intensity is large in the junction, plasmons can be efficiently transferred to connected structure.

H. Wei et al., Nano Lett. 11, 471 (2011)

Assembly of nanowire networks with a micromanipulator

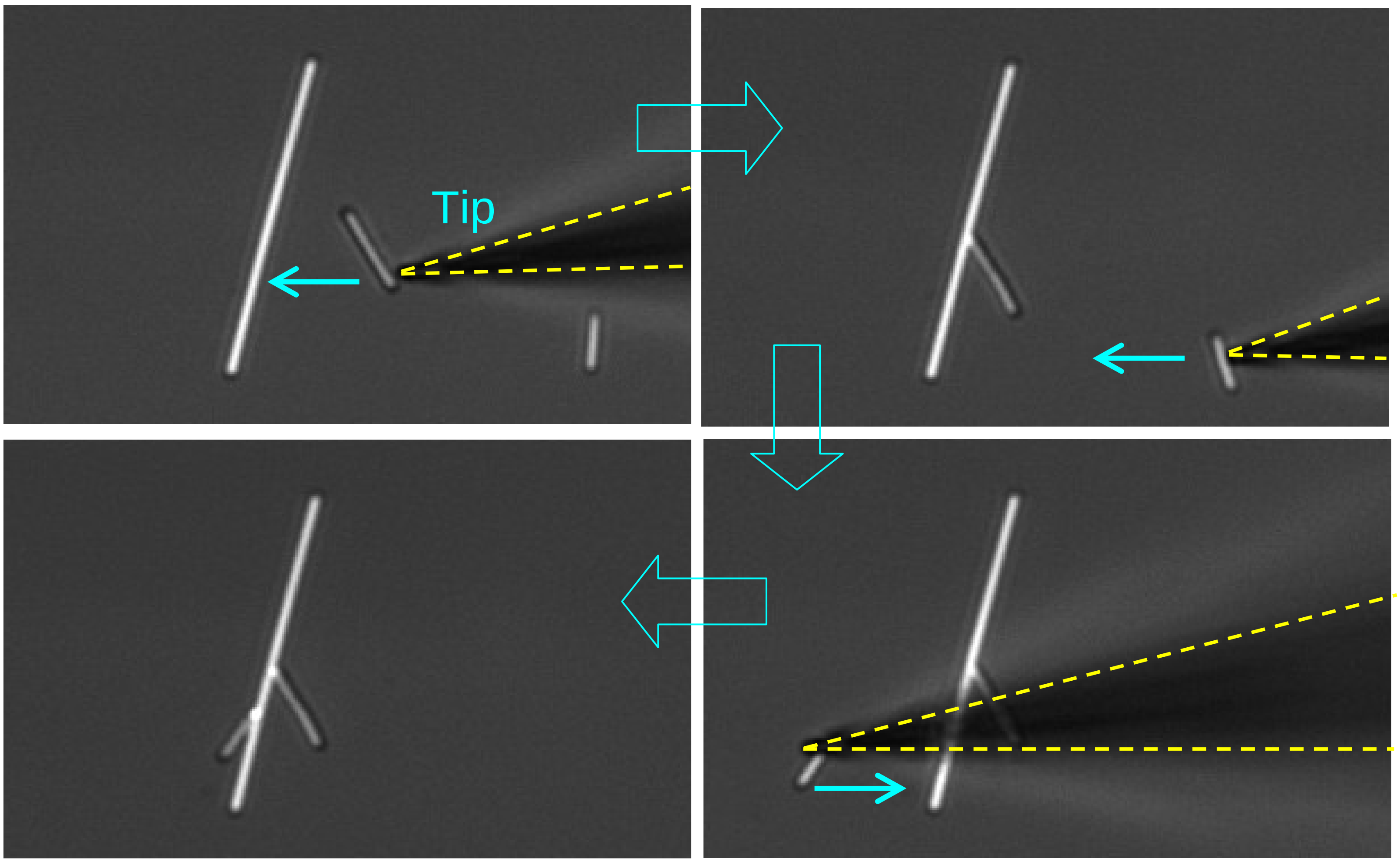

Plasmon Router/Splitter

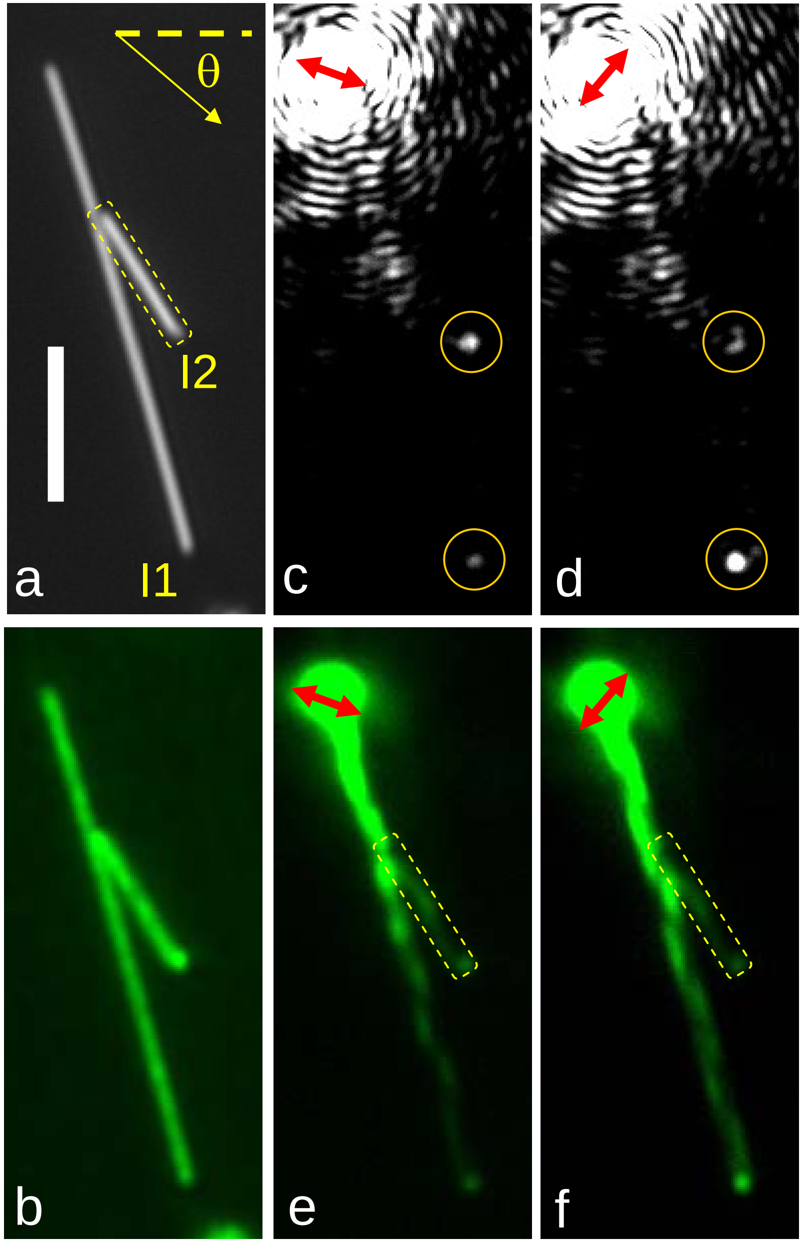

Output intensity as function of incident polarization angles I1 and I2

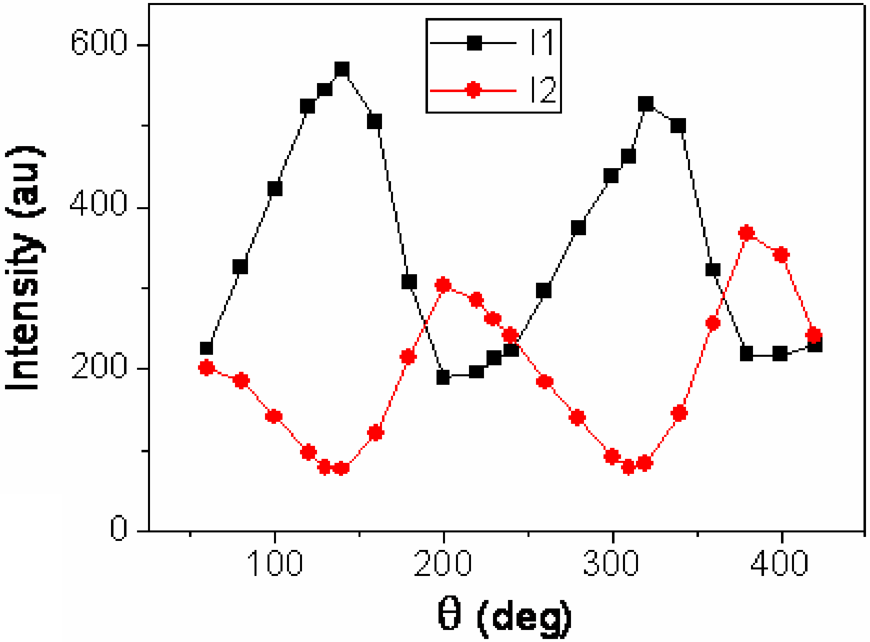

When the near field in junction is large, the energy will be routed to the branch NW.

Controllable Plasmon Routers

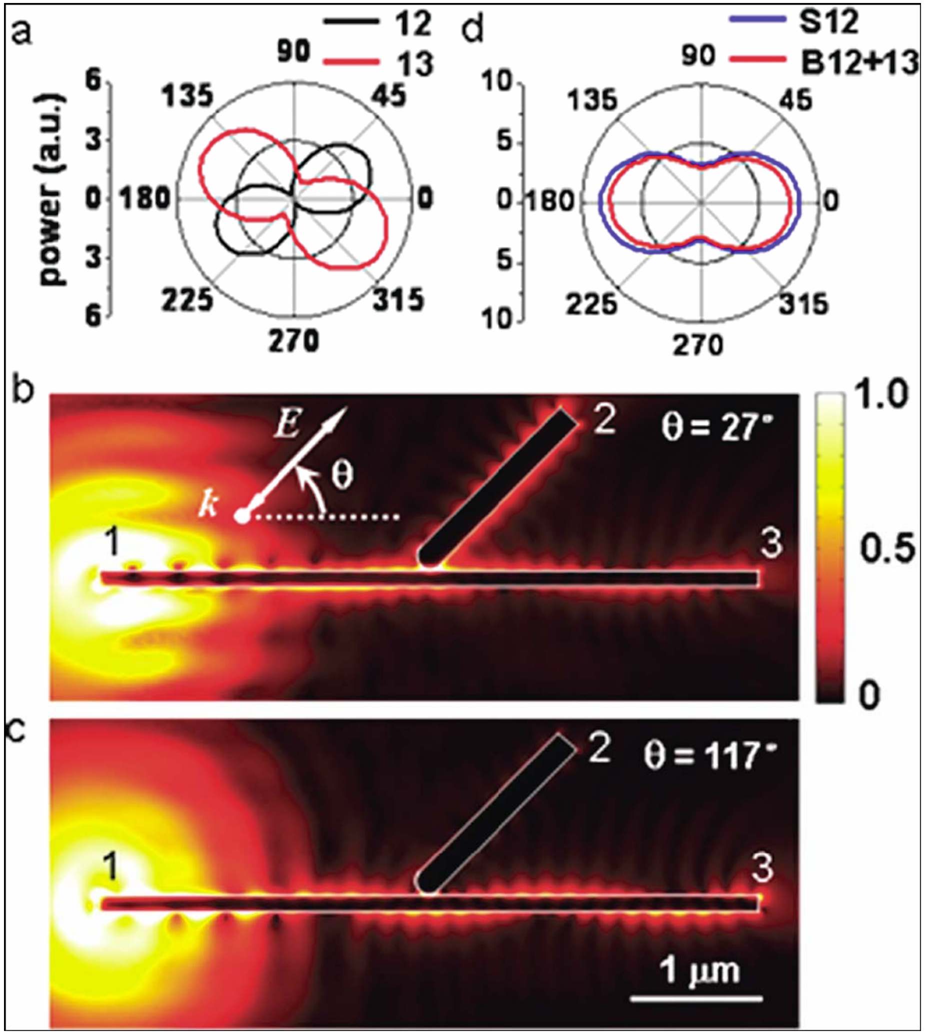

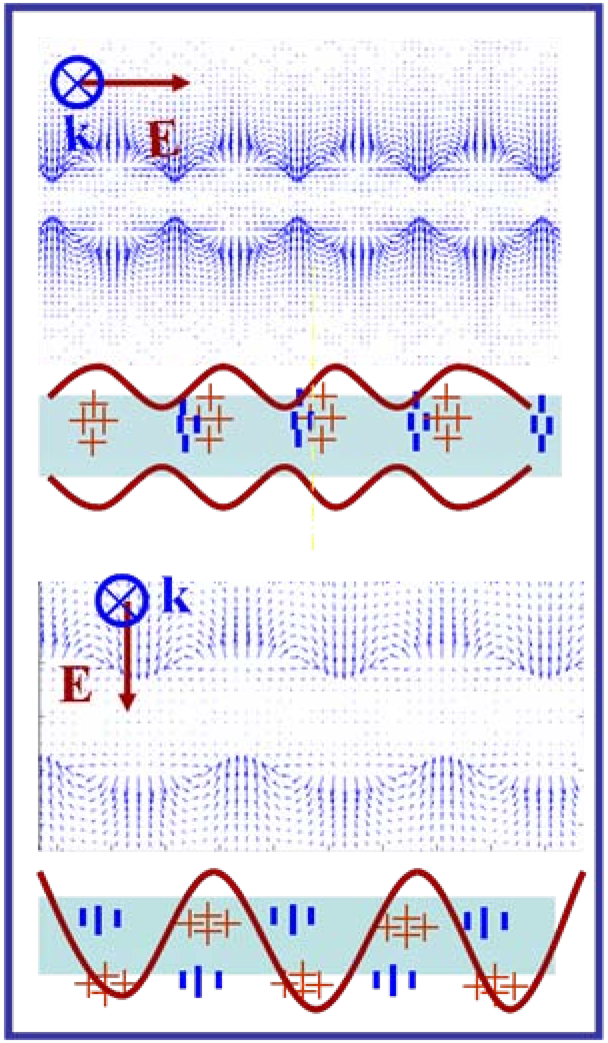

Fang et al, Nano Lett 10, 1950 (2010)

Plasmon Switchs in Plasmonic Network

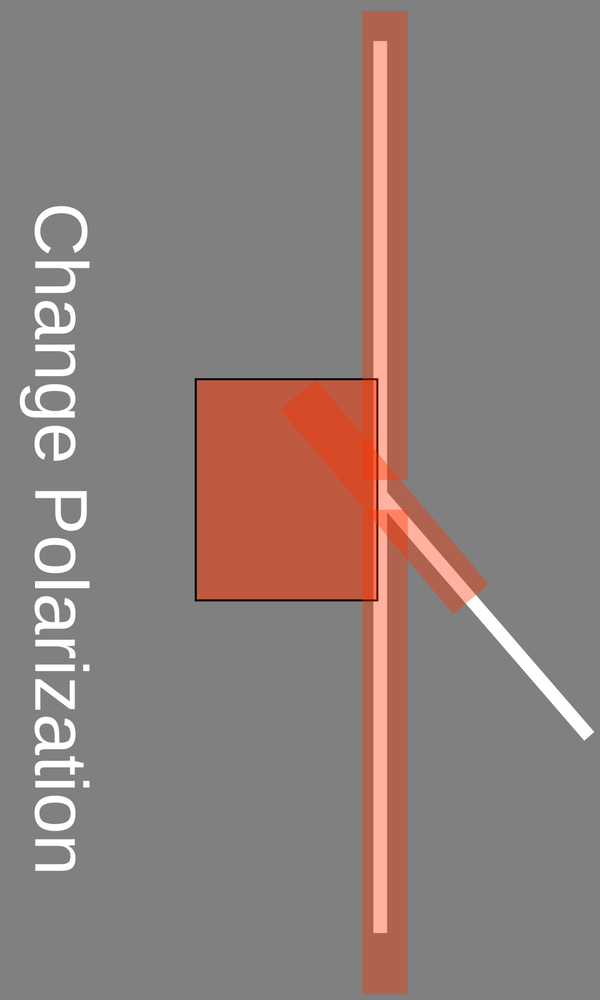

Plasmon Switch #1

III. Plasmon interference and networks

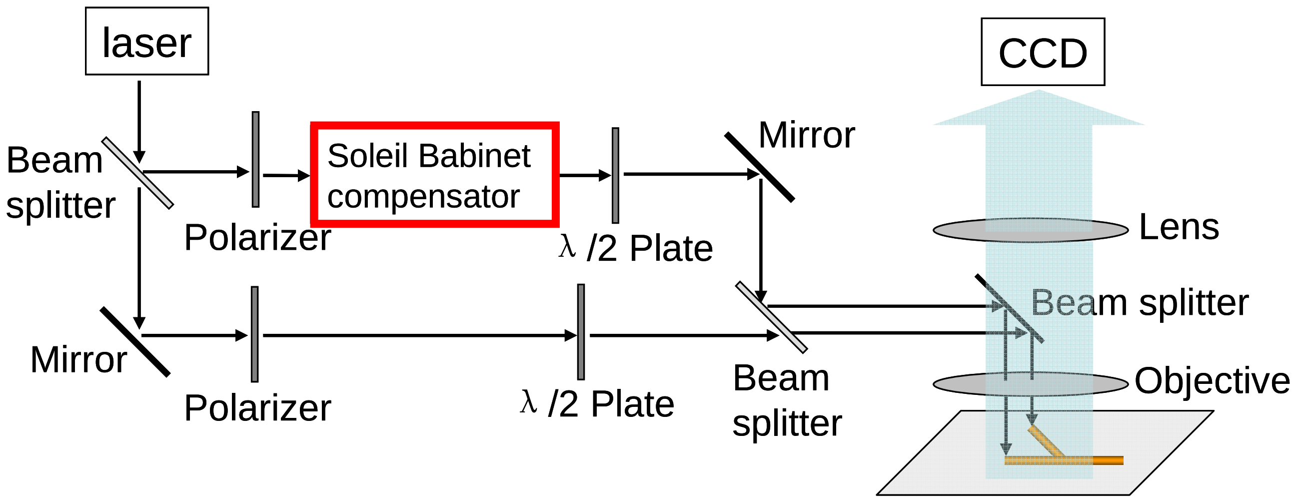

SB Compensator:

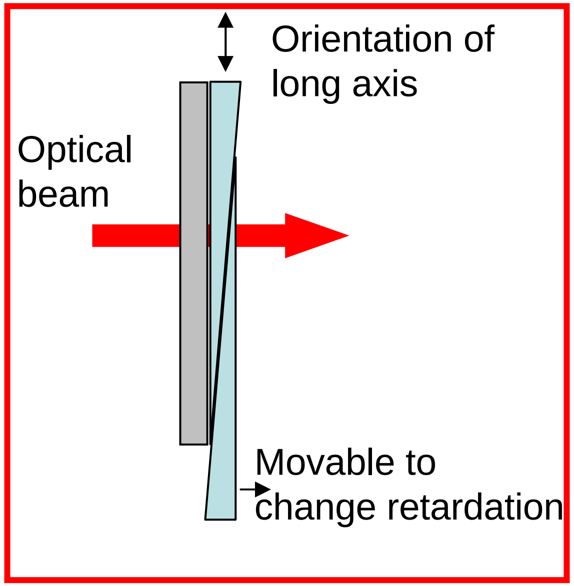

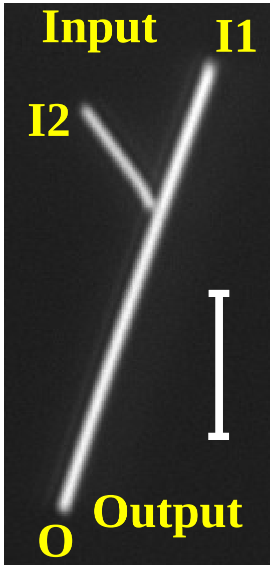

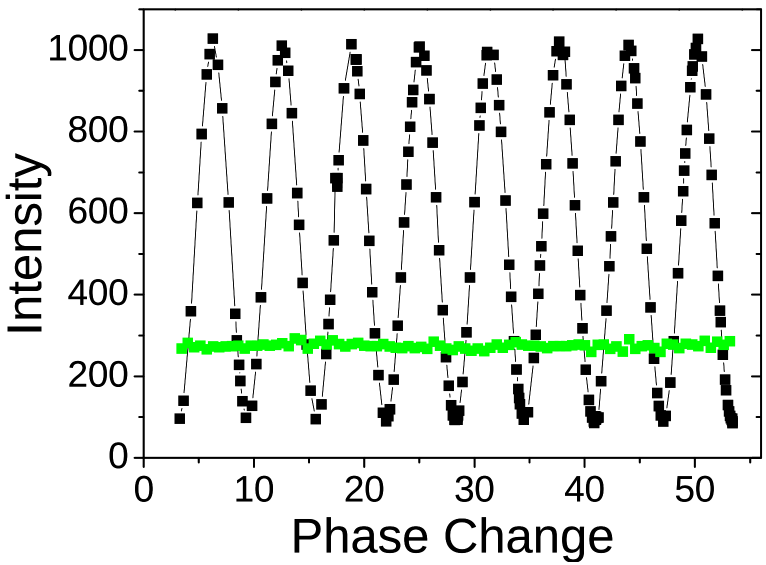

By changing the relative phase of I1 and I2 inputs, the output intensity oscillates.

H. Wei et al. Nano Lett. 11, 471 (2011)

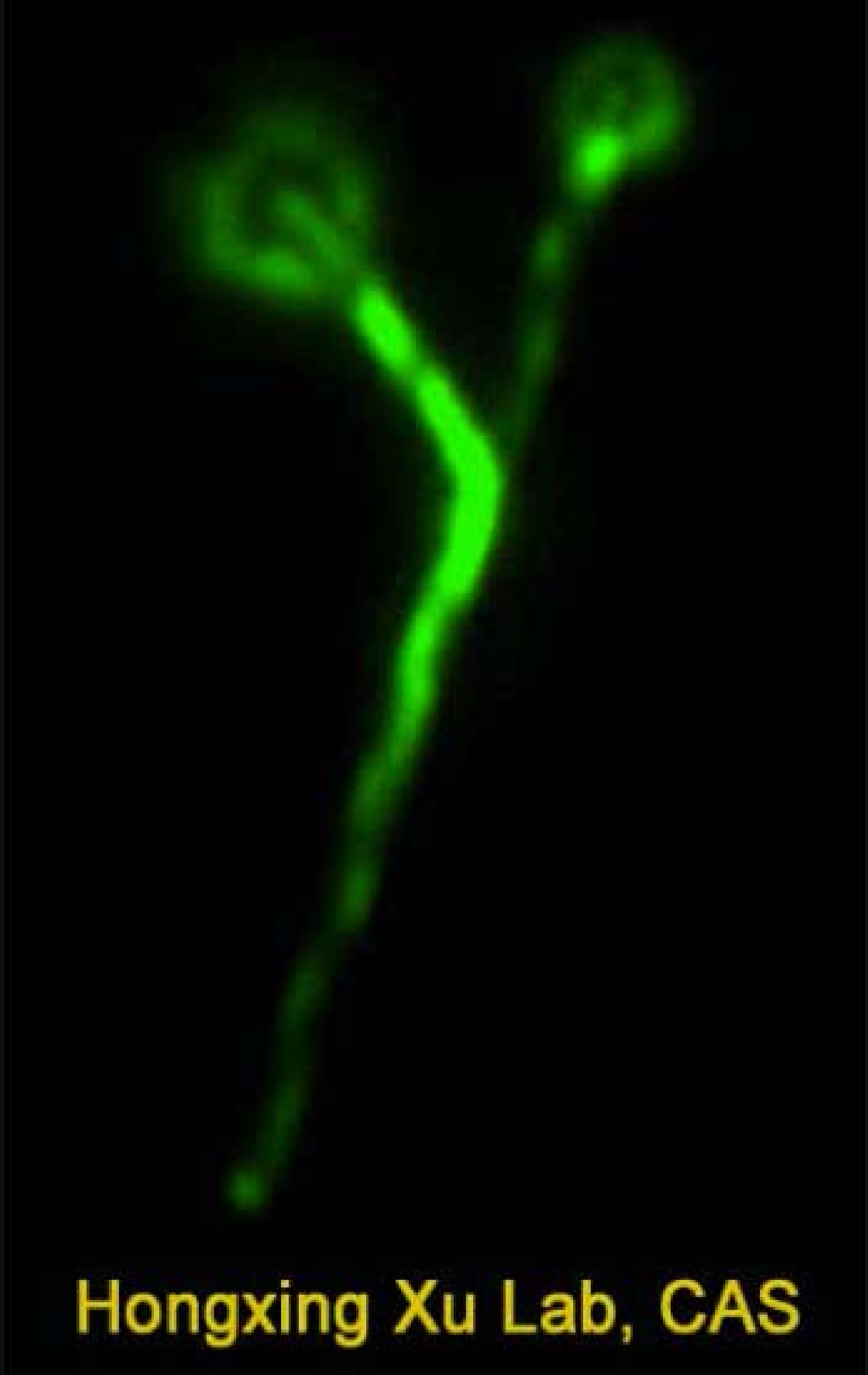
Hongxing Xu Lab, CAS

Plasmon Switchs in Plasmonic Network

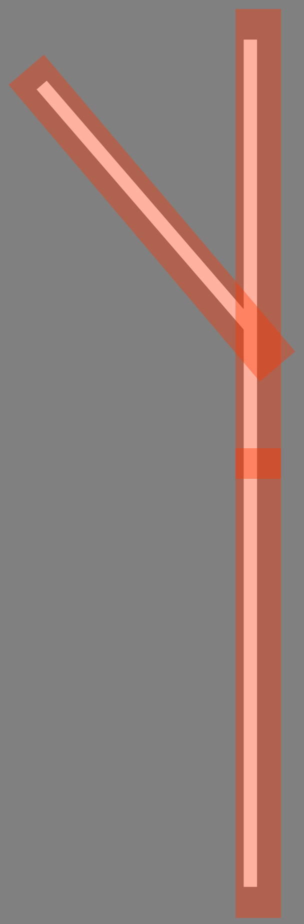

Change Incident Phases

Plasmon Switch #2

Plasmon interference and networks

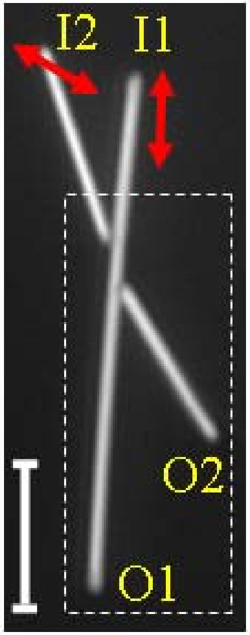

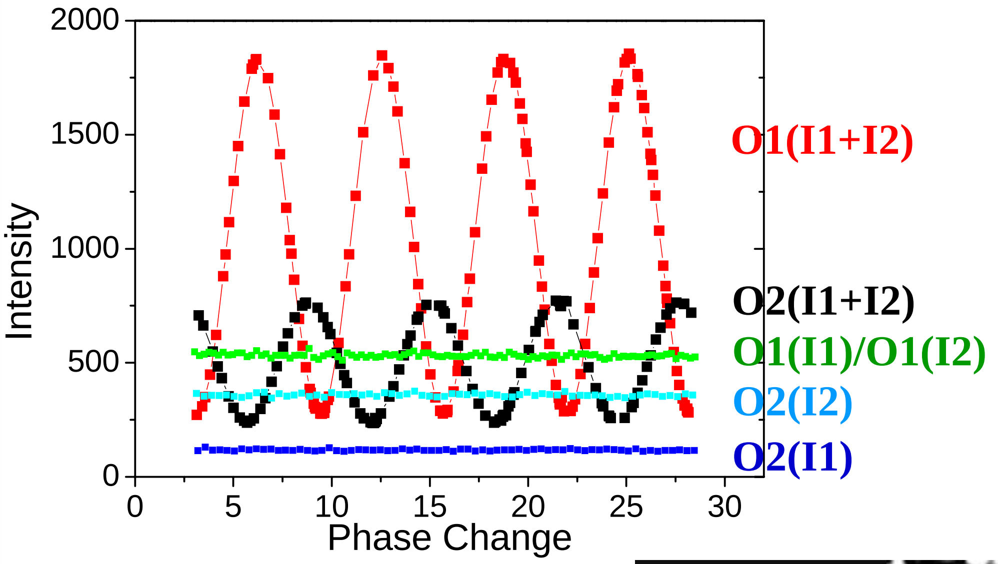

Red: output at **O1** terminal for inputs at both I1 and I2
Black: output at **O2** terminal for inputs at both I1 and I2

The interference between SPPs generated at inputs I1 and I2 determines output at O1 and O2.

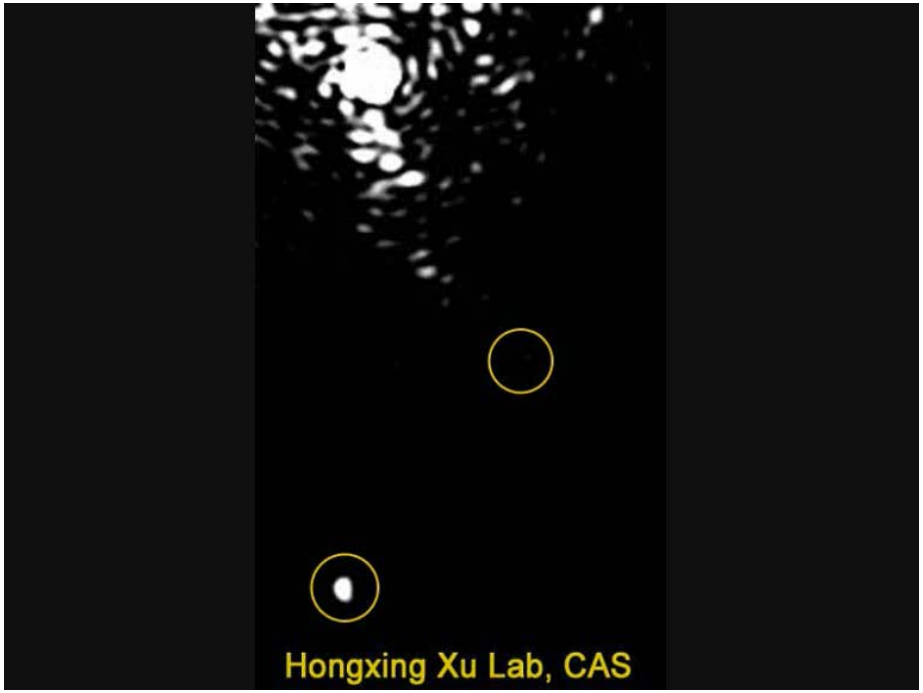

H. Wei et al. Nano Lett. 11, 471 (2011)

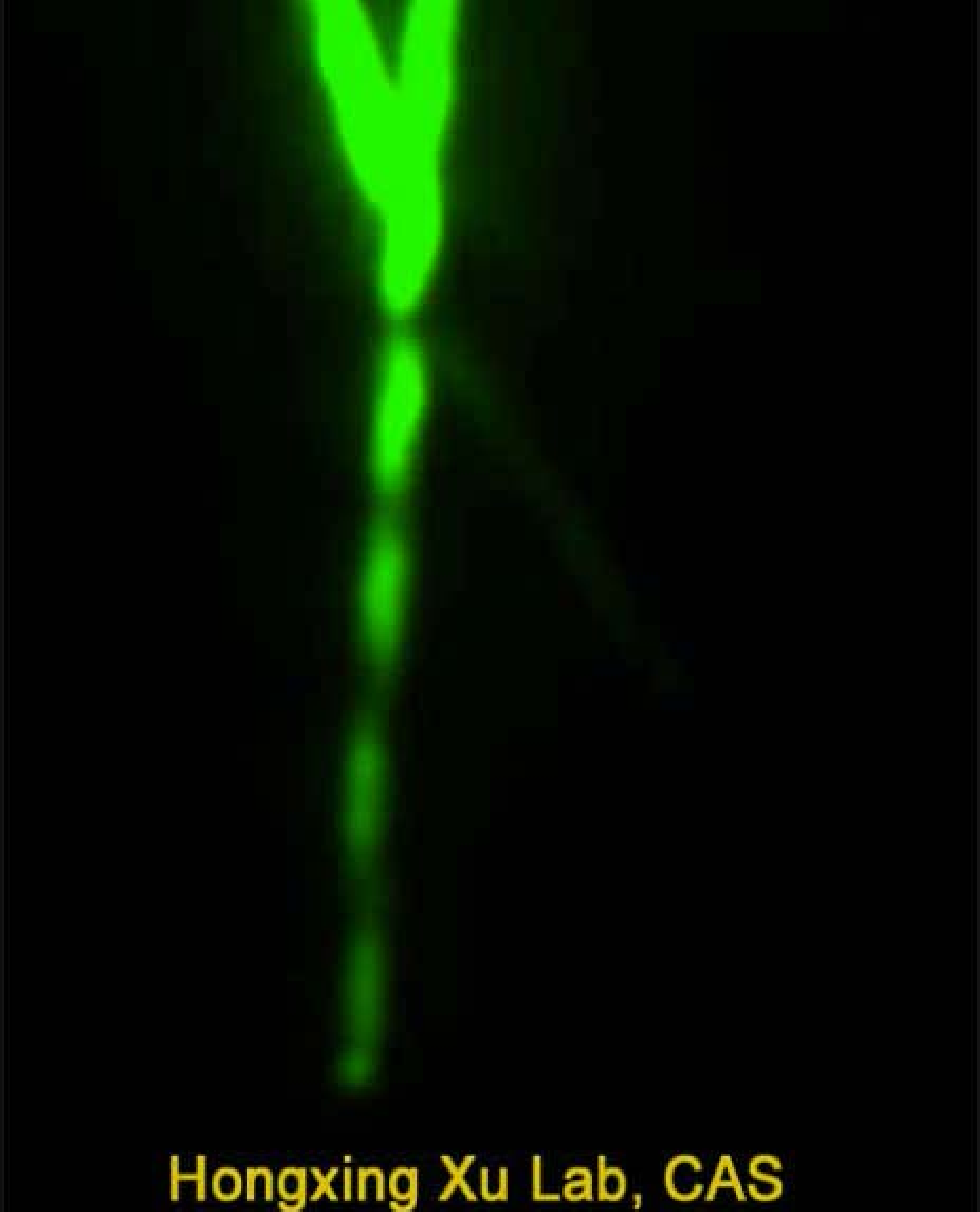
Hongxing Xu Lab, CAS

Plasmon Switchs in Plasmonic Network

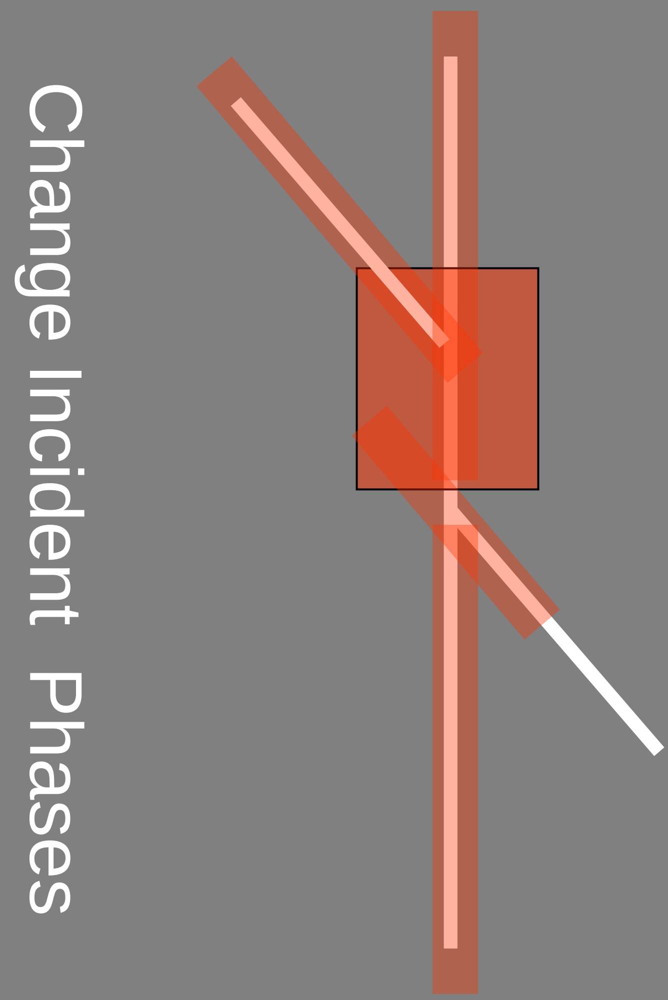

Plasmon Switch#3

Plasmon Switchs in Plasmonic Network

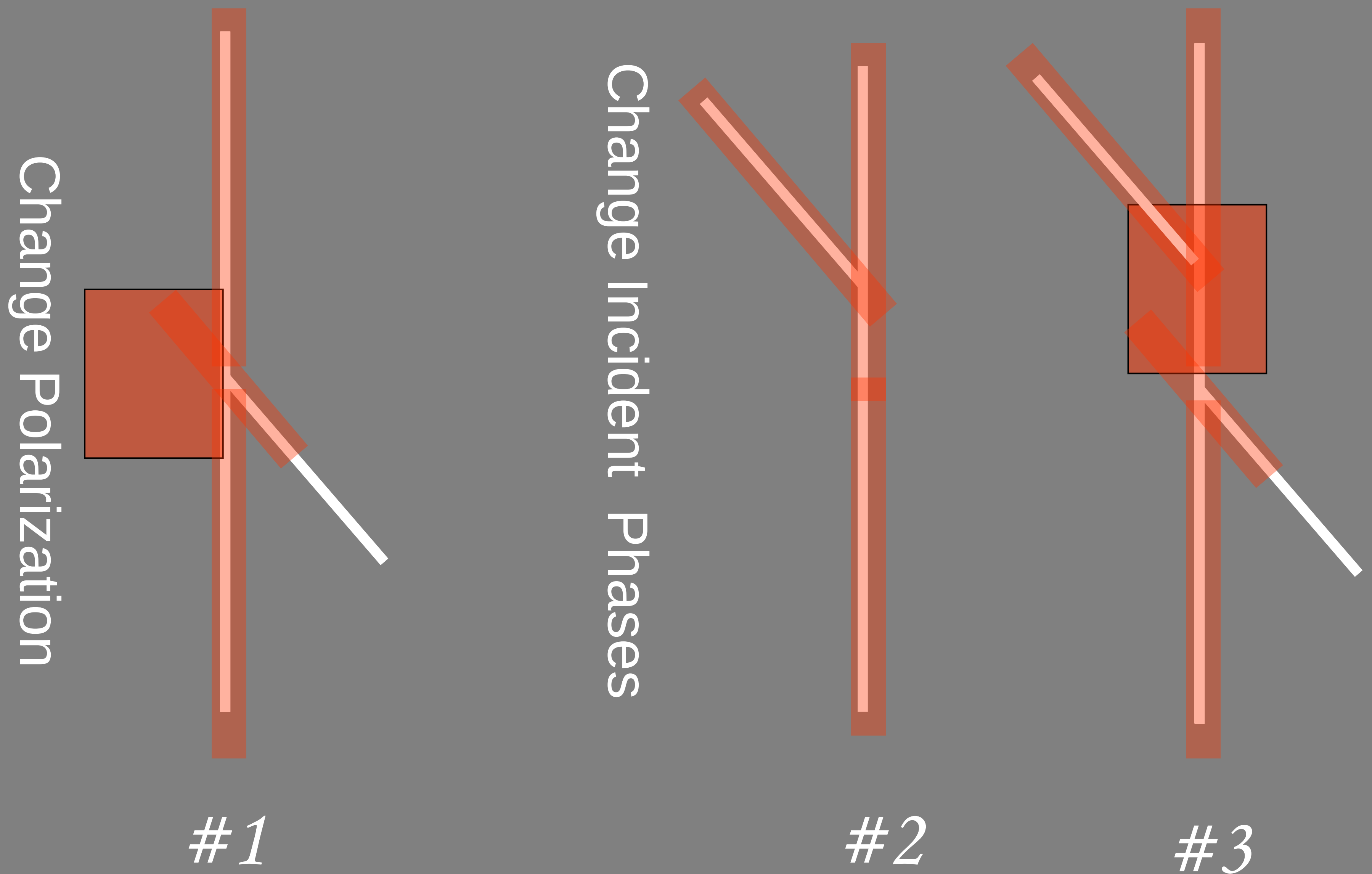

Plasmon-Based Interferometric Logic and Computing

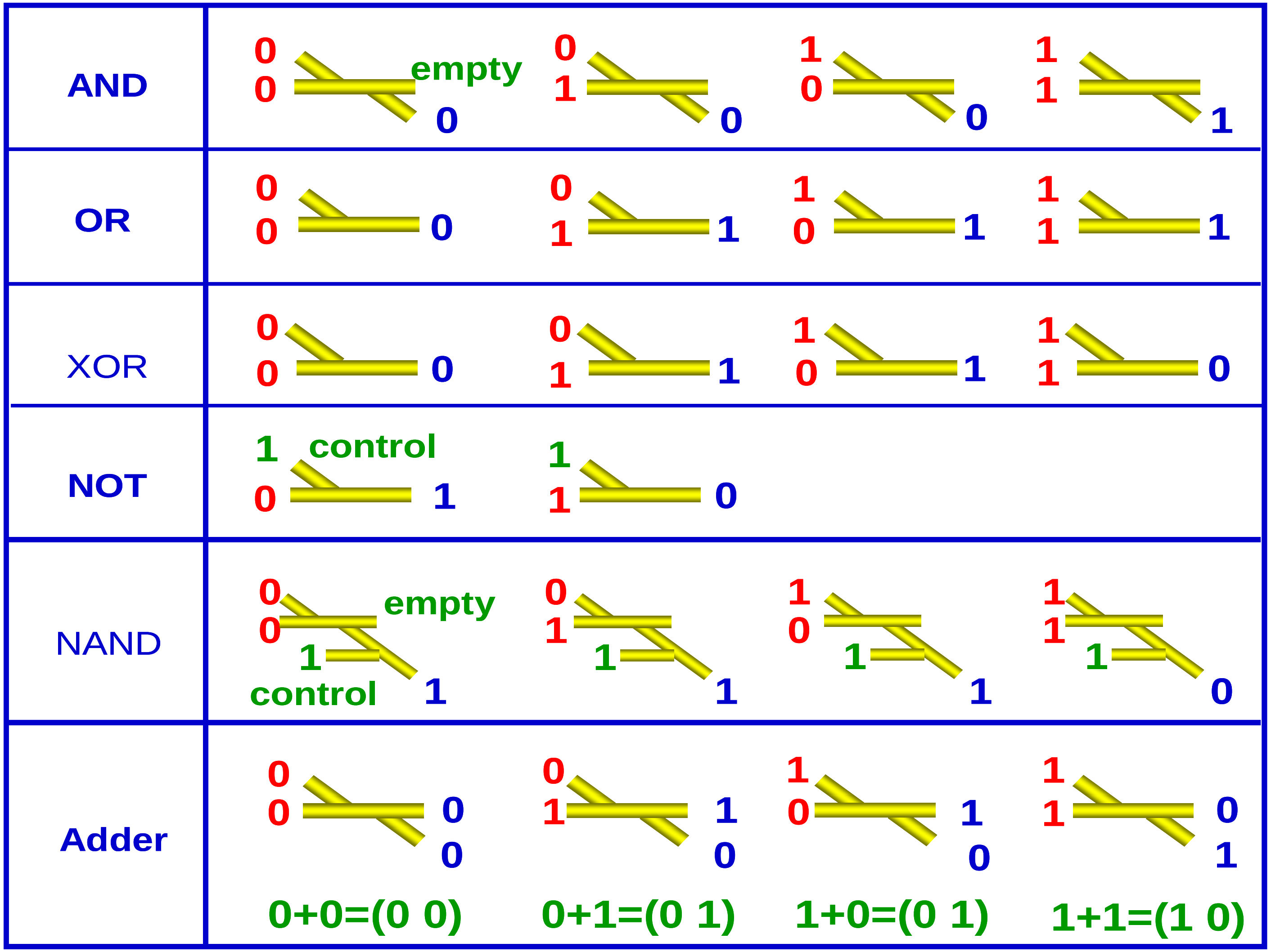

Complete set of Boolean logic functions can be realized!

H. Wei et al. Nano Lett. 11, 471 (2011)

- **Examples of Boolean Logic**

OR Gate

Boolean logic

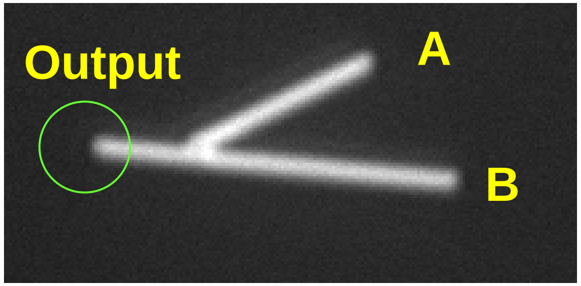

(A, B) → Output

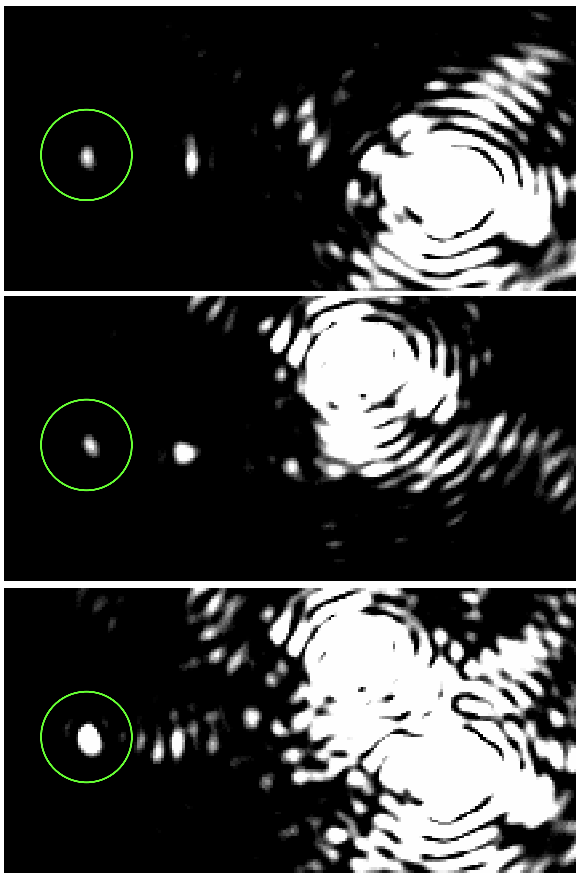

(0, 1) → 1

(1, 0) → 1

(1, 1) → 1

Input		Output
A	B	A OR B
0	0	0
0	1	1
1	0	1
1	1	1

NOT Gate

Boolean logic

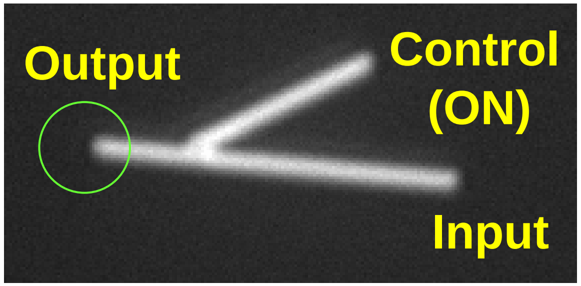

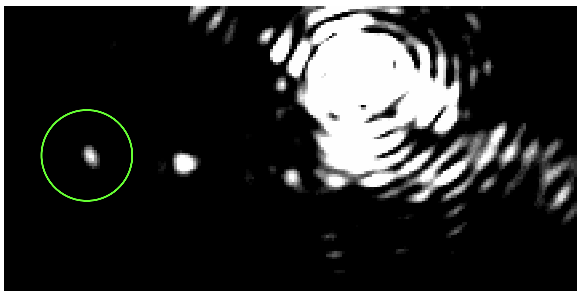

Input → Output

0 → 1

1 → 0

Input	Output
0	1
1	0

AND Gate

Boolean logic

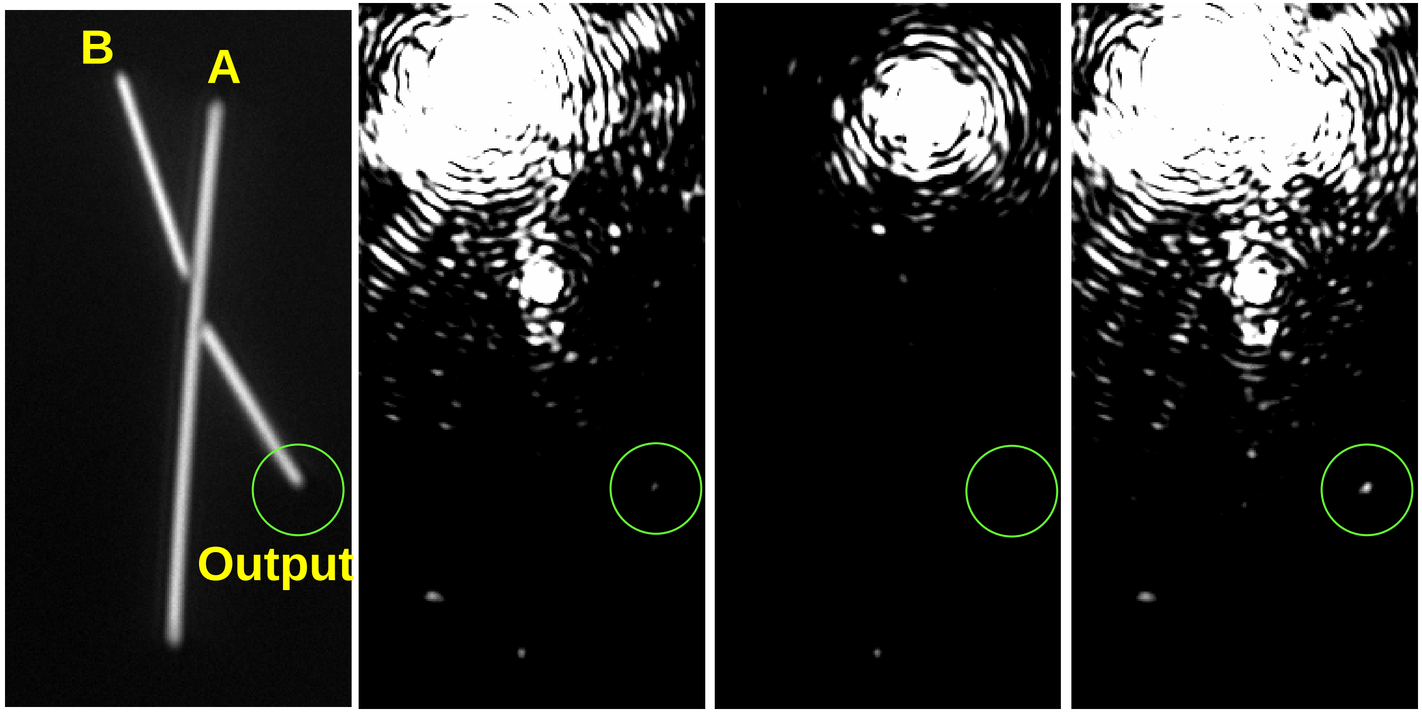

(0, 1) → 0 (1, 0) → 0 (1, 1) → 1

Input		Output
A	B	A AND B
0	1	0
1	0	0
1	1	1

Half Adder

Beyond Boolean logic

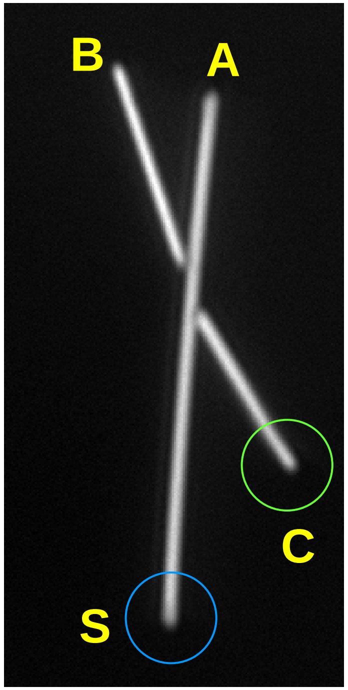

Half-adder:
Add two one-bit binary number **A** and **B**.
S is the sum, **C** is the value carried on to the next addition.

A+B=(C S)

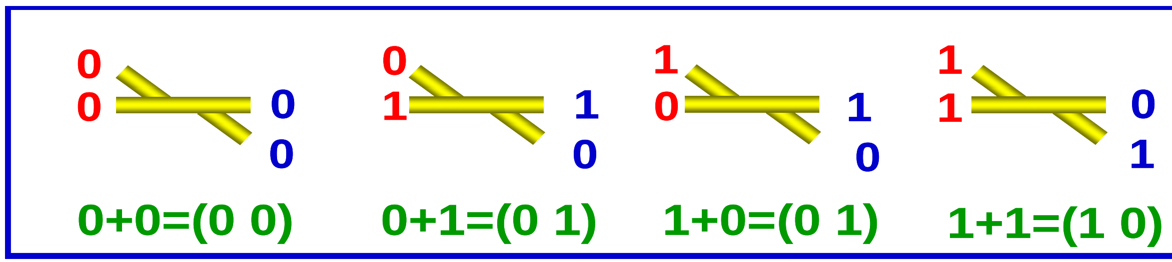

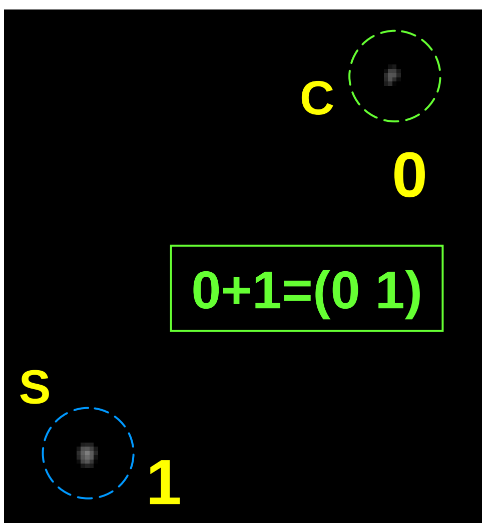

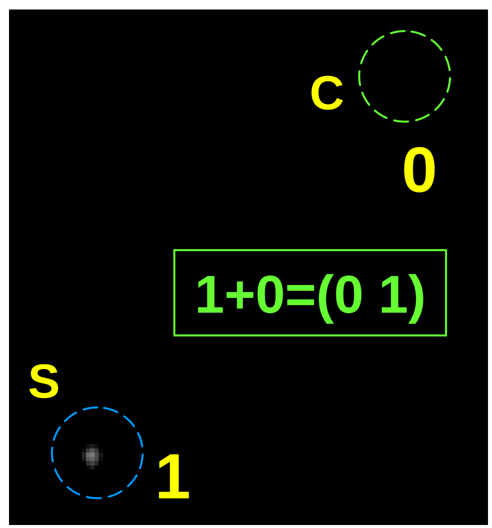

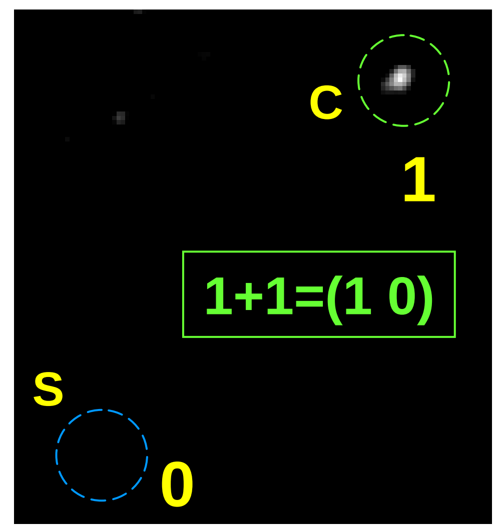

Cascaded Plasmonic Logic Gates

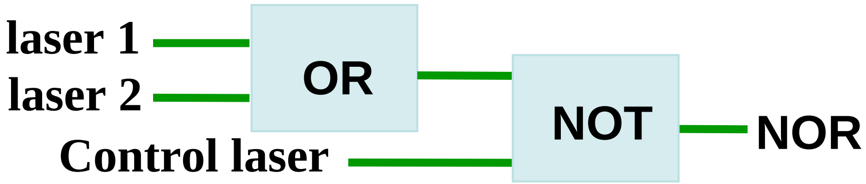

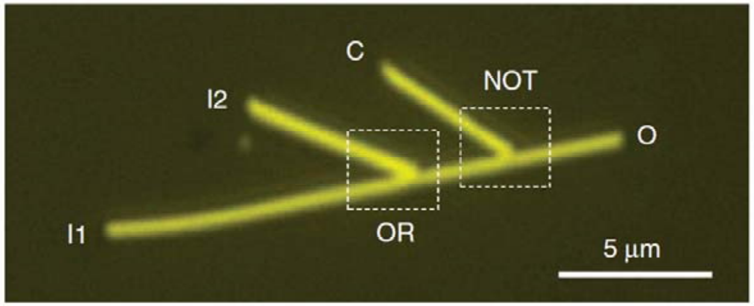

The control signal inverts the output of the *OR* gate, resulting in the *NOR* operation.

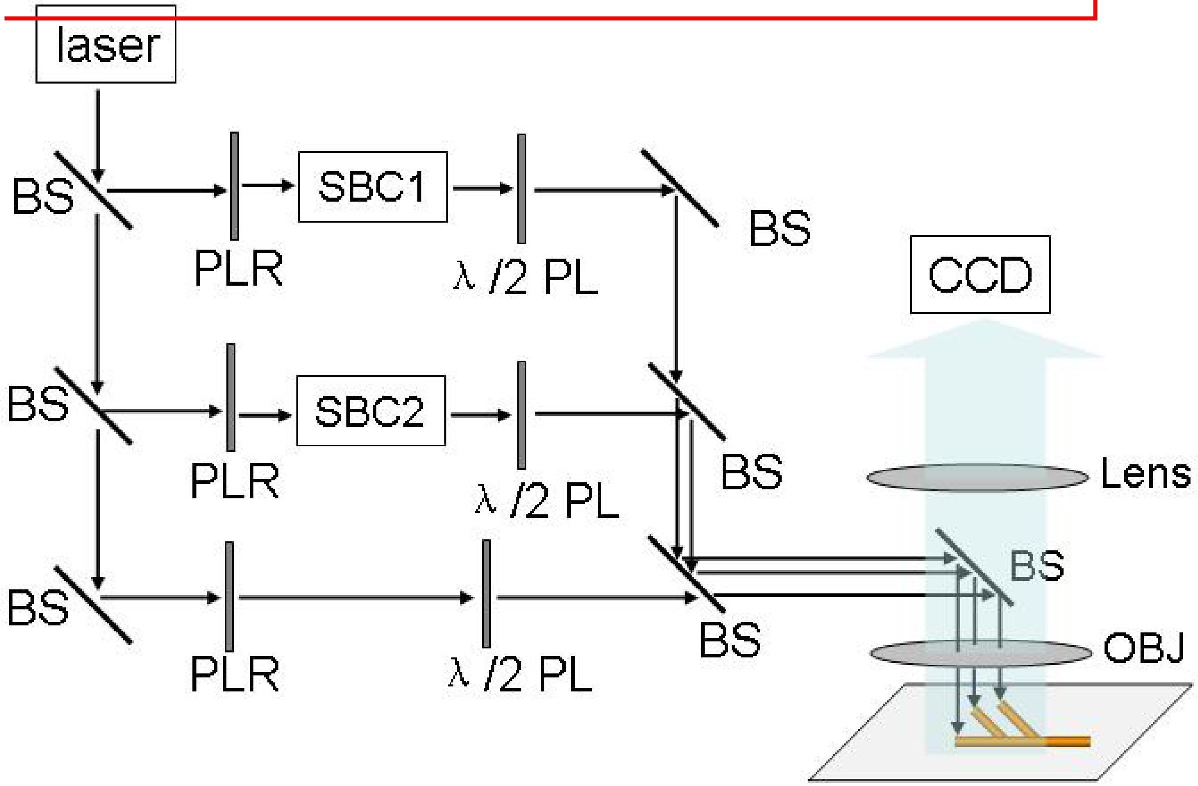

Wei *et al.*, *Nature Communications* 2, 387 (2011)

Cascaded Plasmonic Logic Gates

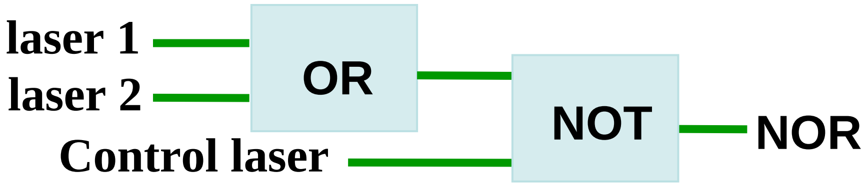

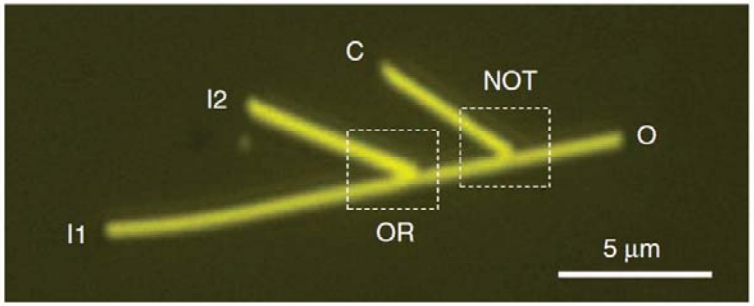

The control signal inverts the output of the *OR* gate, resulting in the *NOR* operation.

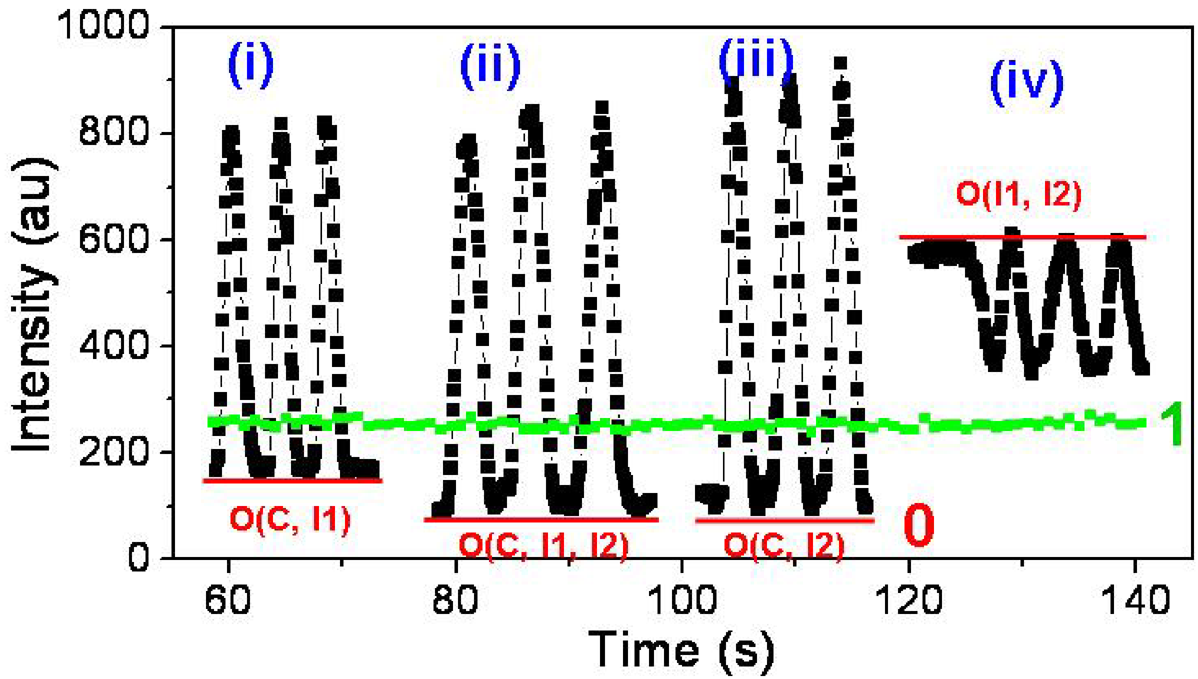

Wei *et al.*, *Nature Communications* 2, 387 (2011)

Cascaded Plasmonic Logic Gates

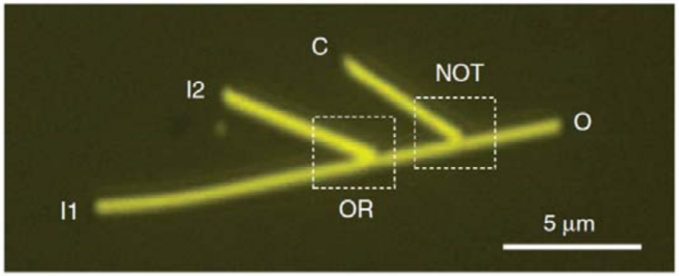

Table 1 | Outputs of logic gates.

Input			Output		
I1	**I2**	**C**	**O1=I1 OR I2**	**(O1, C)=NOT O1**	**O=I1 NOR I2**
0	0	1	0	1	1
0	1	1	1	0	0
1	0	1	1	0	0
1	1	1	1	0	0

OR

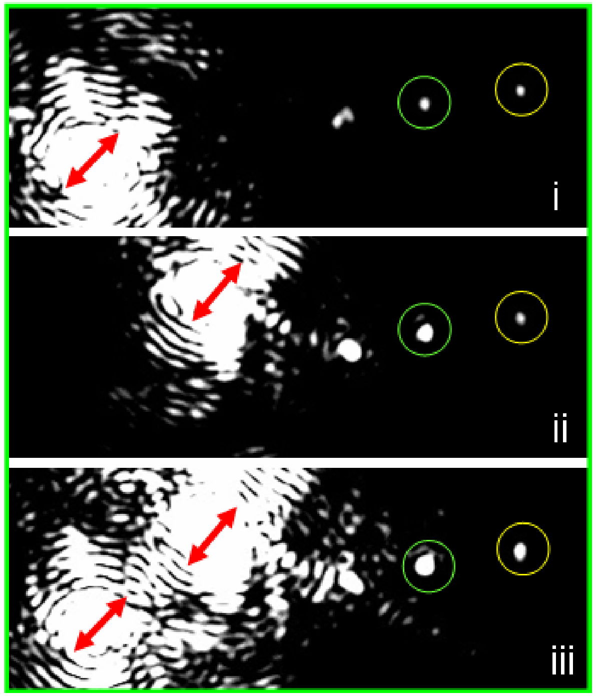

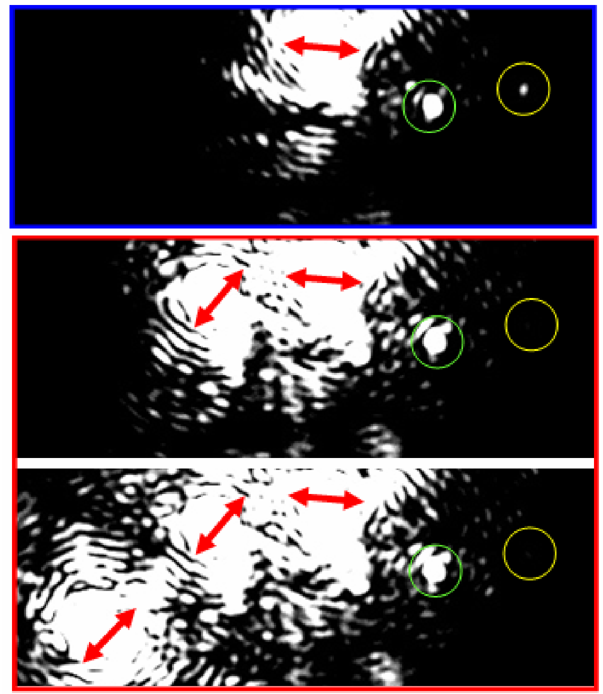

NOT

NOR

The control signal inverts the output of the *OR* gate, resulting in the *NOR* operation.

Wei *et al.*, *Nature Communications* 2, 387 (2011)

Mechanism

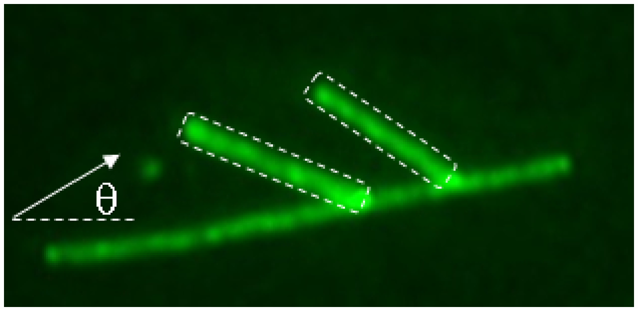

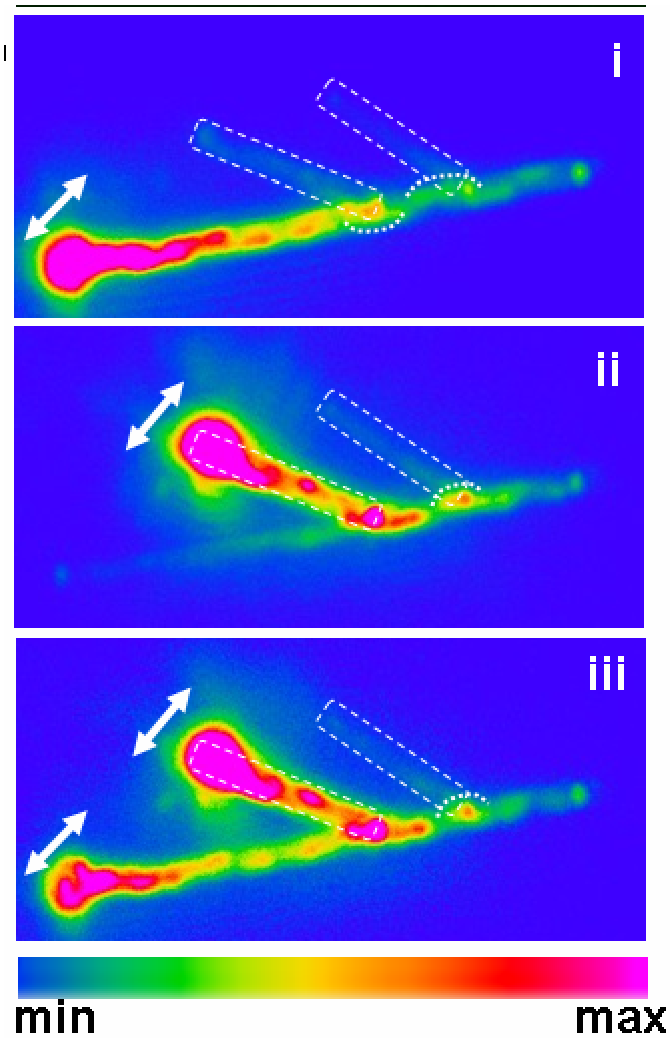

The local field intensity at the C branch junction determines how well the interference can be, i.e., determines if the *OR* operation can be inverted by the control beam.

Wei *et al., Nature Communications* 2, 387 (2011)

Outline

- Near-field, Network and Logic
- **Wire plasmon modes/Chiral wire plasmons**
- Tunable wire plasmons
- Substrate-Mediated Plasmon
- Plasmon Amplification

Plasmon modes excited in metal nanowire

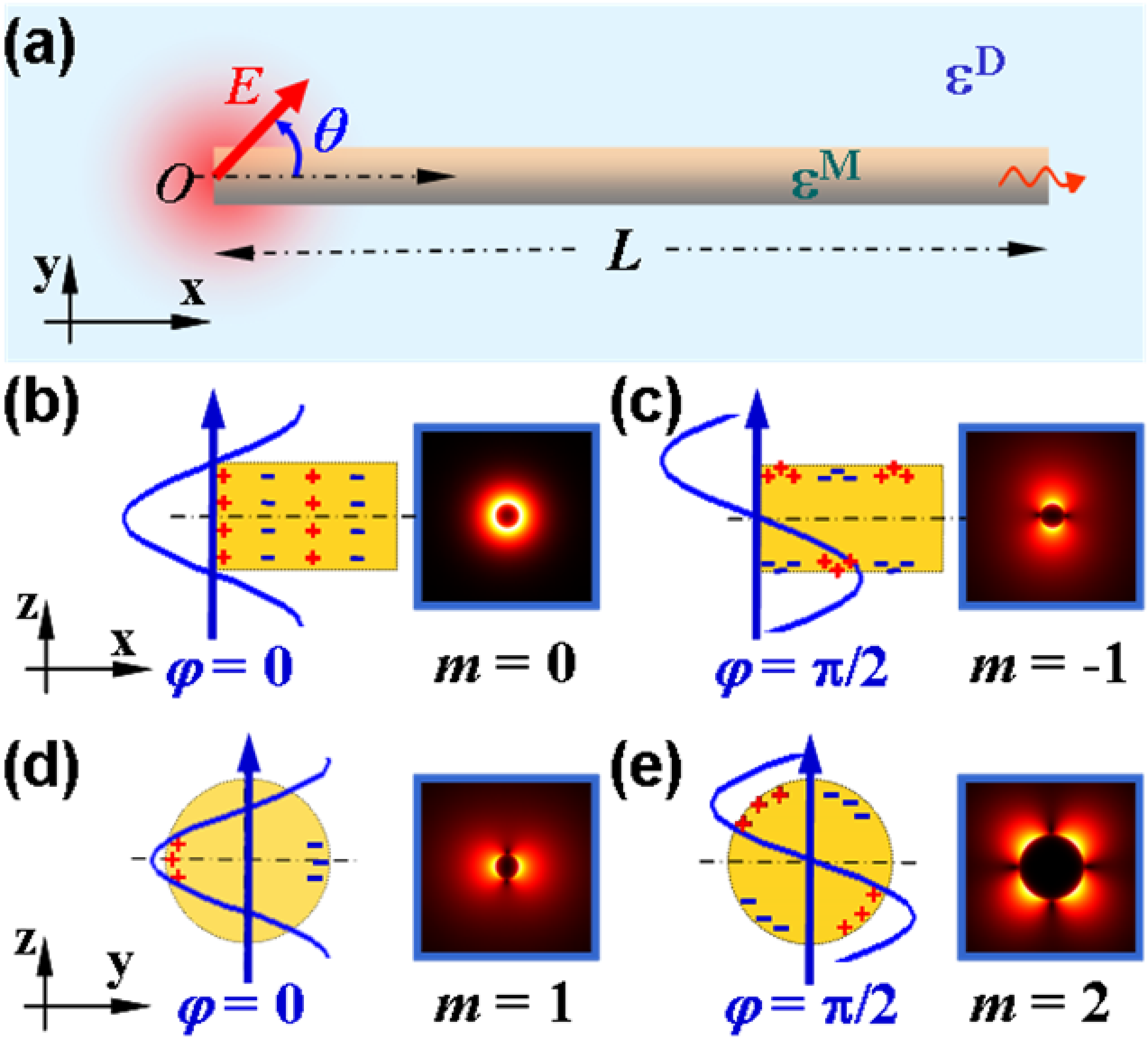

Zhang et al., PRL 107, 096801 (2011)

Mode characteristic

Field distribution outside Ag nanowire:

$$E_m(\vec{r}) = A_m K_m(k_\perp r)\exp(ik_P z)$$

Effective refractive index:

$$n_{eff} = k_P / k_0$$

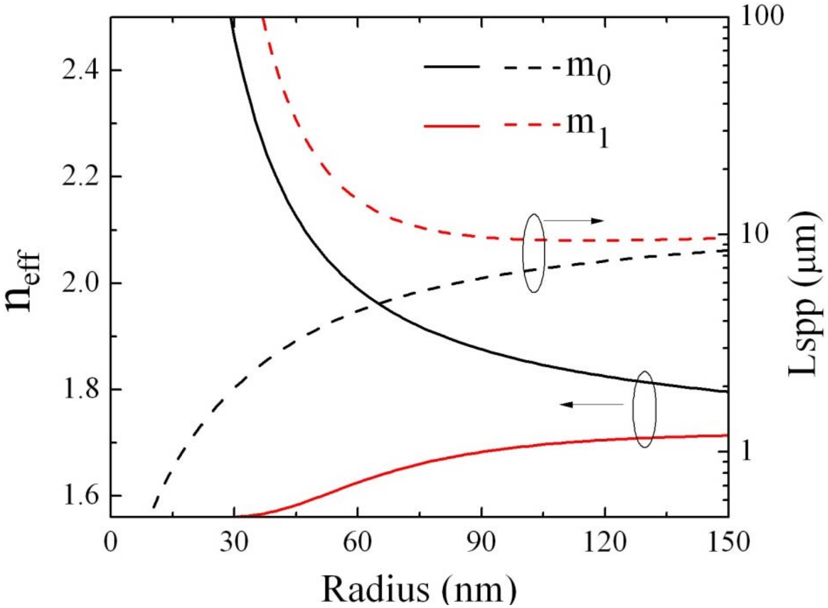

λ =633nm n_d=1.56

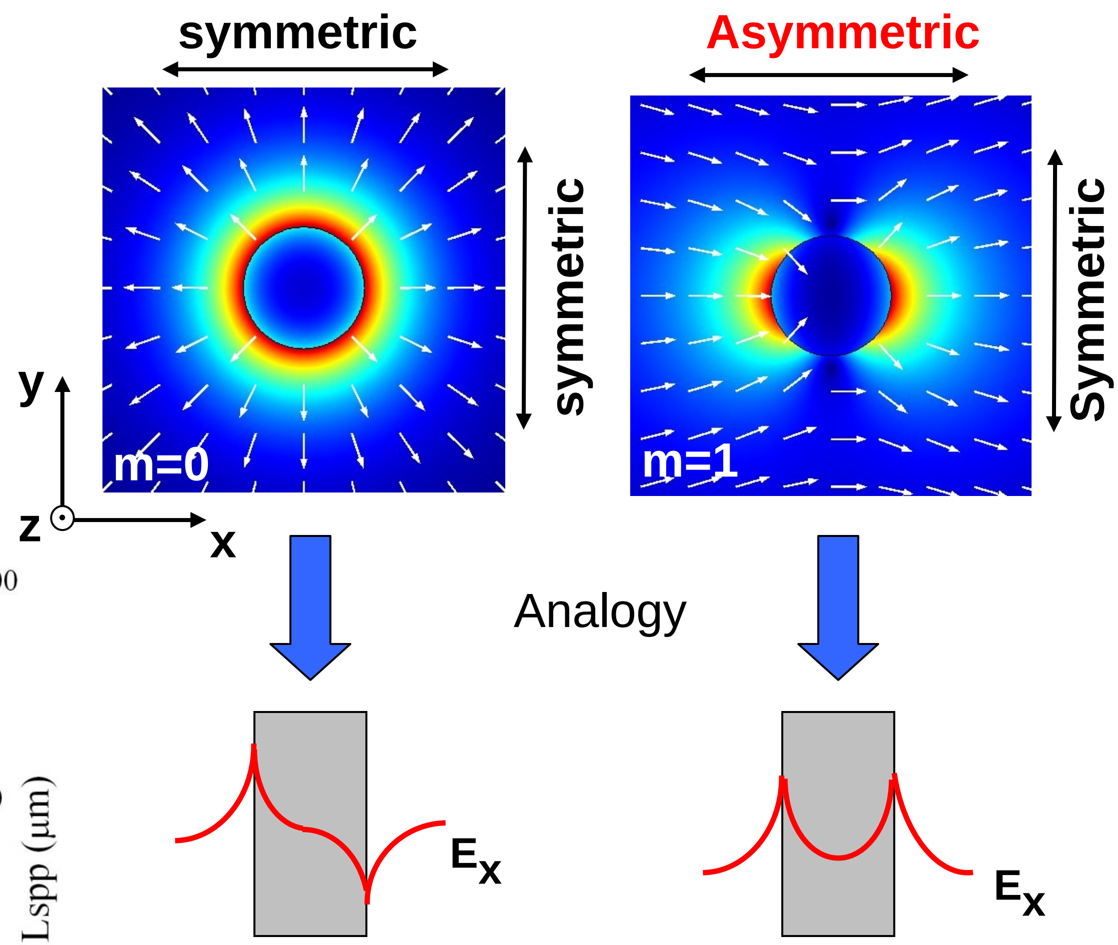

R → 0

Stop propagation for increasing loss

R → 0

Evolve into plane wave

Mode superposition

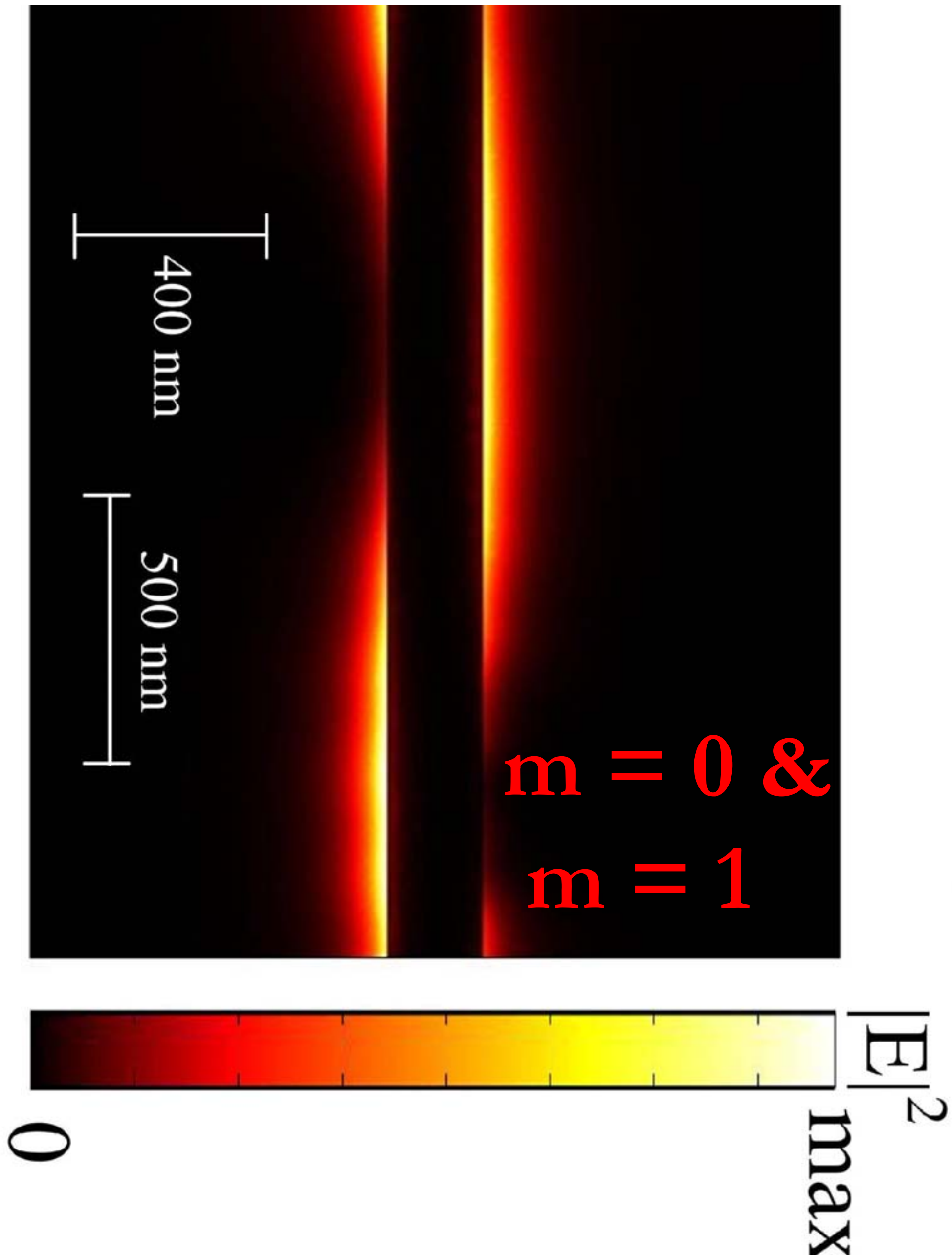

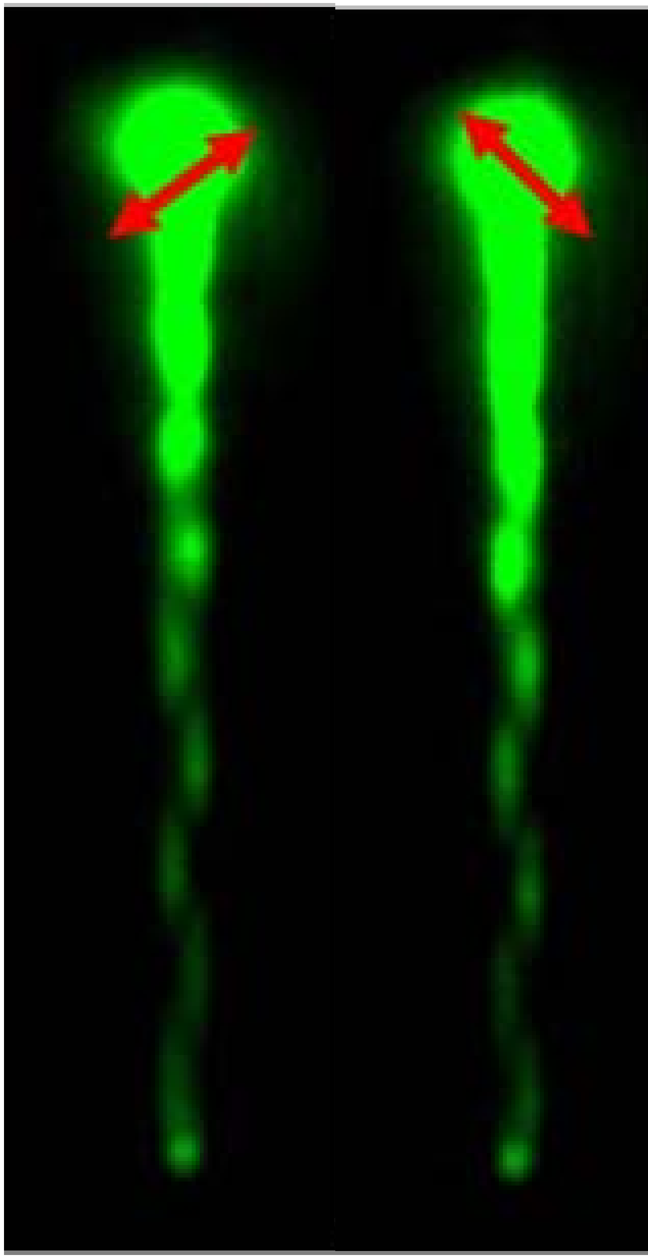

Chiral surface plasmon polaritons

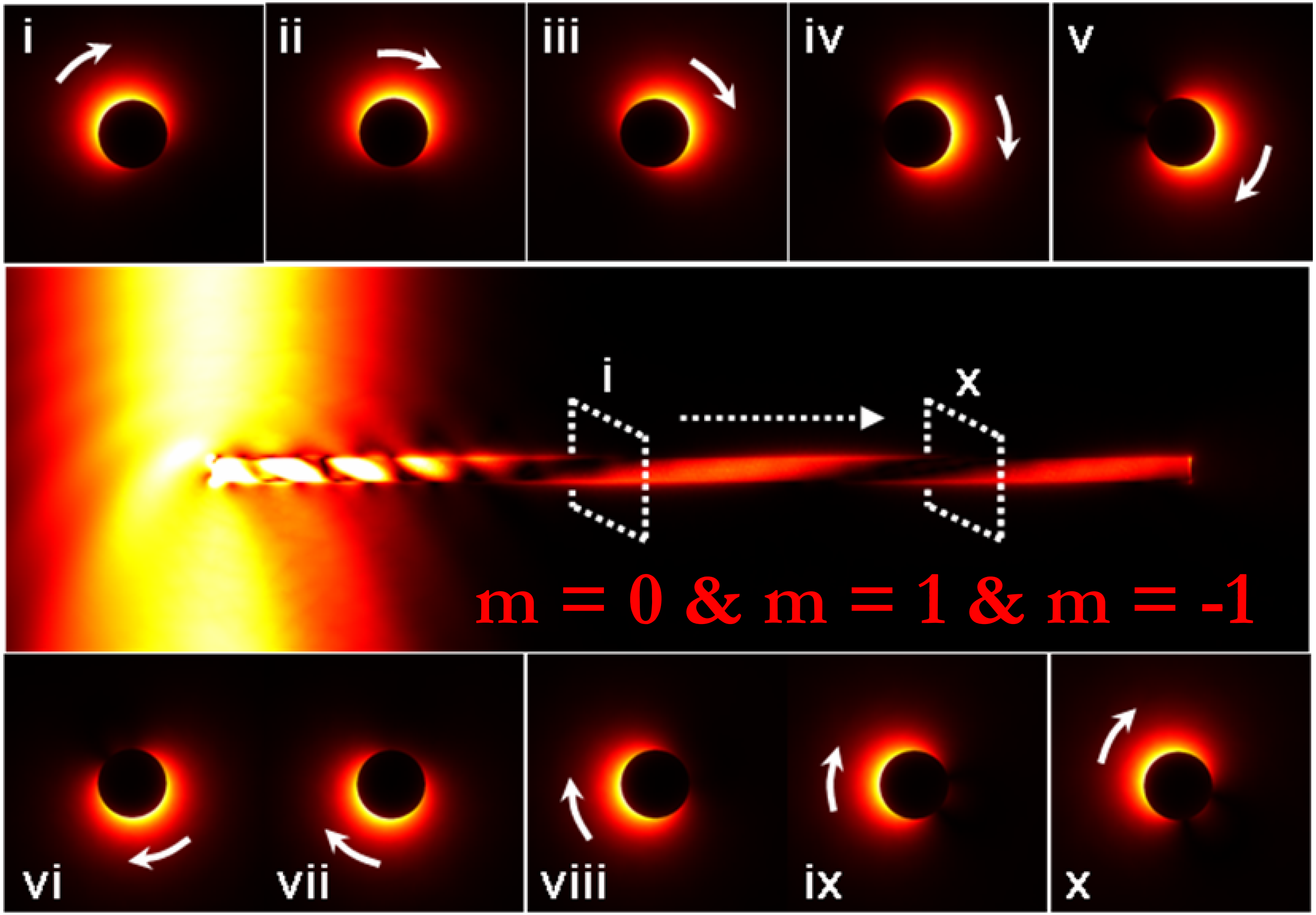

Zhang et al., PRL 107, 096801 (2011)

Chiral surface plasmon polaritons

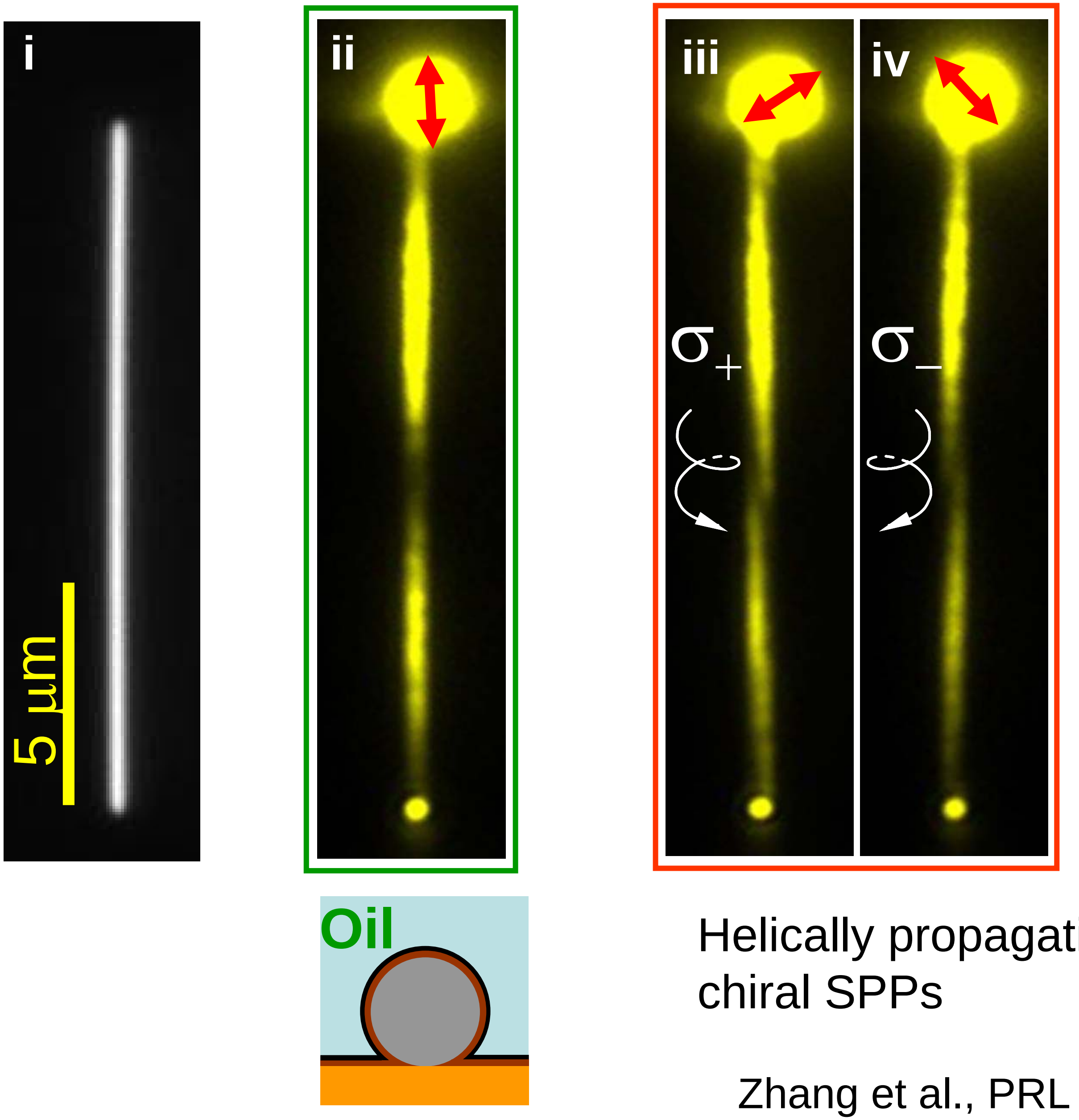

Helically propagating chiral SPPs

Zhang et al., PRL 107, 096801 (2011)

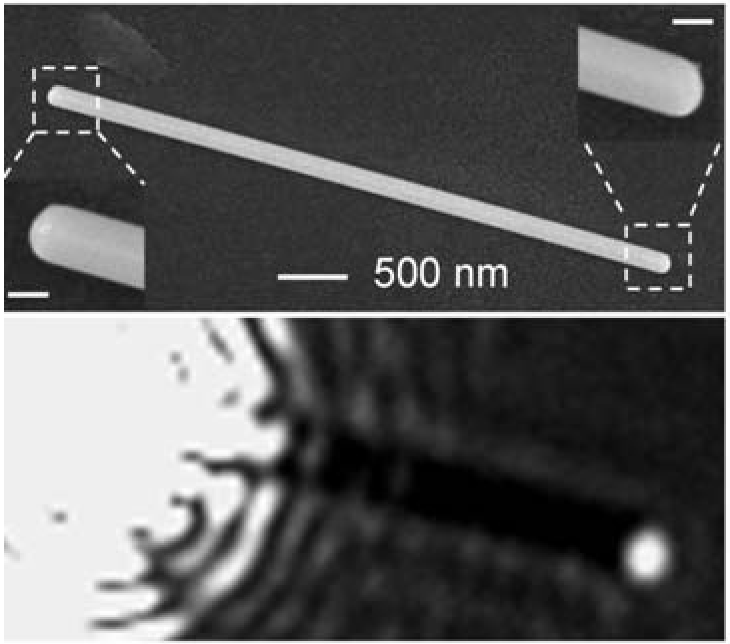

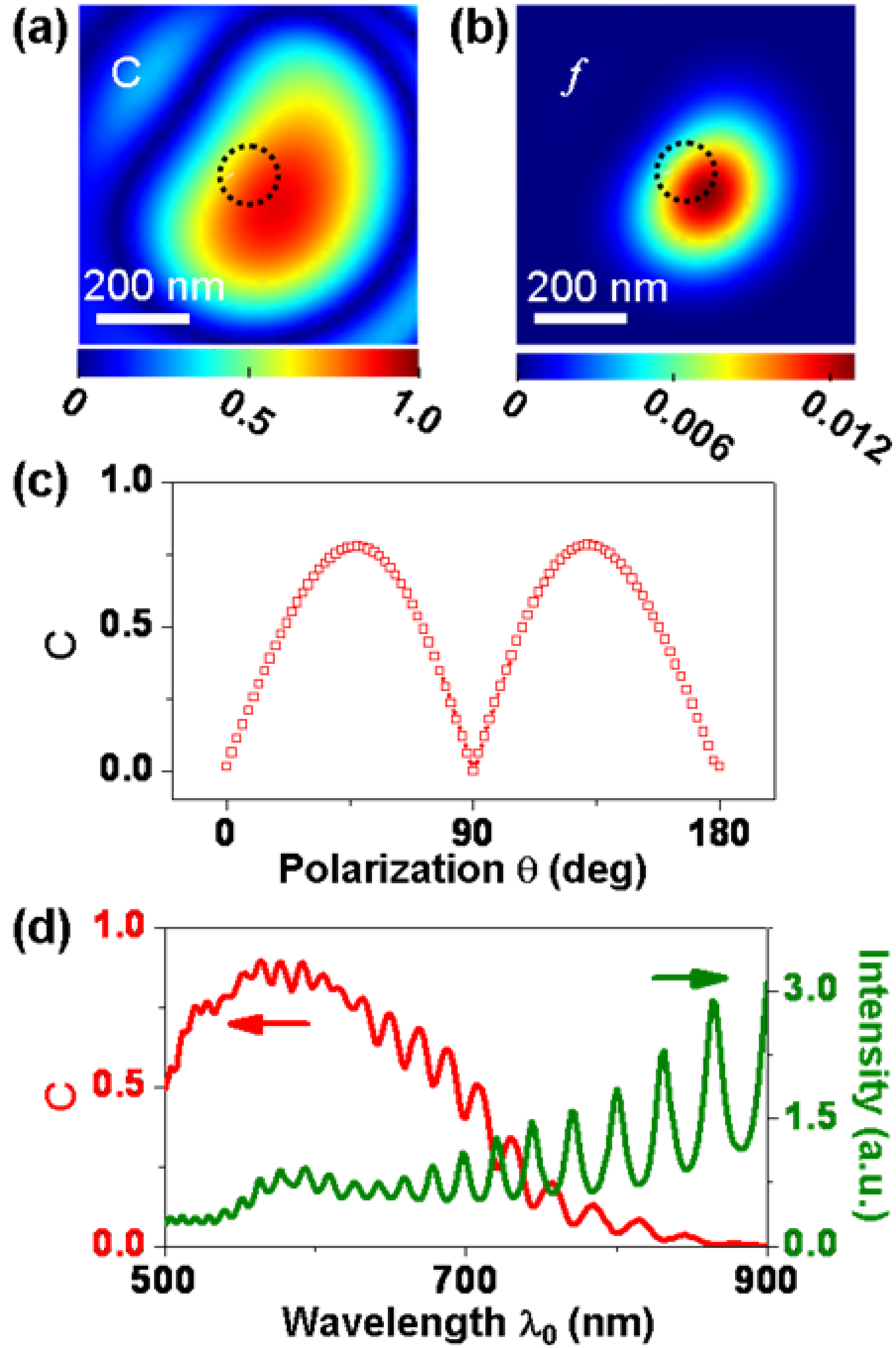

Degree of circular polarization C

$$C = \frac{2\langle E_y(t)E_z(t)\sin(\delta_y - \delta_z)\rangle}{\langle E_x^2(t)\rangle + \langle E_y^2(t)\rangle + \langle E_z^2(t)\rangle}$$

Figure of merit *f*

$$f = I \times C^2$$

Zhang et al., PRL 107, 096801 (2011)

Outline

- Near-field, Network and Logic
- Wire plasmon modes/Chiral wire plasmons
- **Tunable wire plasmons**
- Substrate-Mediated Plasmon
- Plasmon Amplification

等离激元传播的调控— Controlling near field beating period

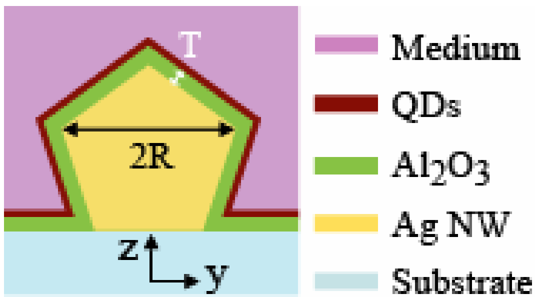

Al_2O_3 thickness

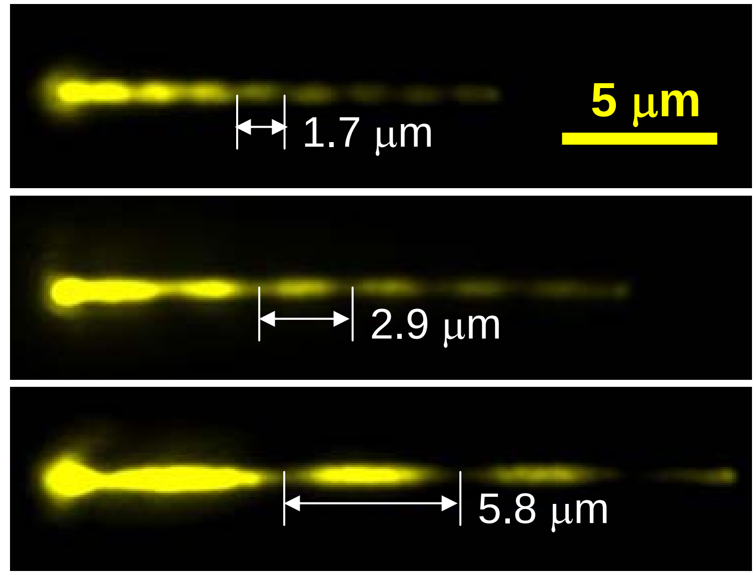

30 nm

50 nm

80 nm

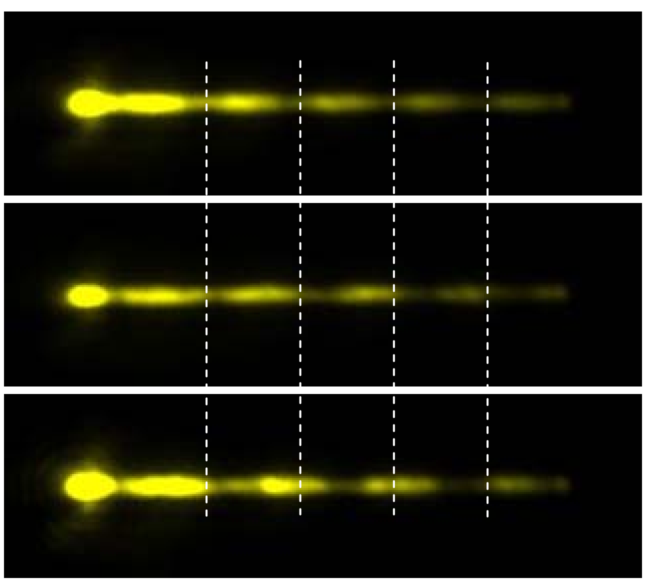

Ag NW of radius 155 nm coated with 30 nm Al_2O_3

2.9 μm

+ 5 nm Al_2O_3

3.3 μm

+ 10 nm Al_2O_3

3.8 μm

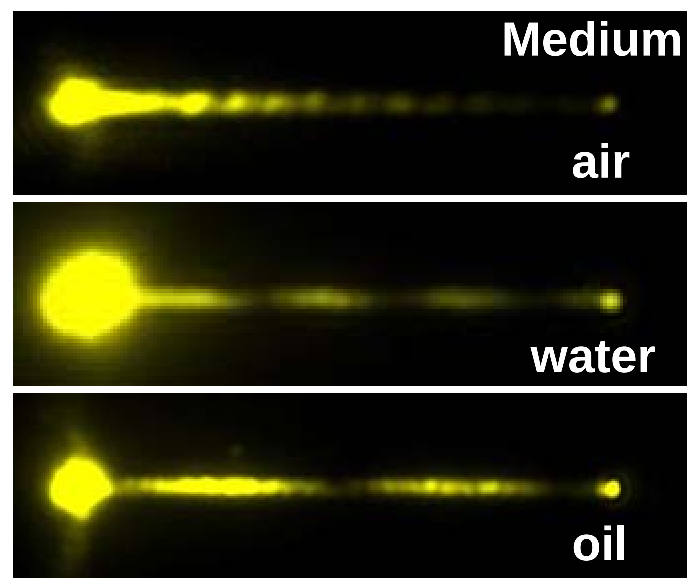

Period

1.3 μm

4.4 μm

7.2 μm

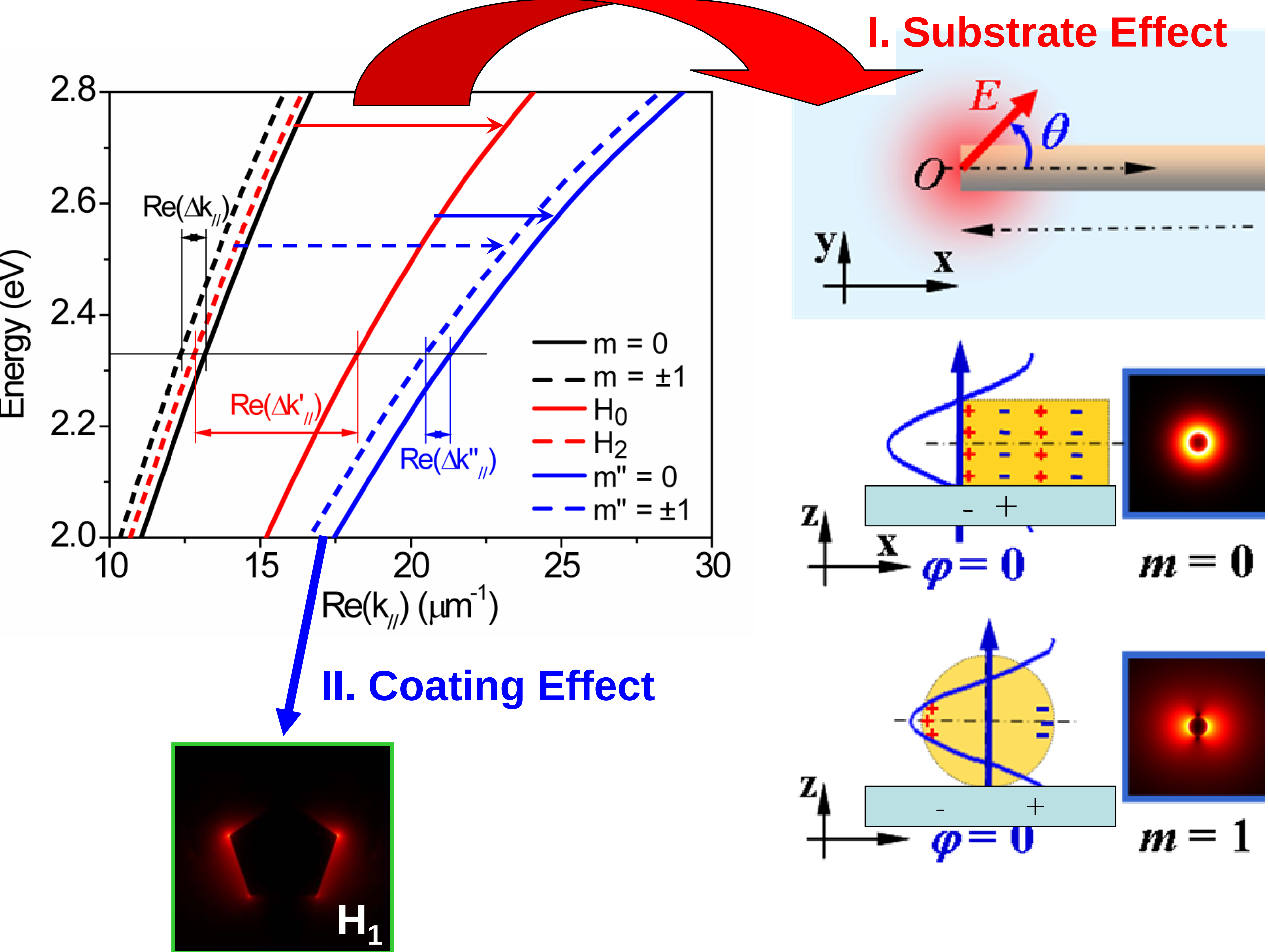

I. Substrate Effect
II. Coating Effect
Energy (eV)
Re(k//) (μm-1)
Re(Δk//)
Re(Δk'//)
Re(Δk"//)
m = 0
m = ±1
H0
H2
m" = 0
m" = ±1
E
θ
O
y
x
z
x
φ = 0
m = 0
z
φ = 0
m = 1
H1

Controlling plasmon transmission in NW networks

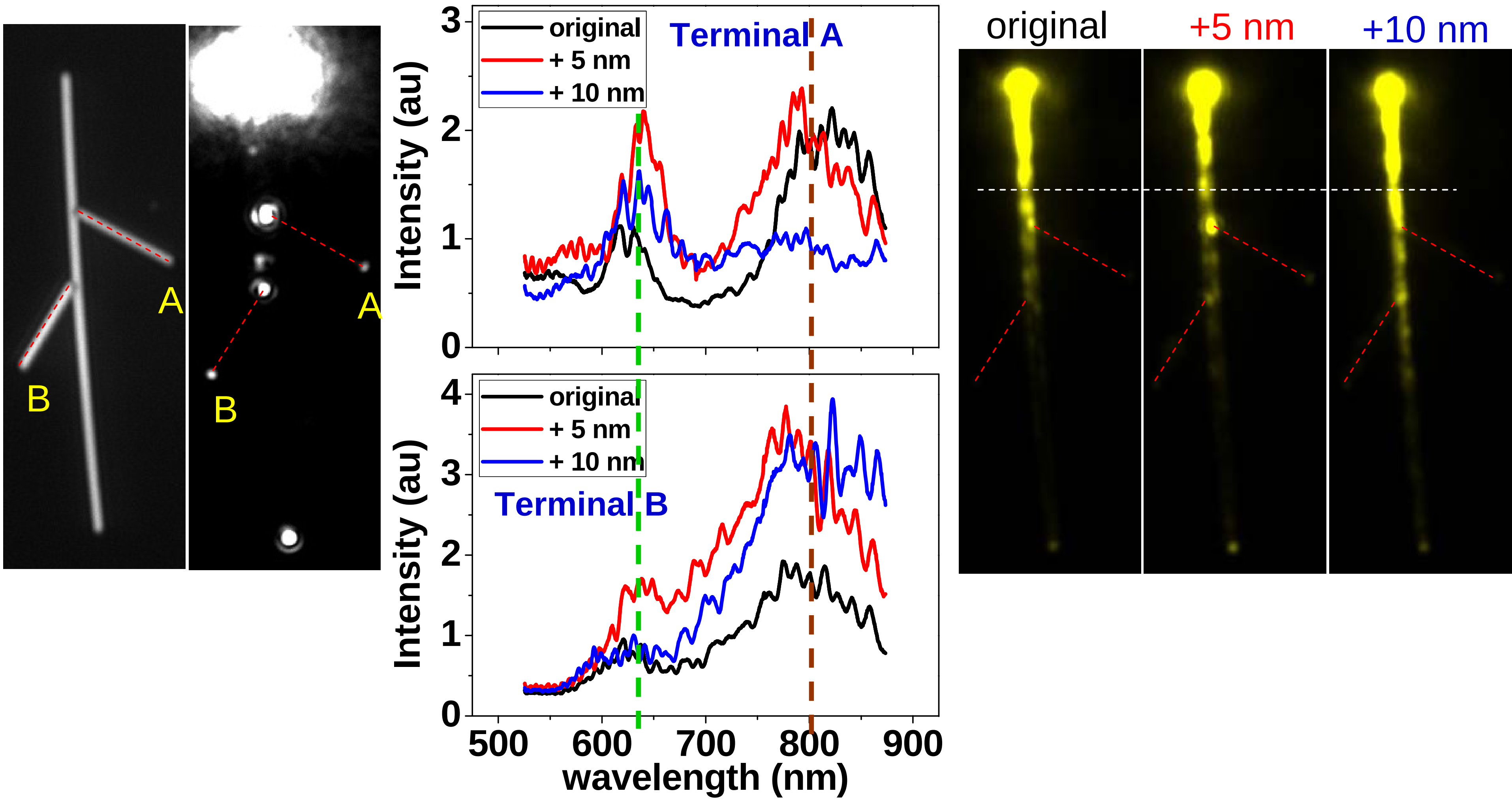

By controlling the dielectric coating thickness, plasmons of certain wavelengths can be routed to different branches.

Mode conversion

Induced by Structure Symmetry Broken

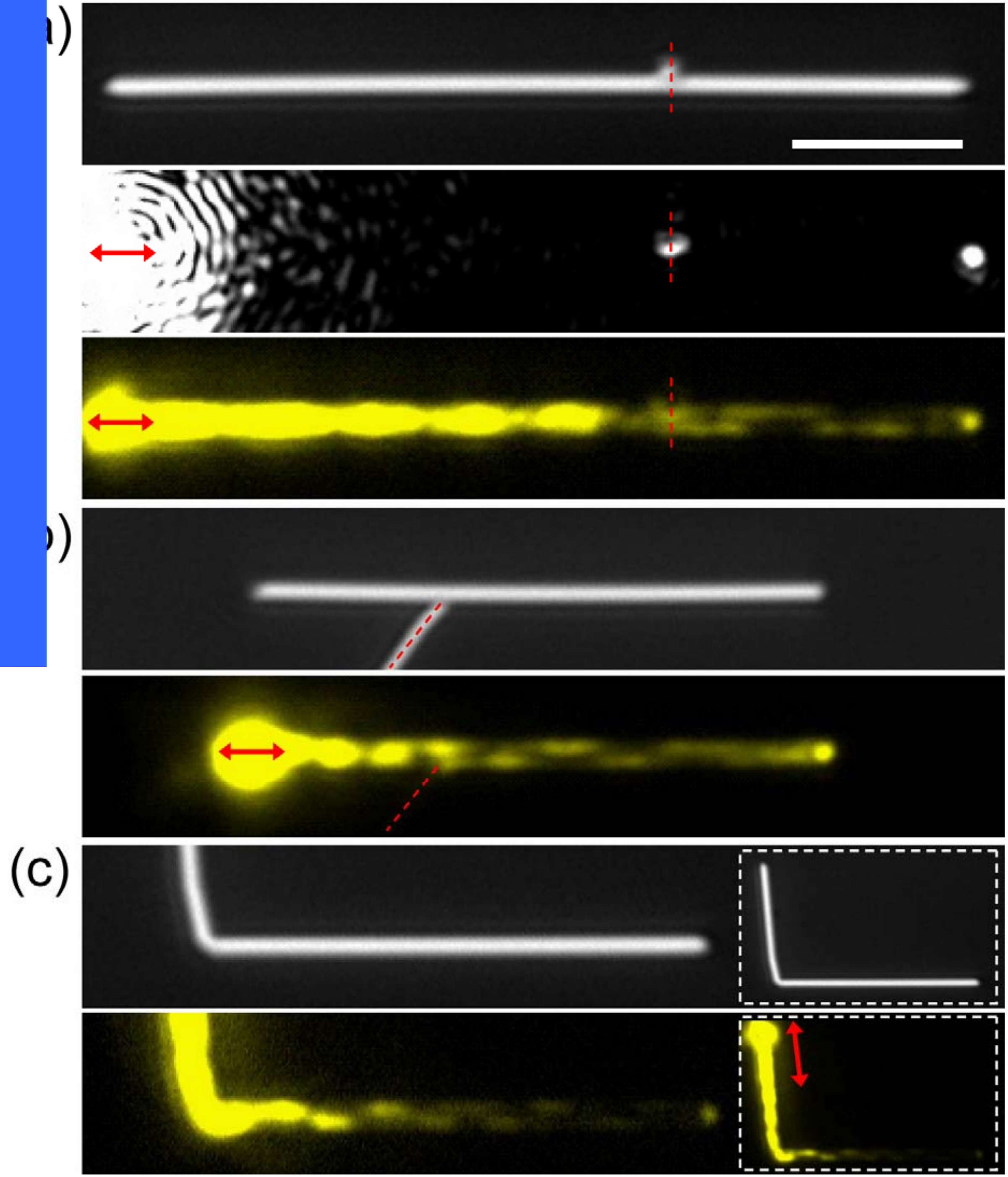

Particle-mediated mode conversion

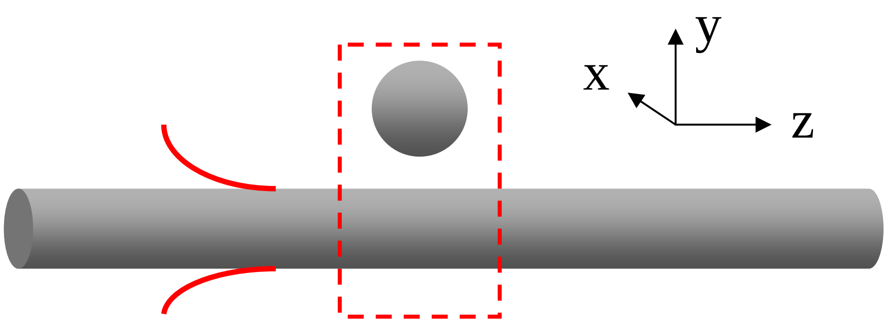

$$\hat{S} \cdot [I_{m0} \quad I_{m1}]^T = [I'_{m0} \quad I'_{m1}]$$

Symmetry:

y direction: broken

x direction: preserved

$\hat{S}$ is Hermitan matrix

Off-diagonal element is conversion efficiency

Simulation for conversion from m0 to m1

mode

m=0

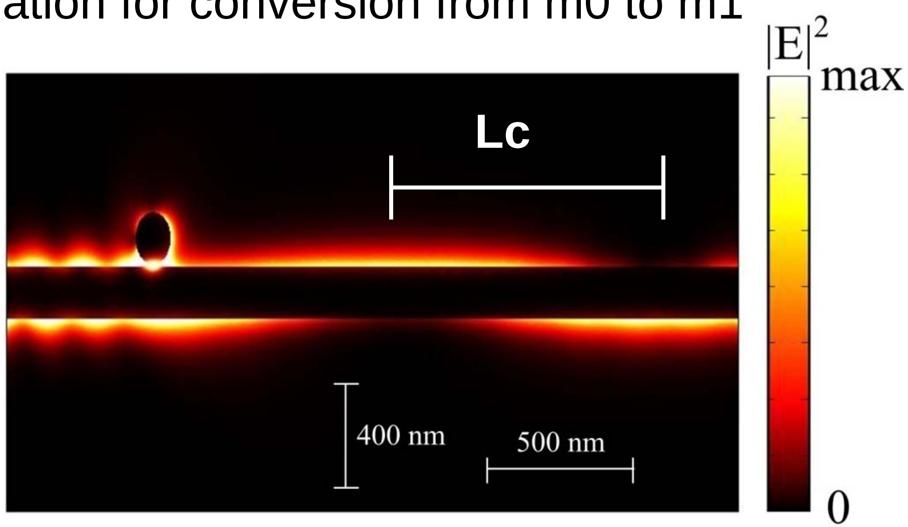

$$(n_{eff,m0} - n_{eff,m1})\frac{2\pi}{\lambda}L_C = \pi$$

$$\hat{S} \cdot [I_{m0} \quad 0]^T = [S_{11}I_{m0} \quad S_{21}I_{m1}]$$

Experiment proof

nanowire radius: 150nm

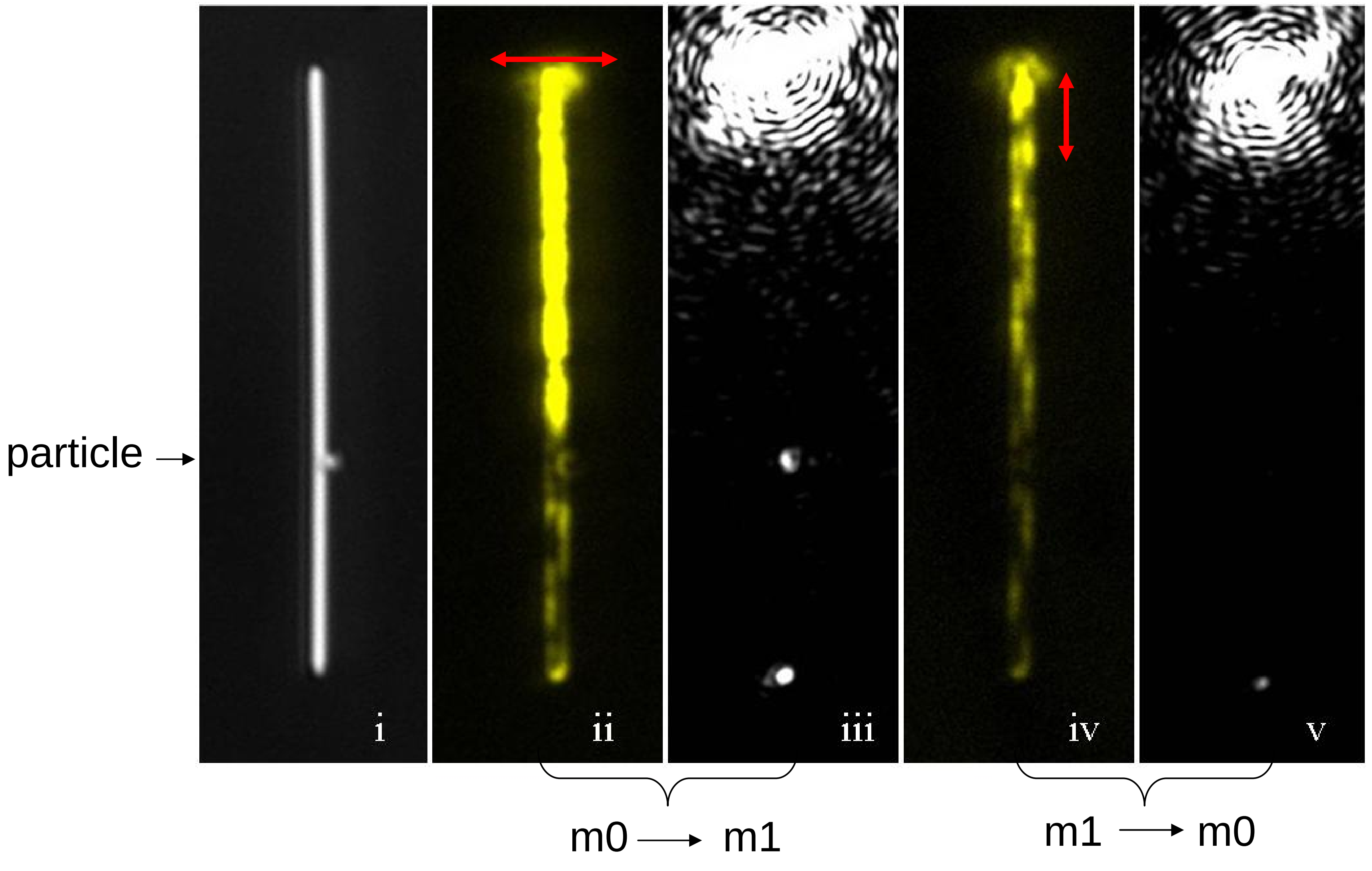

Theoretical description

◆ Expression of plasmon modes

$$|\varphi_0\rangle = \{-E \quad E\} \qquad |\varphi_1\rangle = \{E \quad E\} \qquad \phi = 0: \{0 \quad 2E\} \qquad \phi = \pi: \{2E \quad 0\}$$

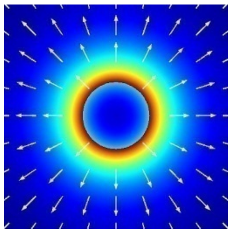

$+\ e^{i\phi}$

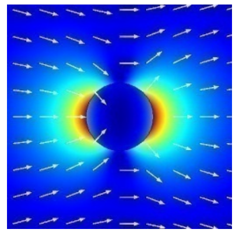

$=$

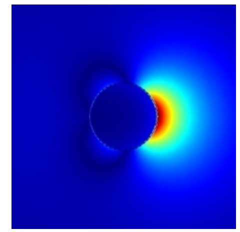

or

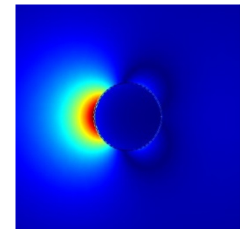

Power of the two modes: $\mathrm{I}_0 \approx \mathrm{I}_1$

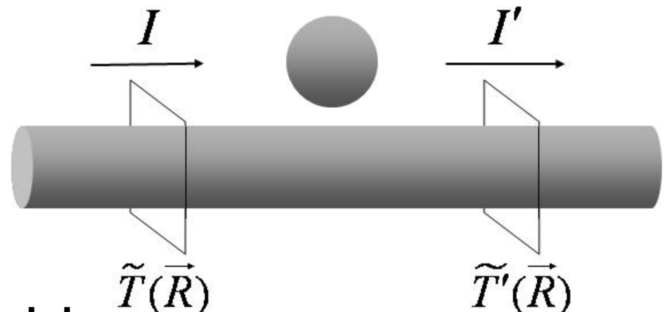

◆ TM_0 as incident: $\tilde{T}_0 = |\varphi_0\rangle = \{-E \quad E\}$

scattering mainly influence field on one side

$$\tilde{T}' = \{-\tilde{t}_0 E \quad E\} = (\tilde{t}_0 + 1)/2|\varphi_0\rangle - (\tilde{t}_0 - 1)/2|\varphi_1\rangle$$

$$I' = \left(|\tilde{t}_0|^2 + 1\right) I_0 / 2$$

$$S_{11} = (\tilde{t}_0 + 1)^2 / 4 \qquad S_{21} = (\tilde{t}_0 - 1)^2 / 4$$

Two conversion processes

I Direct scattering:

Dipole: radiative

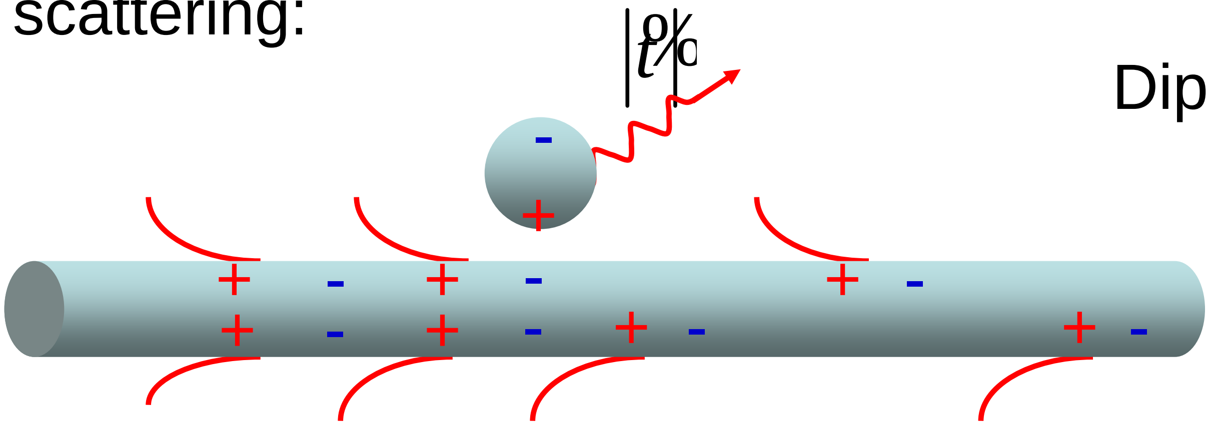

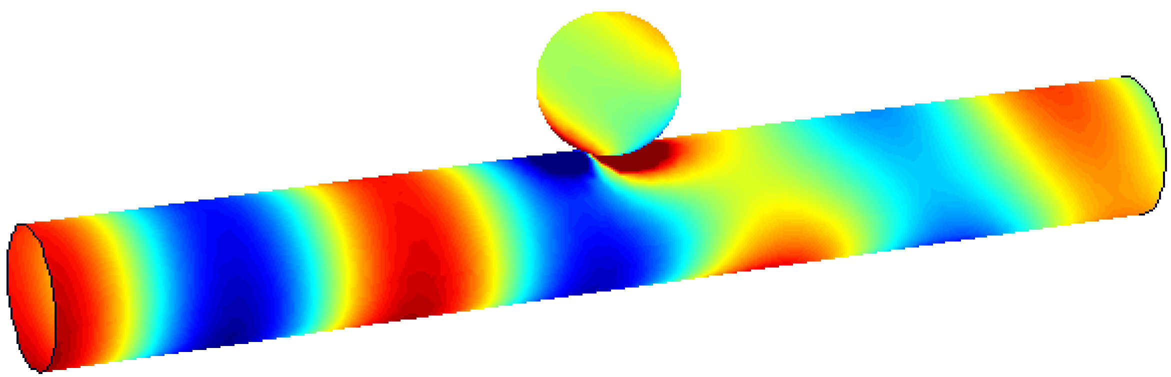

λ = 633 nm

Off Resonance

Two conversion processes

II Recollection: $\arg\left(t\%\right)$

Quadrupole:
near field coupling

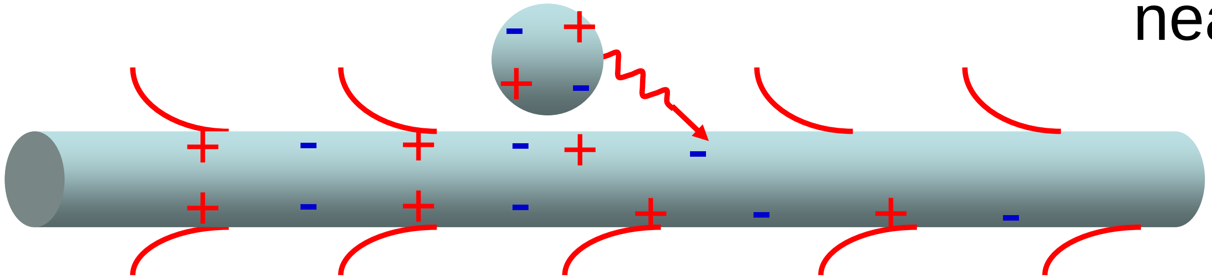

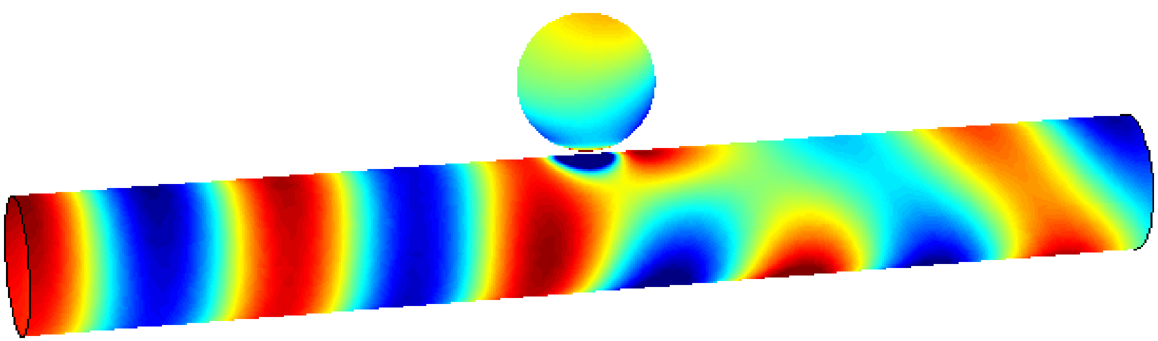

$\lambda =$ **500 nm**
Phase retardation

Process I dominant region:

Power of two modes at output for varying h. (Normalized by input power)

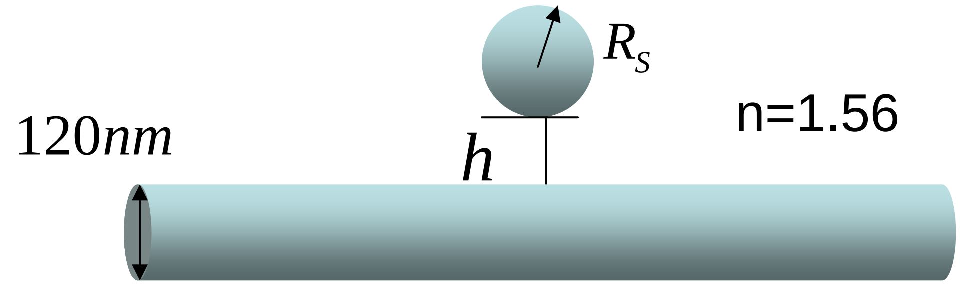

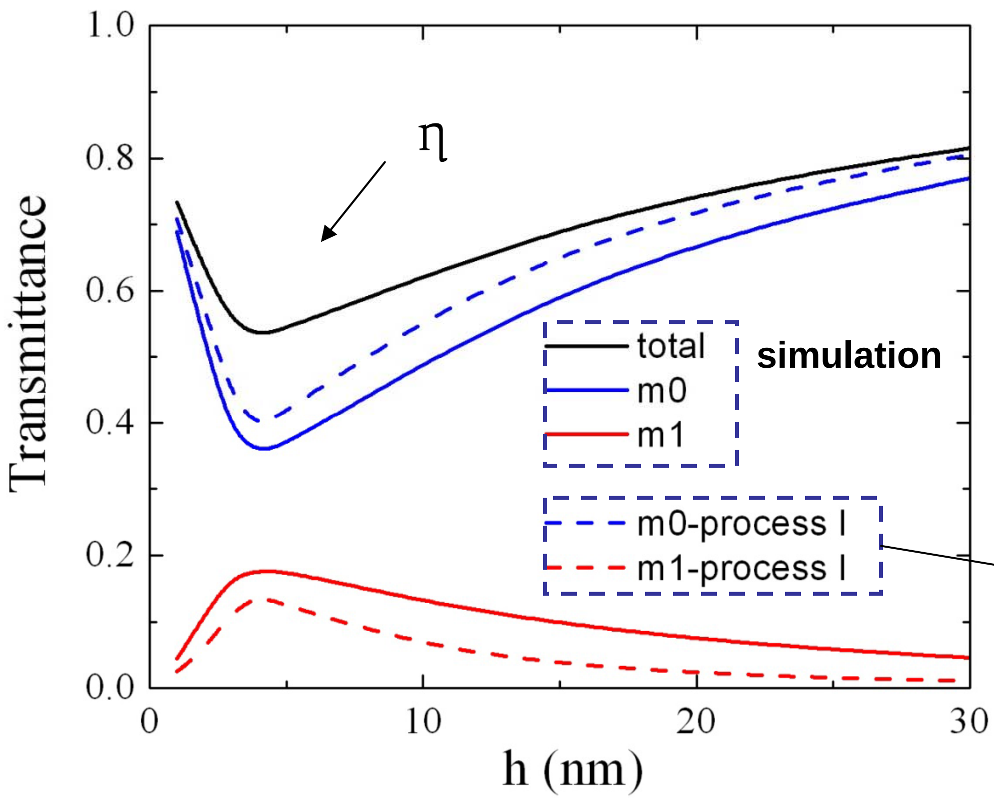

1. Get simulation result
2. Coefficient |t|:

$$|t| = \sqrt{2\eta - 1}$$

3. Conversion efficiency of through process **I**

$$\left(|t| \pm 1\right)^2 / 4$$

$\lambda = 633nm$ Rs=60nm far away from quadrupole resonance $\omega_{\mathbf{quad}}$

Process II dominant region:

Power of two modes at output for varying wavelength (h=7nm)

Conversion efficiency for Process II

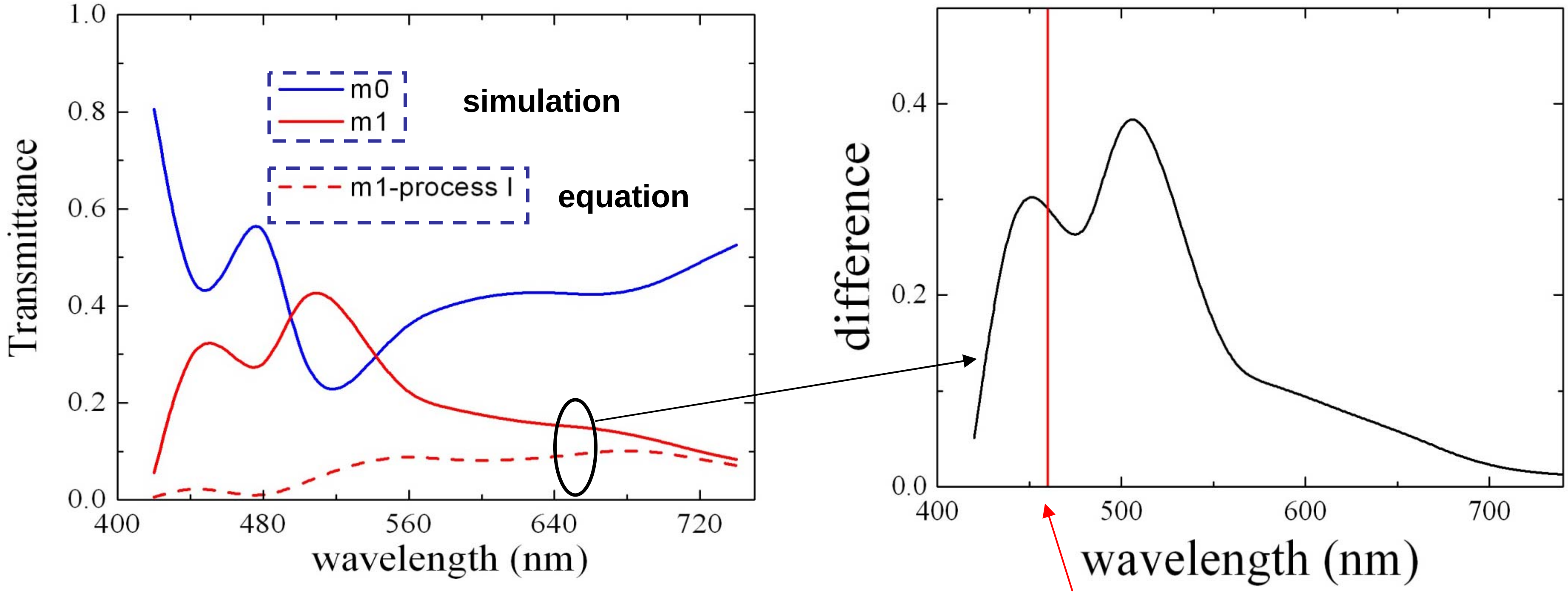

Process II dominat:

Far from $\omega_{\mathbf{quad}}$

Process I dominat:

Far from $\omega_{\mathbf{quad}}$

Quadrupole resonance

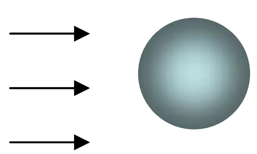

$n_{eff,m0}$

Application for switch

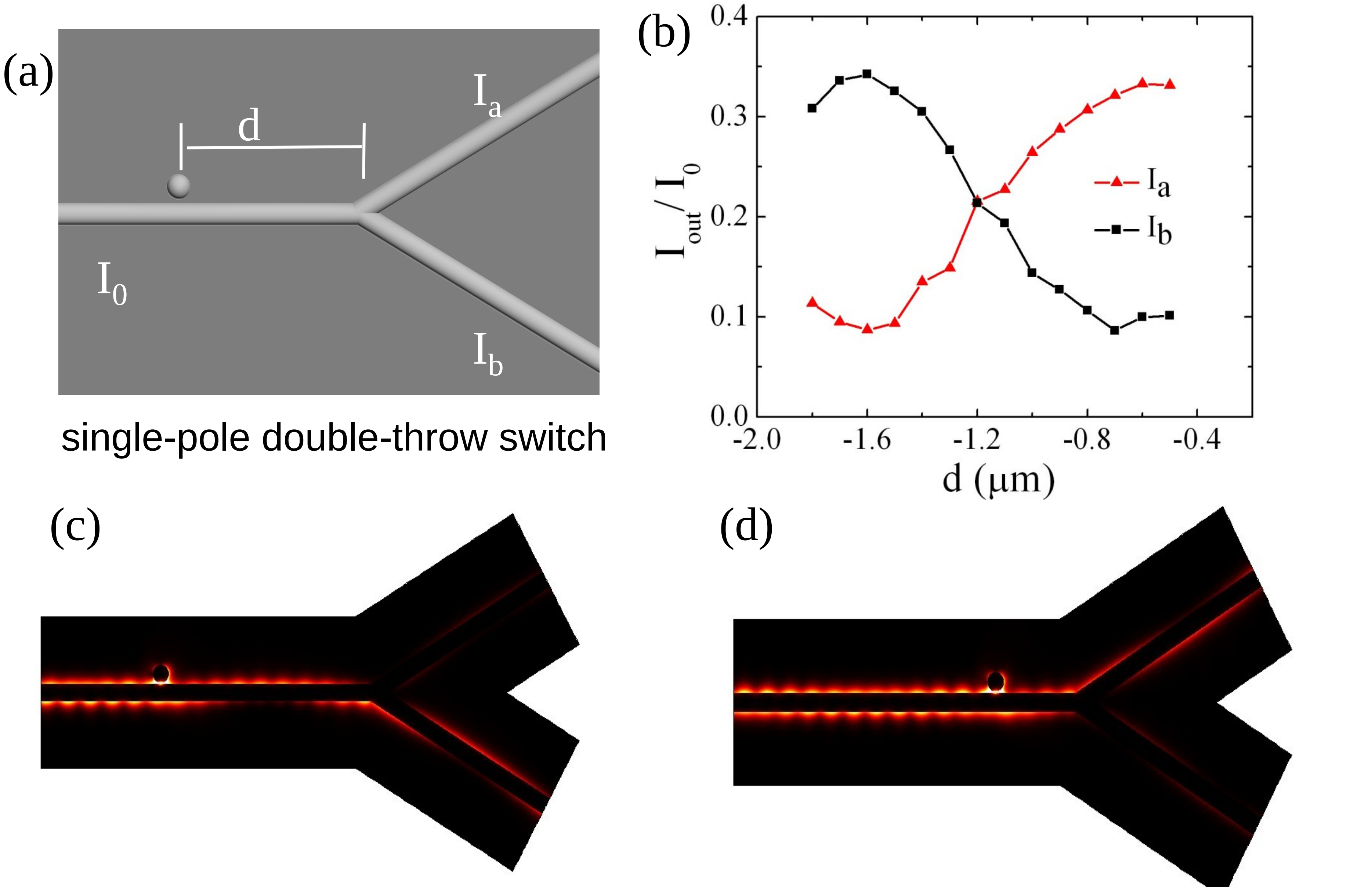

Outline

- Near-field, Network and Logic
- Wire plasmon modes/Chiral wire plasmons
- Tunable wire plasmons
- **Substrate-Mediated Plasmon**
- Plasmon Amplification

Substrate-Mediated Plasmon Coupling

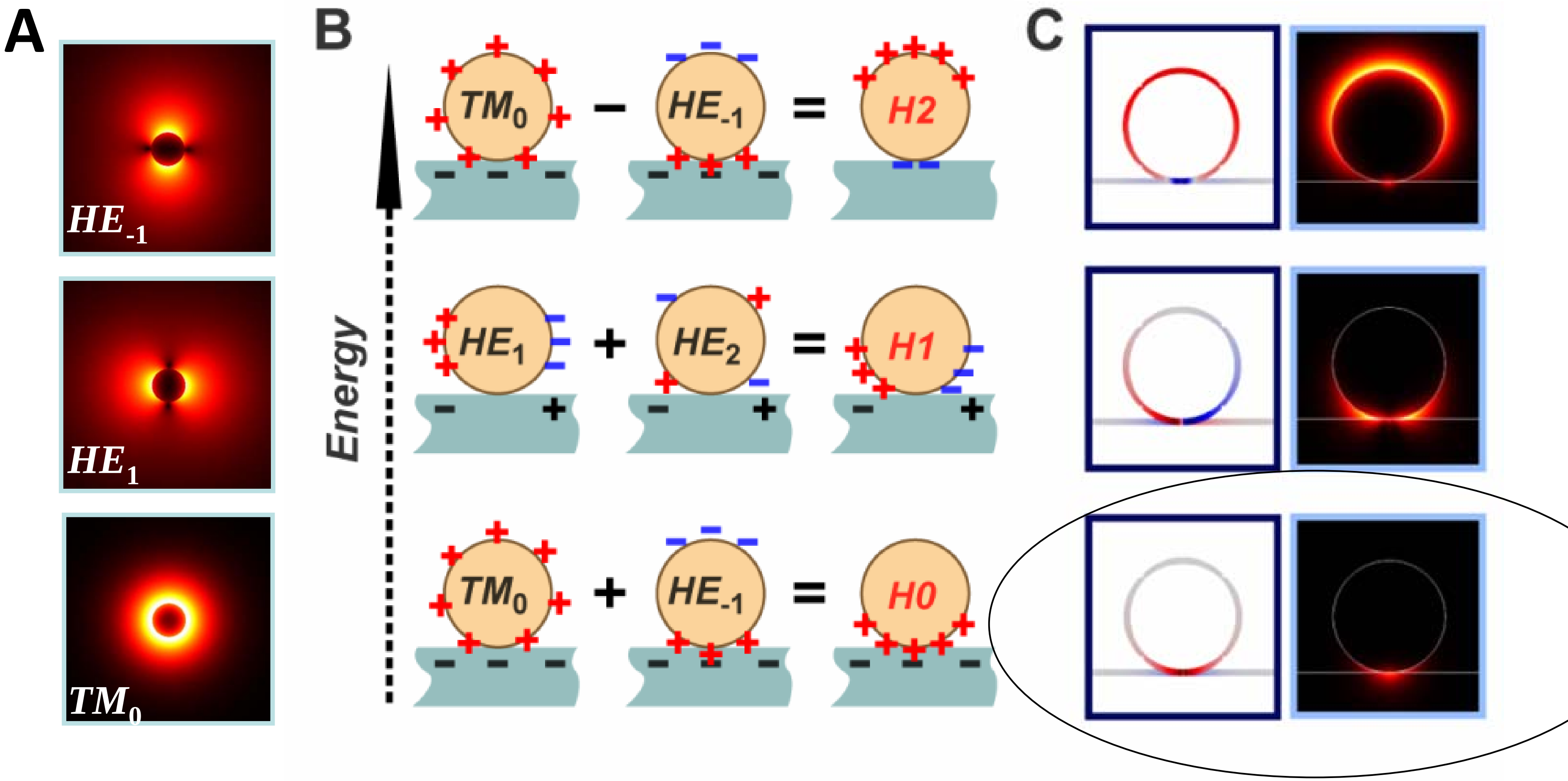

wire SPPs in air + Coupling via substrate = Hybridized modes

Zhang & Xu ACS Nano, accepted

Leaky radiation into substrate

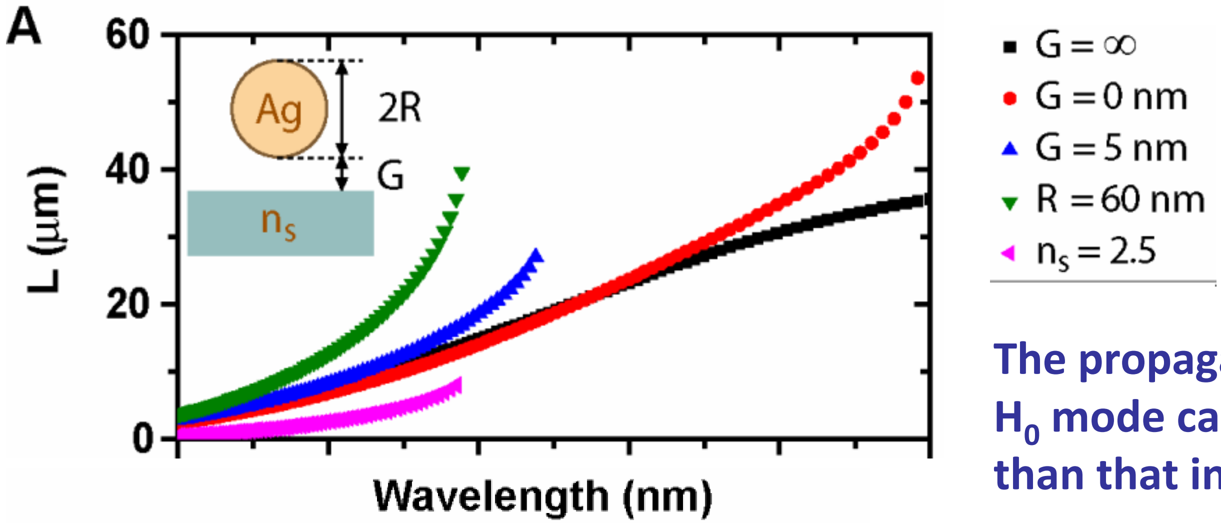

The propagation length of the H_0 mode can be larger in NWOS than that in air.

When the phase constant $\beta < n_s \cdot k_0$, the mode can leak into the substrate as it propagates along the nanowire. This is an big drawback for the NWOS configuration.

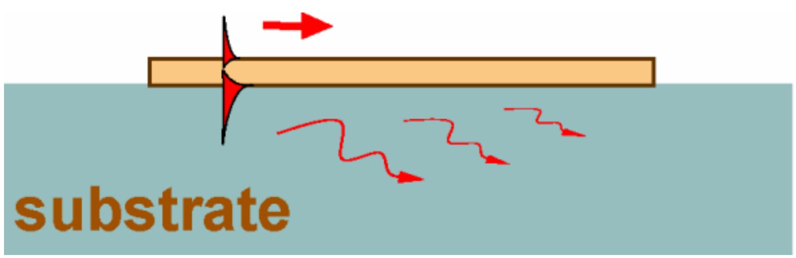

Shegai T et al., Unidirectional Emission …
Nano Lett. 11, 706–711 (2011)

Leaky region

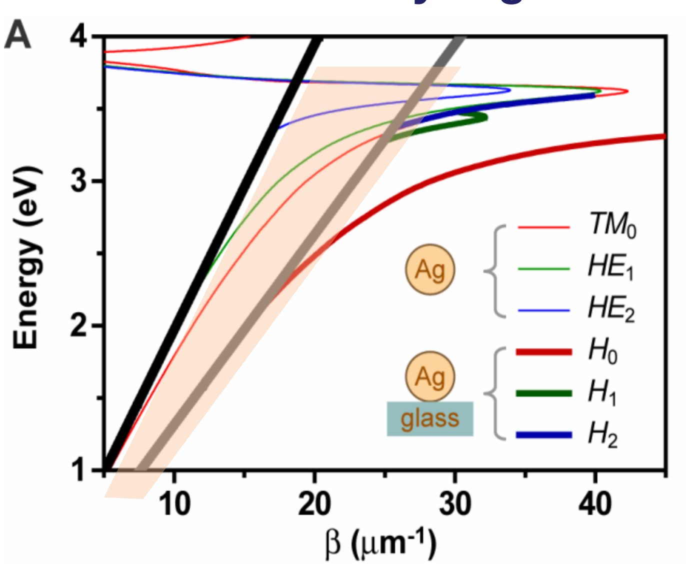

Zhang & Xu ACS Nano, accepted

Bound vs. Leaky region

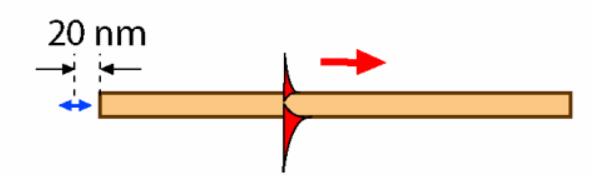

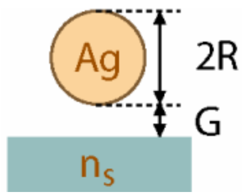

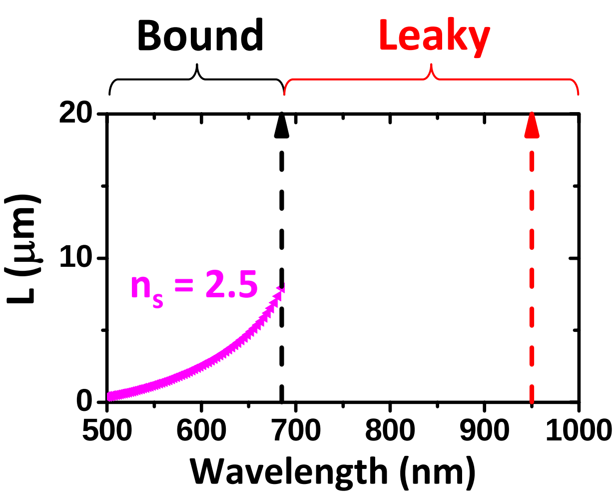

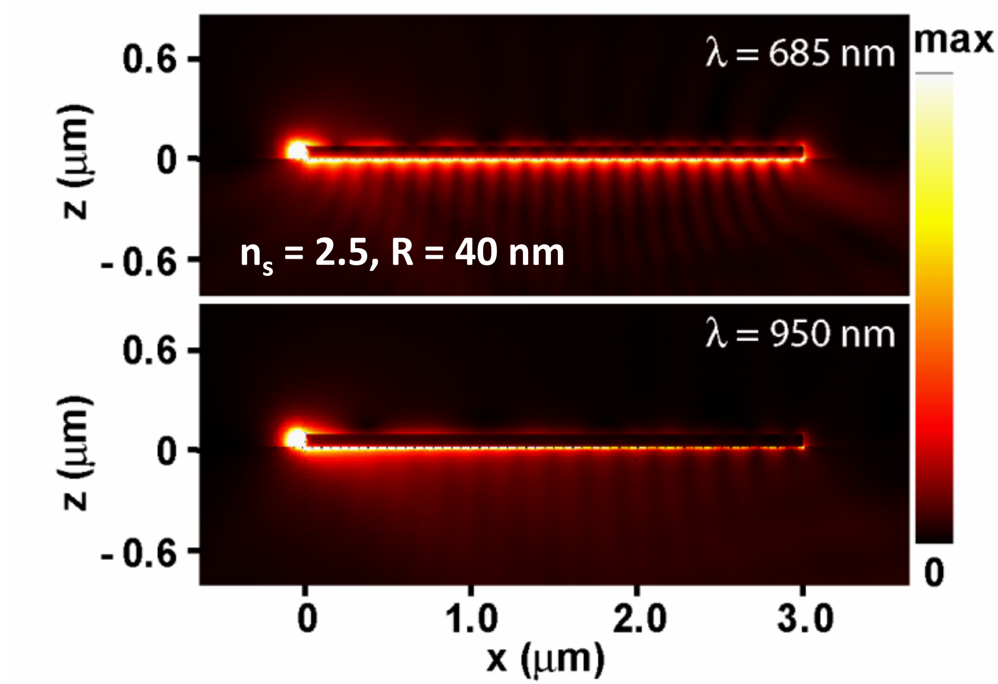

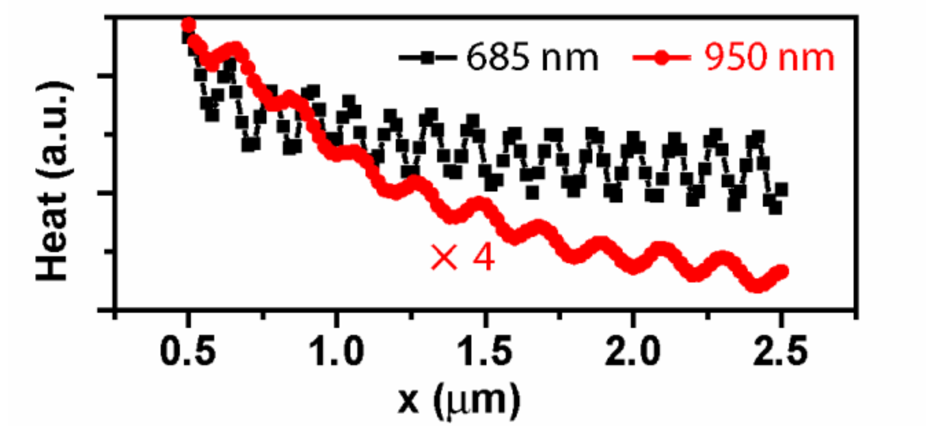

Leakage raises the propagation losses, which prevents the NWOS to work with high-permittivity substrate and in long-wavelength region

Zhang & Xu ACS Nano, accepted

Layered substrate provides an optical barrier

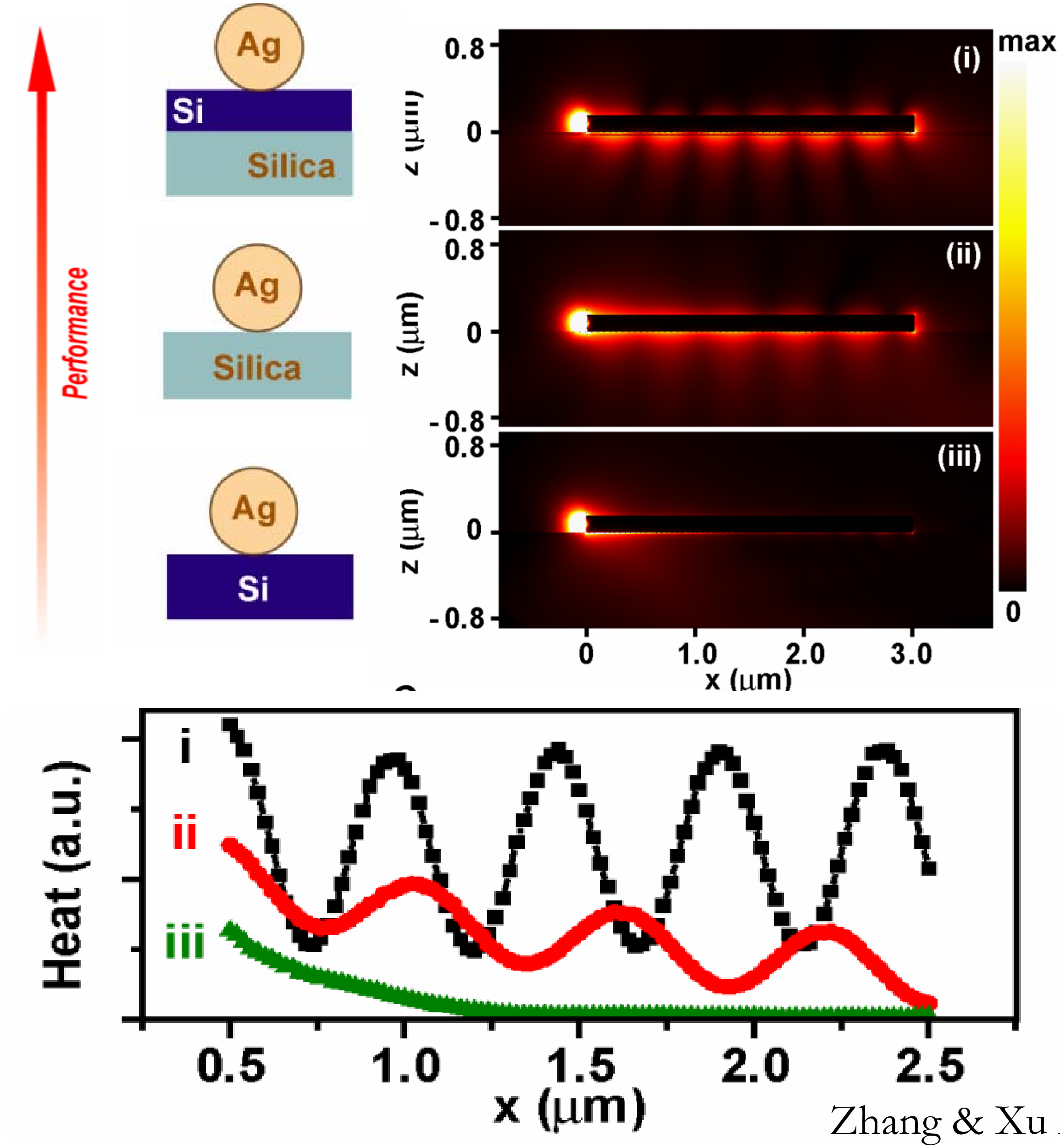

λ = 1550 nm

The thickness of the Si layer T = 30 nm in (i).

Zhang & Xu ACS Nano, accepted

Outline

- Near-field, Network and Logic
- Wire plasmon modes/Chiral wire plasmons
- Tunable wire plasmons
- Substrate-Mediated Plasmon
- **Plasmon Amplification**

CdSe nanobelt/Al_2O_3/Ag hybrid plasmonic waveguide

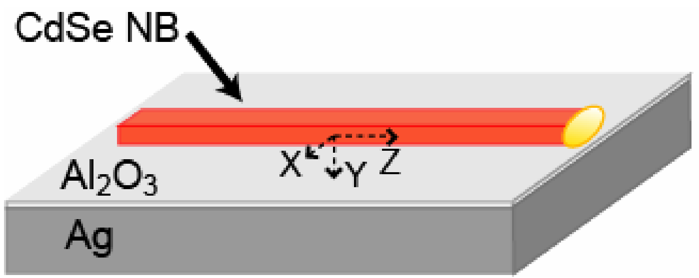

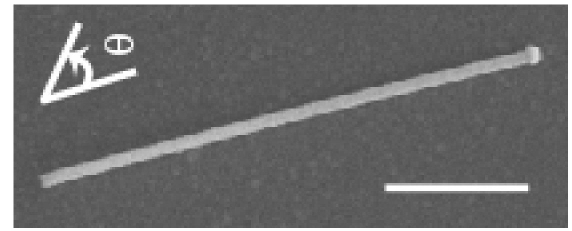

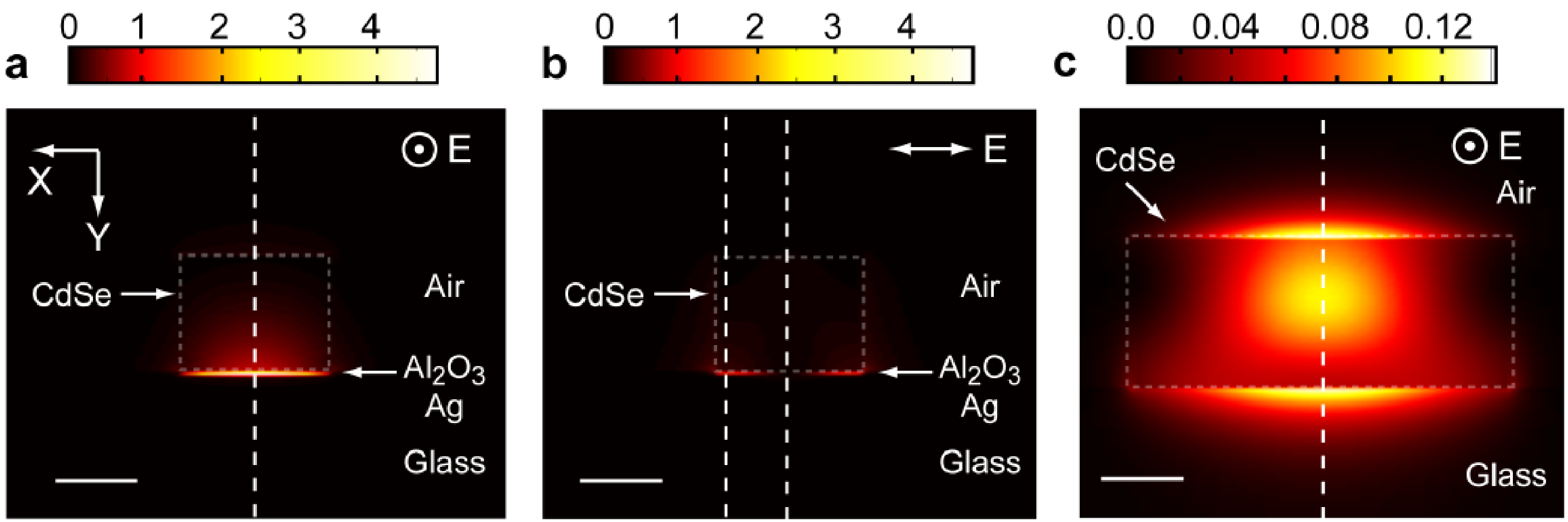

plasmonic

photonic

Liu N, *et al*., Scientific Reports 3, 1967 (2013)

Weak signal amplification in plasmonic waveguides

"Pump-Probe" setup to measure optical gain of plasmonic waveguides

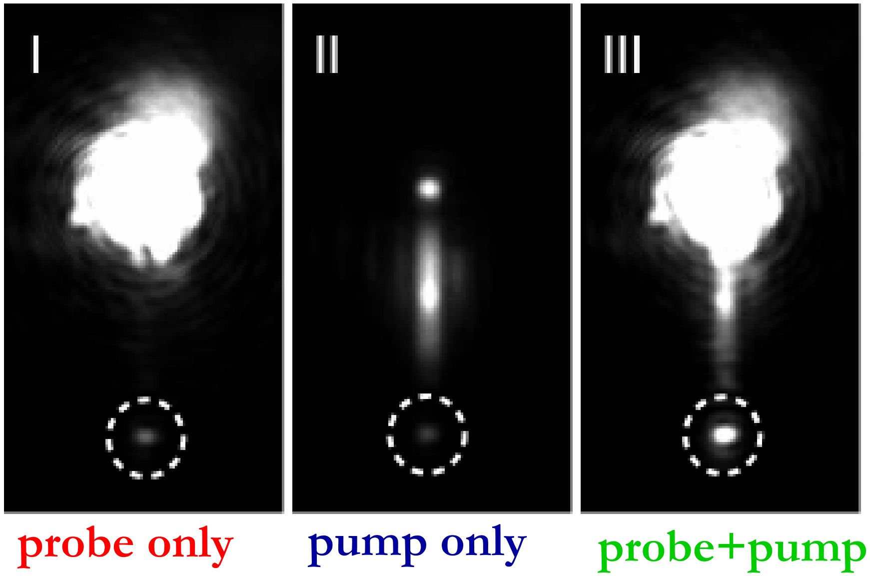

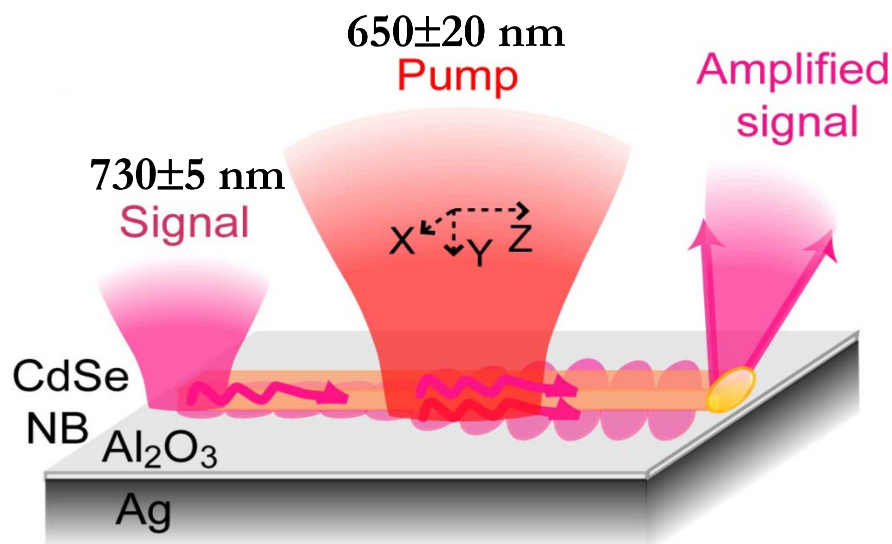

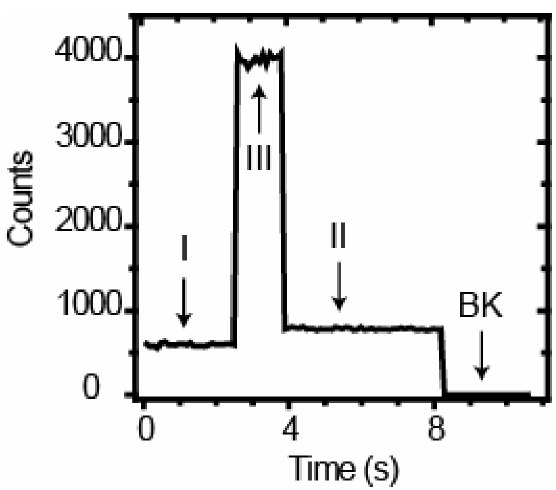

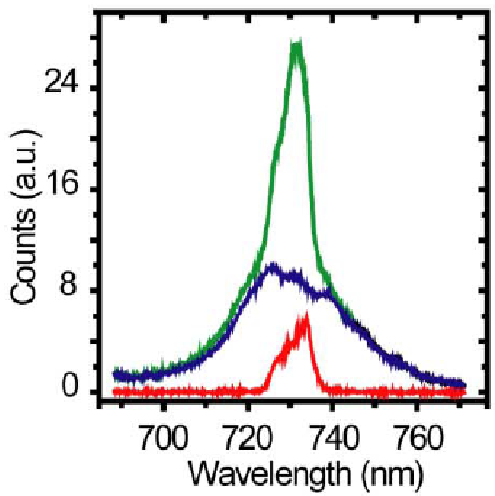

All wavelengths in the probe signal, spanning over 10 nm, are amplified.

broadband loss compensation

Liu N, *et al.*, Scientific Reports 3, 1967 (2013)

gain for TM and TE modes

$$G(\mathrm{dB}) = 10\log\left(\frac{I_{on} - I_{sp}}{I_{off}}\right) = 10\log(G)$$

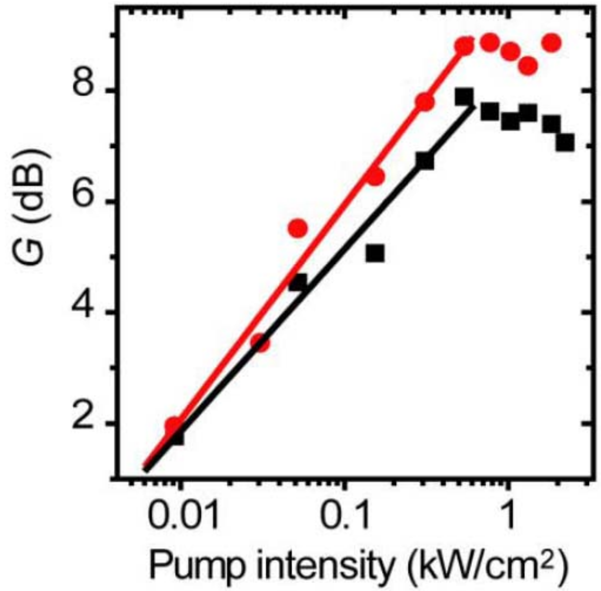

■ : parallel polarization (TM)

● : perpendicular polarization (TE)

Internal gain coefficient:
g = 6140 cm-1 for TM mode;
g = 6755 cm-1 for TE mode.

output intensity *vs* pump location

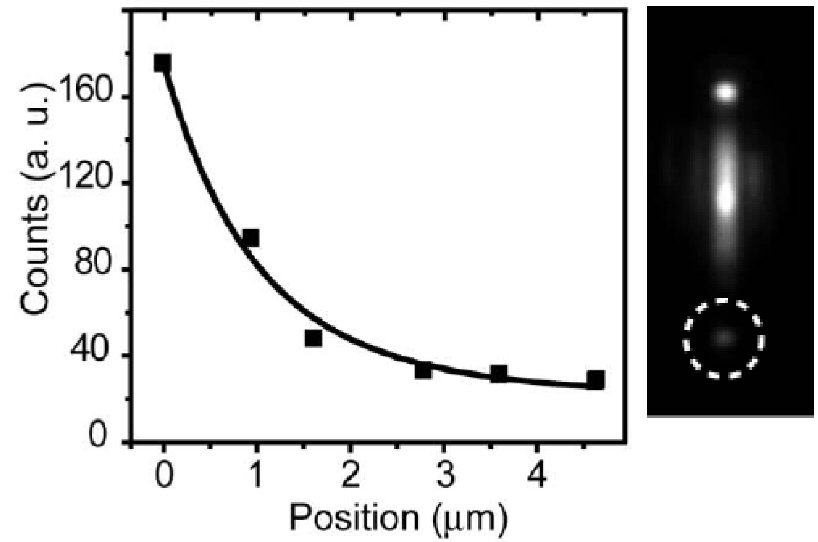

Propagation loss coefficient:
6230 cm-1 for TM mode;
11420 cm-1 for TE mode.

The propagation loss of TM mode was almost fully compensated.

Liu N, *et al.*, Scientific Reports 3, 1967 (2013)

Emission polarization for input signals of TM and TE polarization

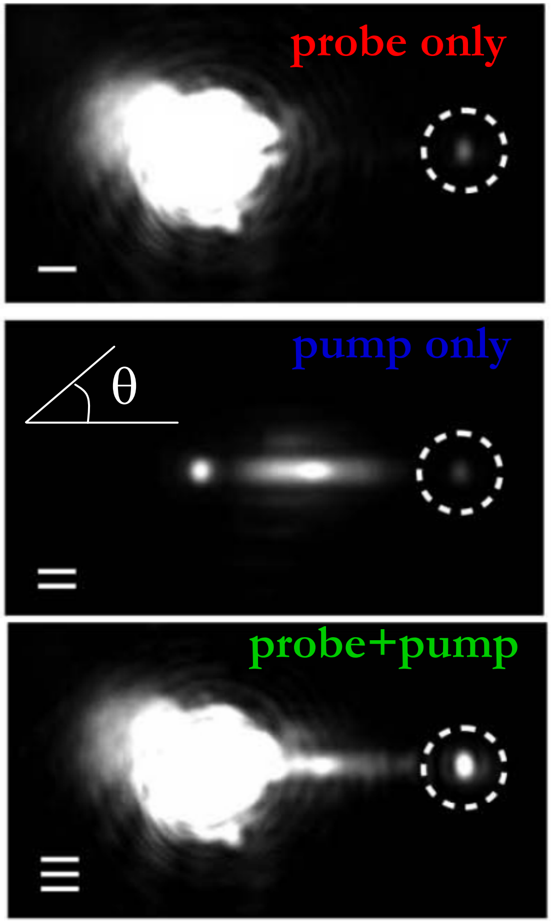

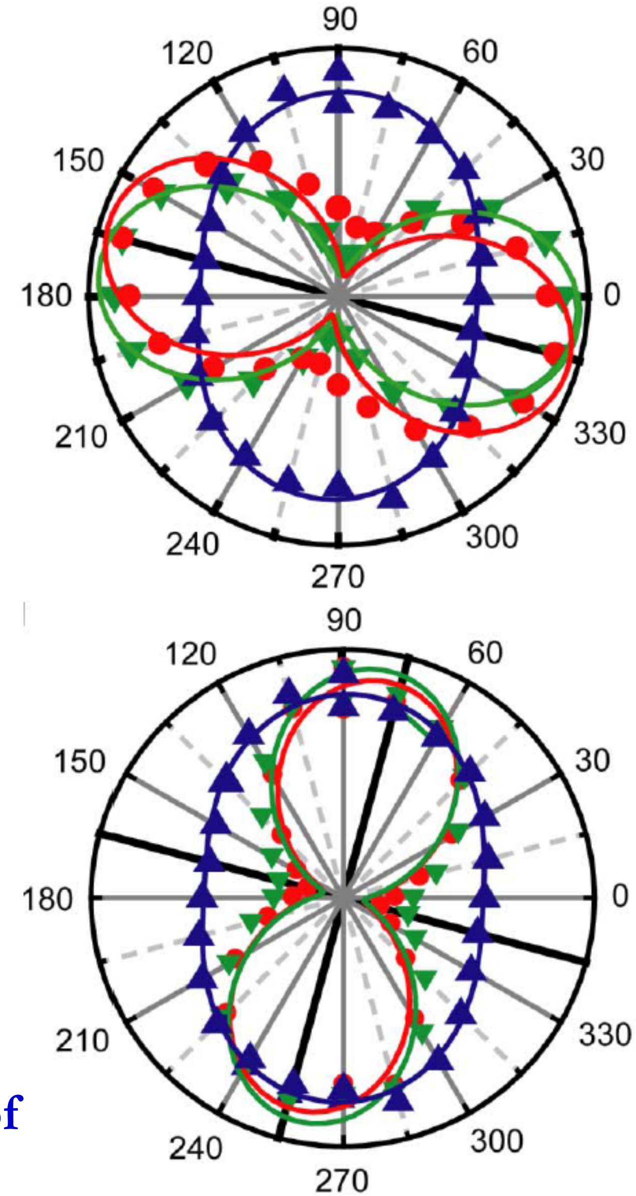

probe: $\theta = 0$
pump: $\theta = 0$

probe: $\theta = 90$
pump: $\theta = 0$

The polarization of the compensated signal (green) follows the polarization of the probe signal (red).

Liu N, *et al.*, Scientific Reports 3, 1967 (2013)

Comparison of gain in plasmonic and photonic waveguides

$$G = G_0 \ln \frac{I}{I_{tr}}$$

I_{tr}: transparency pump intensity, indicating the start of gain

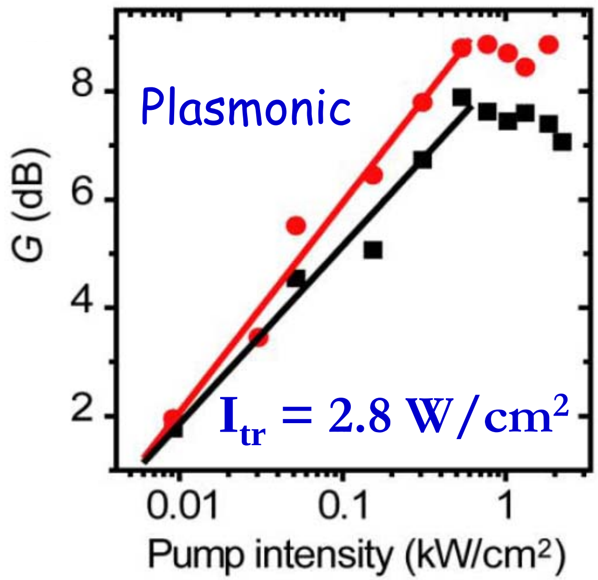

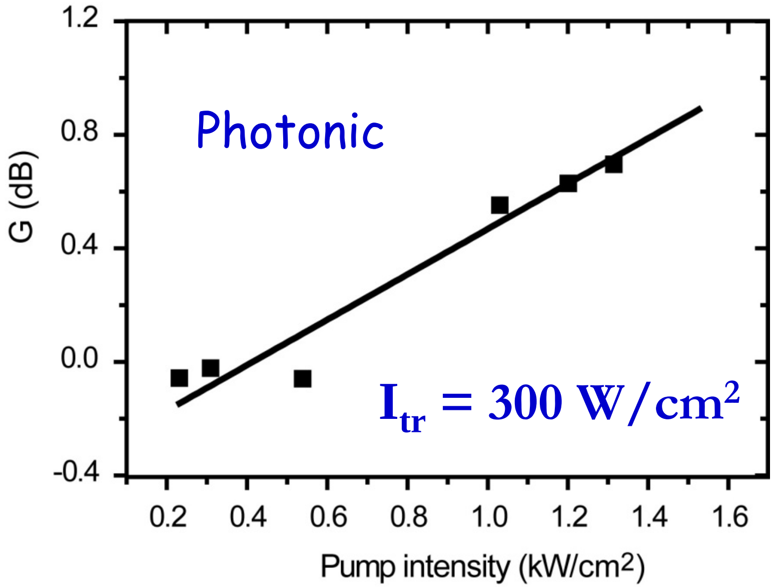

Internal gain coefficient $g = fg_m$

f: fractional factor as the ratio of electric field in CdSe nanobelt and in entire structure.

f=0.64 for plasmonic, f=0.52 for photonic

g_m: material gain coefficient

Pump rate determined by the electric field intensity within the CdSe nanobelt: **2.34**

The transfer of photo-generated hot electrons from Ag film to CdSe nanobelt results in th large difference of I_{tr} for plasmonic and photonic waveguides.

Summary

- **Quantum dot near field imaging**
- **Plasmon-based nanowire devices: switch, splitter, router, λ/4 wave plate, …**
- **Interferometric logic, cascade**
- **Effect of dielectric environment, controlling the beating periods**
- **Directional propagation in Ag film**

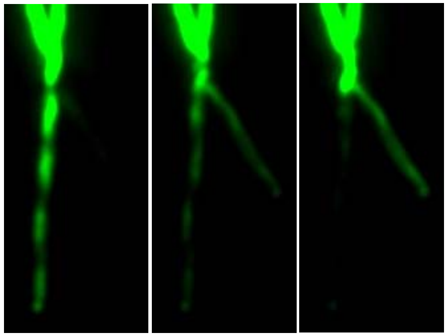

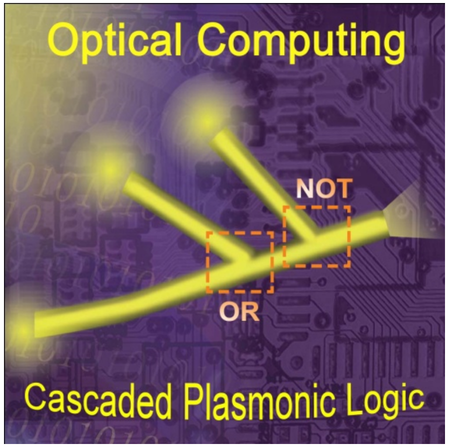

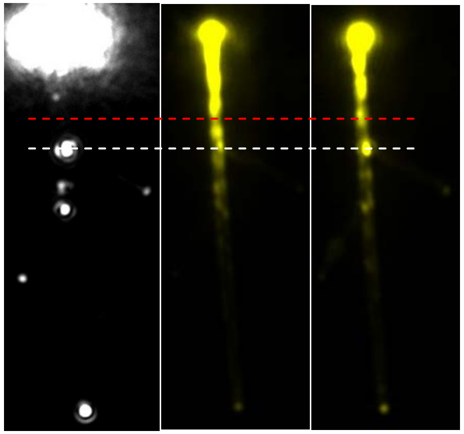

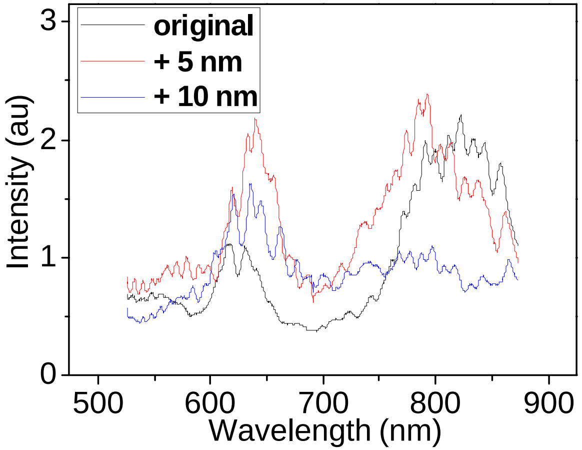

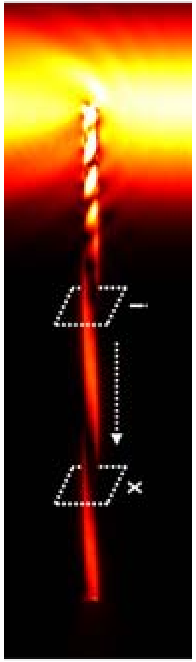

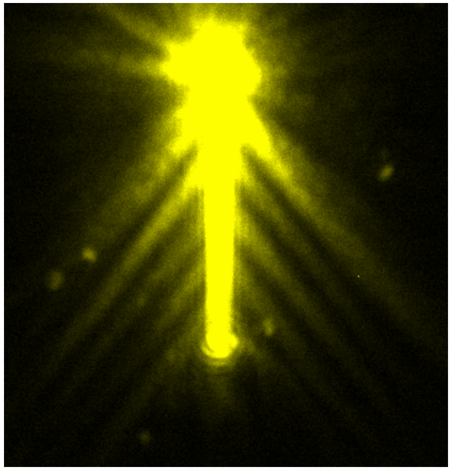

Hongxing Xu Group: http://n03.iphy.ac.cn

Position openings:

- International Young Scientist Fellowship (Post Doc)
- Research Scientist (Staff)

Contact: Prof Hongxing Xu, hxxu@iphy.ac.cn

Acknowledge: Support from CAS, NSF, MOST

Acknowledgement

Hong Wei, Shunping Zhang, Xiaorui Tian, Zhuoxian Wang, Zhipeng Li
Naomi Halas, Peter Nordlander (Rice University)
Mikael Kall (Chalmers University of Technology)

Support from IOP, CAS, NSF, MOST

Hongxing Xu Group http://n03.iphy.ac.cn